The Use of Virus Induced Gene Silencing to Investigate Septoria Leaf Blotch in Wheat

LEE, JACK,ALEXANDER

The Use of Virus-Induced Gene Silencing to Investigate Septoria Leaf Blotch in Wheat

Jack Alexander Lee

Submitted for the Degree of Doctor of Philosophy by Research

School of Biological and Biomedical Sciences

2015

Abstract

Septoria leaf blotch, caused by the fungal pathogen *Zymoseptoria tritici*, is one of the most damaging diseases of wheat (*Triticum aestivum*), a crop plant of significant worldwide importance.

Using the system of Virus-Induced Gene Silencing, to create transient knockdowns of target genes, a novel wheat gene, *TaR1*, was identified as playing a key role in the host response to this pathogen. Silencing this gene leads to the earlier onset of disease symptoms, but reduced reproduction of the causal pathogen.

Sequence analysis, confocal microscopy and protein-protein interaction assays were used to determine that the protein TaR1 localises the nucleus, where its function involves the binding of histones. Precisely, TaR1 is able to bind the Histone 3 subunit, specifically methylated on Lysine 4.

Through this action, the host defence response is delayed, and successful pathogen colonisation is promoted. It is hypothesised that this is an example of the pathogen 'hi-jacking' TaR1 from its original function, in order to complete its lifecycle.

Contents

Abstract I

Contents II

List of Figures VII

List of Tables IX

Acknowledgements X

Declaration XI

Statement of Copyright XI

1. Introduction 1

1.1. Overview 1

1.2. Plant Immunity 2

1.2.1. Summary 2

1.2.2. PAMP-Triggered Immunity 3

1.2.3. Effector-Triggered Immunity 9

1.2.4. Necrotrophic Pathogens 13

1.2.5. Crop Immunity 14

1.3. The Importance of the Wheat-*Zymoseptoria tritici* Interaction 15

1.3.1. Wheat as a Crop 15

1.3.2. Septoria Leaf Blotch 16

1.4. Post-Translational Modifications in Plant Immunity 18

1.4.1. Post-Translational Modification 18

1.4.2. The Ubiquitin-Proteasome System 19

1.4.3. Chromatin Remodelling 21

1.5. Virus-Induced Gene Silencing 25

1.6. Study Objectives 27

2. Materials and Methods **28**
2.1. Materials **28**
2.1.1. Chemicals **28**
2.1.2. Vectors **28**
2.1.3. Bacterial and Fungal strains **29**
2.1.4. Plants **29**
2.2. RNA Extraction **29**
2.3. cDNA Synthesis **29**
2.4. Polymerase Chain Reaction (PCR) **30**
2.4.1. Primers **30**
2.4.2. Taq Polymerase PCR **30**
2.4.3. Q5 Polymerase Proof-Reading PCR **30**
2.4.4. Colony PCR **31**
2.4.5. Site-Directed Mutagenesis **31**
2.4.6. Quantitative Real Time PCR (qPCR) **32**
2.5. Gel Electrophoresis **32**
2.6. Gel Extraction **32**
2.7. Cloning **33**
2.7.1. Gateway Cloning **33**
2.7.2. Destination Vector Recombination **33**
2.7.3. Ligation-Independent Cloning **33**
2.8. Transformation **26**
2.8.1. Competent *E. coli* Production **34**
2.8.2. *E. coli* Transformation **34**
2.8.3. Competent Agrobacterium Production **35**
2.8.4. Agrobacterium Transformation **35**
2.9. Plasmid Purification **36**
2.10. Protein Analysis **36**
2.10.1. SDS PAGE **36**
2.10.2. Coomassie Blue Staining **36**

2.10.3. Western Blotting **36**
2.11. Protein Expression **37**
2.12. Protein Purification **38**
2.13. *In Vitro* Histone Binding Assay **39**
2.14. Antibody Purification **39**
2.15. Plant Growth Conditions **40**
2.16. Agrobacterium Infiltration **41**
2.17. Plant Total Protein Extraction **41**
2.18. Immunoprecipitation **41**
2.19. Plant Nuclear Isolation **42**
2.20. Virus Induced Gene Silencing **42**
2.21. *Zymoseptoria tritici* Infection **43**
2.21.1. Infection **43**
2.21.2. Scoring **43**
2.22. Plant Tissue Culture **44**
2.23. Genomic DNA Extraction **44**
2.24. Confocal Microscopy **44**
2.22.1. DAPI Staining **44**
2.22.2. Microscopy **44**
2.23. Sequence Analysis **45**

3. Using Virus-Induced Gene Silencing to Identify Genes Involved in the Interaction Between Wheat and *Zymoseptoria tritici*. 46
3.1. Introduction **46**
3.2. Silencing *PDS* to Determine VIGS Efficacy **47**
3.3. Target Gene Selection **49**
3.4. Preliminary Infection Experiments **51**
3.5. Target Gene Silencing **57**
3.6. *TaR1* Silencing Affects *Z. tritici* Spore Production **58**
3.7. TaR1 Domain Clarification **61**
3.8. Conclusions **63**

4. Characterisation of TaR1 and its Role in *Zymoseptoria tritici* Infection **65**
4.1 Introduction **65**
4.2. TaR1 Domain Analysis **66**
4.3. TaR1 is Nuclear-Localised **69**
4.4. TaR1 Binds to Specifically Modified Histones **72**
4.5. *TaR1* Silencing Reduces *Z. tritici* Reproduction by Disrupting the Timing of the Life Cycle **76**
4.5. Identification of HATs and HDACs in Wheat **83**
4.6. Conclusions **83**
4.6.1. TaR1 Function **83**
4.6.2. Role of TaR1 in *Z. tritici* Infection **85**

5. Analysis of Transgenic *TaR1* Overexpressing Lines **87**
5.1. Introduction **87**
5.2. Transgenic *TaR1* Overexpression Lines **88**
5.3. Transgenic Plant Selection **91**
5.4. Analysing RNA and Protein Expression in Overexpression Lines **93**
5.4.1. Testing Anti-TaR1 Antibody **93**
5.4.2. Improving TaR1 Detection by Anti-TaR1 **93**
5.4.3. Analysing *TaR1* Overexpression by qPCR **97**
5.5. *TaPDS* Silencing in Fielder Variety Wheat **99**
5.6. Infection of Fielder Variety Wheat with *Z. tritici* **99**
5.7. Analysis of Growth and Development of *TaR1* Overexpressing Lines **101**
5.7.1. Growth of *TaR1* Overexpressing Lines **101**
5.7.2. Flowering Development of *TaR1* Overexpressing Lines **102**
5.7.3. Yield of *TaR1* Overexpressing Lines **102**
5.8. Conclusions **103**

6. Discussion **106**
6.1. Introduction **106**

6.2. Virus-Induced Gene Silencing **107**
6.3. TaR1 is Involved in the Interaction Between Wheat and *Z. tritici* **108**
6.4. TaR1 as a Link Between Defence and Chromatin Remodelling **110**
6.5. Stable Transgenics Overexpressing *TaR1* **116**
6.6. TaR1-Specific Antibody **117**
6.7. Summary **119**

Appendix **120**

Bibliography **122**

List of Figures

1.1. The Two-Phase Model of Plant Immunity 3

1.2. PTI Signalling 6

1.3. Comparison of the Guard and Decoy Models 11

1.4. *Zymoseptoria tritici* Lifecycle 17

1.5. Ubiquitination in Plant Defence 21

1.6. BSMV Vector Map 27

3.1. *TaPDS* Sequence 48

3.2. *TaPDS* Silencing 48

3.3. Expression Profiles of *TaU1-5* and *TaR1-5* After *Z. tritici* Infection 52

3.4. UBC Protein Sequence Alignment 53

3.5. RING Protein Sequence Alignment 54

3.6. Nucleotide Sequences of *TaU1-5* 55

3.7. Nucleotide Sequences of *TaR1-5* 56

3.8. Preliminary Spore Count Experiment 59

3.9. qPCR Primer Products 59

3.10. Silencing qPCR 60

3.11. *TaR1* and *TaU1*-Silenced Spore Count Data 60

3.12. Conserved Domain Database Search Results for TaR1 62

3.13. Phylogeny of RING and PHD Domains 62

4.1. TaR1 PHD Domain Alignment and Phylogenetic Tree 67

4.2. TaR1 AL Domain Analysis 68

4.3. YFP-TaR1 Confocal Microscopy 70

4.4. Western Blotting of Infiltrated *N. benthamiana* 71

4.5. RFP-TaR1 Confocal Microscopy 71

4.6. Co-Immunoprecipitation of YFP-TaR1 and HA-H3 73

4.7. Co-Immunoprecipitation of HA-TaR1 and YFP-H3 73

4.8. Purification of His-TaR1 75

4.9. Histone Peptide Pulldown Assay 75

4.10. Infection Phenotyope of *TaR1*-Silenced Plants 77

4.11. Green Area Percentage of *Z. tritici* Infected Leaves 78

4.12. Repeated *TaR1*-Silenced Spore Count 78

4.13. *TaR1*-Silenced Picnidia Count 79

4.14. Histone Acetyl Transferase Multiple Sequence Alignments 80

4.15. Histone Deacetylase Multiple Sequence Alignments 81

5.1. Kanamycin Selection Plates 90

5.2. Kanamycin Selection Lateral Roots 90

5.3. PCR Amplification of *NPTII* 92

5.4. αTaR1 Test 92

5.5. High Protein Concentration αTaR1 Western Blot 94

5.6. αTaR1 Western Blot Optimisation 94

5.7. Nuclear Isolation Western Blot 96

5.8. Antibody Purification Western Blot 96

5.9. Western Blot with Purified αTaR1 98

5.10. *TaR1* Expression qPCR 98

5.11. *TaPDS* Silencing in Fielder Wheat 100

5.12. Fielder Infection with *Z. tritici* IPO323 100

6.1. Possible Mechanism for TaR1 Function 113

List of Tables

Table 2.1. List of Vectors Used 28

Table 2.2. List of Bacterial and Fungal Strains 29

Table 3.1. Target Genes Chosen Based on UPS-related Domains And Expression Changes on Infection 50

Table 5.1. TaR1 Transgenic Lines 89

Table 5.2. *TaR1* Overexpression Adult Plant Growth Analysis 101

Table 5.3. *TaR1* Overexpression Flowering Development Analysis 102

Table 5.4. *TaR1* Overexpression Yield Analysis 103

Acknowledgements

I would firstly like to thank my supervisor, Dr. Ari Sadanandom without whose input and knowledge none of this would have come to pass. I will also be forever grateful to Dr. Cunjin Zhang, who taught me everything I needed to know, Dr. Mark Bailey for three-plus great years of lab companionship, Linda and Alberto for the camaraderie of the wheat team and to Stuart, Charlotte, Gary, Helen, Beatriz, Anjil, Vivek and all my other colleagues and friends. Without you my days would have been far less fun, and my knowledge of Scottish football drastically reduced.

Further thanks must go to my fantastic housemates and PhD colleagues James and Dave, for an entertaining environment that made the whole process much easier. I'd also like to give special thanks to Martin and Anna for visiting regularly so I wasn't left alone with them too often! You've all been wonderful.

I'd like to thank my family for their love and support over the years, and for the effort they made to give the opportunities I have had and to put me where I am now.

And finally my greatest thanks go to Olivia Kent, whose deeds include but are not limited to: talking, listening, helping, drawing, cooking, cleaning, cheering up, entertaining, visiting, proof-reading, shoe buying, cajoling and introducing me to friendly cats. I'd never have made it without you.

Declaration

This thesis is submitted to the University of Durham in support of my application for the degree of Doctor of Philosophy. It has been composed by myself and has not been submitted in any previous application for any degree. The work (including data generated and data analysis) was carried out by the author except where explicitly states otherwise.

Jack Lee

Statement of Copyright

Chapter 1

Introduction

1.1. Overview

Agricultural cultivation of cereal crops is an important practice and contributes to the dietary staples of the majority of people worldwide. With an ever-expanding population and reduced availability of fertile land, greater strain is being placed on increasing the yield of these crops.

Crop plants face a variety of stresses, both biotic and abiotic, in the field. Improving the responses of plants, so that they may continue to grow under stress and to produce high yields, is a very important goal in global food security. In particular, this project focuses on Triticum aestivum (wheat), a crop which is accountable for up to 20% of human calorie intake (Pena et al., 2014), and is currently the target of the wheat 20:20 project, which aims to increase current average yields from 8.4 tonnes per hectare to 20 within the next 20 years (http://www.rothamsted.ac.uk/our-science/2020-wheat).

This project will concentrate on biotic stress of wheat, specifically that caused by Septoria leaf blotch (STB), a disease caused by the fungus Zymoseptoria tritici. The majority of agricultural diseases are controlled through breeding for resistant varieties and application of pesticidal chemicals. However, due to the relatively few known resistance genes and short generation time of the pathogen, which contributes to the development of fungicide resistance, these methods are becoming increasingly less effective.

In order to improve control systems, it is first important to increase understanding of the underlying molecular processes involved in this plant-pathogen interaction. This project will aim to achieve that by examining the role of individual host genes by knocking down their expression through Virus Induced Gene Silencing (VIGS), and examining the infection phenotype created.

1.2. Plant Immunity

1.2.1 Summary

Plants grow under constant threat from the attack of pathogens, delivered through the air and soil that they rely upon. These pathogens consist of a huge variety of organisms, including bacteria, fungi and viruses, amongst others, with a wide array of life histories and modes of infection. Plants must be able to defend themselves against these attacks, in order to successfully grow and reproduce.

Plants rely on physical barriers such as the waxy cuticle and the cell wall as a first line of defence to prevent access to pathogens (Underwood 2012; Serrano et al., 2014). Pathogens have developed methods of circumventing these defences, entering tissue through stomata, hydathodes and wounds (Gudesblat et al., 2009), and can penetrate individual cells through structures such fungal appresoria and nematode stylets (Howard et al., 1991; Lambert and Bekal 2002).

In addition to these barriers, constitutively-active plant defence mechanisms also incorporate a number of toxic and inhibitory compounds, including phenolics, phytoalexins and hydrolytic enzymes targeting pathogen cell walls and proteins (Ahuja et al., 2012; Daayf et al., 2012; Rovenich et al., 2014). However, these defences can also be overcome. In such cases, plants must therefore respond through inducible defences with each plant cell able to recognise and respond to pathogen attack (Spoel and Dong 2012).

The inducible pathogen response of plants follows a two-phase pattern, as seen in Figure 1.1. (adapted from Jones and Dangl 2006). In the first phase, plant receptors detect well-conserved pathogen derived molecules called Pathogen Associated Molecule Patterns (PAMPs), which trigger a response called PAMP-Triggered Immunity (PTI). To counter these, pathogens release compounds called effectors into the plant cell to suppress immunity. Detection of these leads to the second immune phase of the plant, called Effector-Triggered Immunity (ETI) (Jones and Dangl 2006).

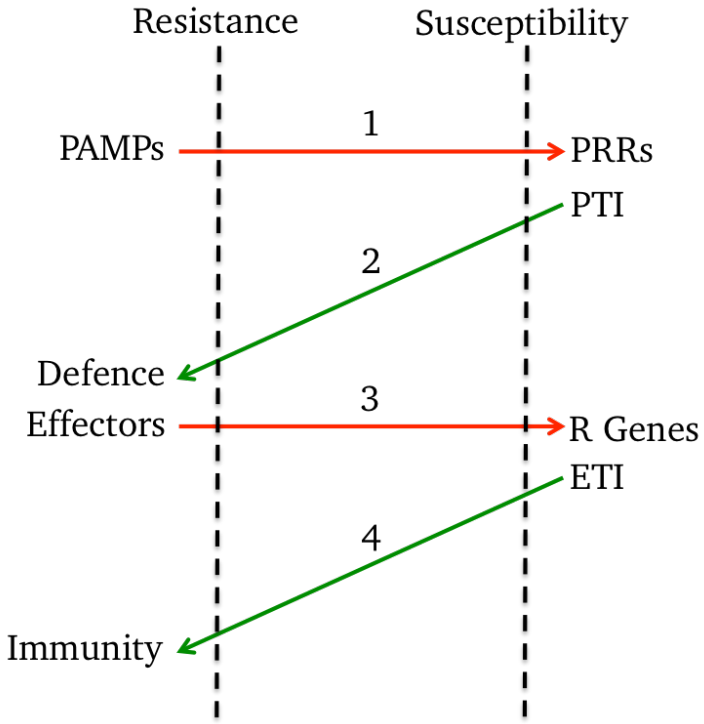

Figure 1.1. The Two-Phase Model of Plant Immunity. An interaction between a pathogen (red) and plant cells (green) can result in a 'zig-zag' pattern between resistance and susceptibility. 1) Pathogens attack the plant and produce PAMPs, which are detected by plant PPRs 2) PRR signalling leads to defence through PTI 3) The pathogen releases effector proteins to suppress the defence response 4) R genes detect individual receptors, signalling ETI and a stronger immune response.

1.2.2. PAMP Triggered Immunity

Recognition

Integral pathogen components, such as flagellin from bacteria and chitin from fungi, are strongly conserved (Felix et al., 1999; Pacheco-Arjona and Ramirez-Prado 2014). Recognition of these PAMPs is the first step in recognition of pathogen attack. Detection of these proteins is known to be mediated through transmembrane receptors known as Pattern Recognition Receptors (PRRs), such as FLAGELLIN SENSING2 (FLS2), which recognises bacterial flagellin, and CHITIN ELICITOR RECEPTOR KINASE1 (CERK1) and CHITIN ELICITOR BINDING PROTEIN (CEBiP), which recognise fungal chitin (Gomez-Gomez and Boller 2000; Kaku et al., 2006; Miya et al., 2007; Boller and Felix 2009).

Plant-derived molecules can also act as PRR ligands to trigger a defence response (Boller and Felix 2009). Many pathogens produce hydrolytic enzymes as a method of surpassing constitutive defences, which damage plant proteins and can be recognised as Damage Associated Molecular Patterns (DAMPs), indirect indicators of pathogen invasion (Moreira et al., 2005; Abramovitch et al., 2006). Examples include oligogalacturonides, which are released by pathogen-derived pectin degrading enzymes and stimulate a number of defence responses, and extracellular ATP, which is released on wounding and plays a role in the regulation of plant defence (Reymond et al., 1995; Chivasa et al., 2009; Choi et al., 2014).

PRRs, PAMP and DAMP immune receptors are localised to the surface of the cell and are currently characterised as either Receptor Kinases (RKs), which have an extracellular ligand-binding domain and an intracellular kinase domain or Receptor-Like Proteins (RLPs), which lack the kinase domain, and so must associate with other surface localised kinases (Zipfel 2014). The Arabidopsis flagellin receptor, FLS2, is a RK that dimerises with another membrane associated RK BRASSINOSTEROID INSENSITIVE ASSOCIATED KINASE (BAK1) following binding of a 22 amino acid sequence at the N-terminus of flagellin (Gomez-Gomez and Boller 2002; Chinchilla et al., 2007).

Similarly, the Arabidopsis chitin receptor CERK1 is also a RK, this time forming a homodimer when bound to chitin, which activates the cytoplasmic kinase domain for downstream signalling (Miya et al., 2007; Liu et al., 2012). In rice, however, the primary chitin receptor is CHITIN ELICITOR BINDING PROTEIN (CEBiP), a RLP. On chitin recognition, CEBiP homodimers undergo a ‘sandwich-type’ dimerisation with the rice CERK1 homolog, forming a hetero-oligomeric complex, through which kinase activity and hence further signalling is established (Kaku et al., 2006, Shimizu et al., 2010; Hayafune et al., 2014). Other RLP PRRs have been discovered and, while their full mechanism is not always known, they presumably also require another membrane-associated kinase to function (Ron and Avni 2004; Zhang et al., 2014).

Many plants accumulate chitinases and other hydrolytic enzymes in response to pathogen detection, combating infection by the breakdown of cell walls. However, they may also provide a secondary function of producing a higher concentration of extracellular chitin to be detected by the PRRs (Punja and Zhang 1993; Rovenich et al., 2014).

In the interaction between wheat and Z. tritici, it is currently known that wheat homologues of the CERK1 and CEBiP receptors are required for chitin-induced responses in wheat. CERK1 or CEBiP deficient plants were impaired in their ability to resist Z. tritici (Lee et al., 2014). Treatment with beta-1,3 glucan fragments, purified from Z. tritici cell walls increased the resistance of previously susceptible plants (Shetty et al., 2009), suggesting that wheat recognises this through an as yet unknown receptor, inducing a defence response.

Downstream Signalling

PPRs are restricted to the cell membrane and therefore, even after activation of their kinase domain, require a partner to link their kinase activity to downstream signalling. In particular, Receptor-Like Cytoplasmic Kinases (RLCKs) have been identified as important direct interactors of PRRs, positively regulating PTI signalling. One such RLCK, BOTRYTIS-INDUCED KINASE (BIK1), has been shown to be activated by phosphorylation, through interaction with both the CERK1 homodimer and the FLS2/BAK1 heterodimer (Lu et al., 2010; Zhang et al., 2010). This suggests that perhaps there is some convergence of the two pathways here, as PTI is intended to defend against a broad spectrum of pathogens.

After activation by the receptor, RLCKs can perform an extensive role in PTI induction. Firstly, the receptor components FLS2 and BAK1 are phosphorylated on association with BIK1, suggesting that it has a role in amplifying the receptor signal. Downstream, BIK1 is also involved in callose deposition, Reactive Oxygen Species (ROS) bursts and Salicylic Acid (SA) accumulation, all of which are related to the defence response. Whilst the mechanism behind some of these downstream events remains unknown, stimulation of ROS by BIK1 was proven to be via direct phosphorylation, of RESPIRATORY BURST OXIDASE-D (RbohD), an NADPH oxidase (Lu et al., 2010; Zhang et al., 2010; Li et al., 2014). This pathway is further described in Figure 1.2.

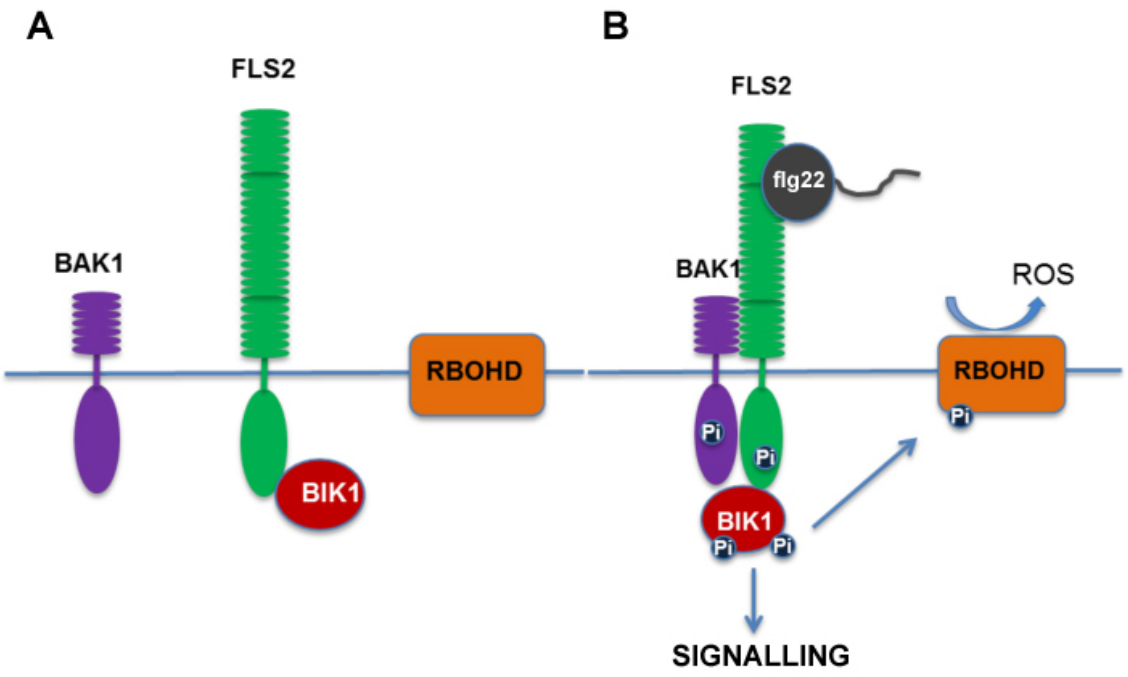

Figure 1.2. PTI Signalling. A) FLS2, BAK1 and BIK1 before pathogen recognition. B) Recognition of the PAMP flg22 causes FLS2 and BAK1 to dimerise and phosphorylate BIK1. The activated BIK1 then phosphorylates RBOHD, stimulating ROS production. Activated BIK also brings about further downstream signalling, presumably through further phosphorylation, although the exact mechanism is currently unknown.

The activation of Mitogen-Activated Protein Kinase (MAPK) signalling cascades is also well-established as having a function in the plant immune response, often occurring very shortly after pathogen recognition (Asai et al., 2002). BIK1 is thought to act upstream of any MAPK cascade components, and although the mechanism is currently poorly understood, it may act as a link between PRR recognition and MAPK cascade signalling (Lu et al., 2010).

While the involvement of wheat CERK1 and CEBiP in the recognition of Z. tritici is known (Lee et al., 2014), nothing is currently known of the downstream signalling through which this is processed. However, the involvement of wheat BAK1-like proteins have been implicated in the response of wheat to other fungal pathogens (Ding et al., 2011).

Plant Responses to Pathogen Recognition

Pathogen recognition by PRRs and subsequent signalling pathways elicit a rapid reaction, with the most immediate responses including calcium influxes, bursts of ROS and MAPK cascades (Boller and Felix 2009). ROS bursts and MAPK cascades are regularly associated with plant pathogen responses, while the influx in calcium was shown to be key to the activation of NADPH oxidases, and hence ROS bursts, which are an early cellular response to pathogen attack, and are important signals in many responses (Torres et al., 2006; Ogasawara et al., 2008). These responses include the accumulation of SA, a plant hormone strongly associated with plant defence responses, and the transcription of defence responsive genes (Navarro et al., 2004; Tsuda et al., 2008; Li et al., 2014).

The defence responses brought about by this can act in a number of ways. The deposition of the cell wall polymer callose at sites of pathogen penetration, to prevent further access to the cell, is a commonly seen PTI response and an example of a mechanical defense to pathogen entry (Jacobs et al., 2003). Similar to this, stomata, a common site of pathogen entry, reduce in opening on recognition of pathogen attack (Melotto et al., 2006). Such mechanical defences as callose deposition and other cell wall fortifications have been noted in wheat, though they have not been studied in relation to Z. tritici.

In addition to these mechanical defences, which aim to prevent further pathogen entry, many plants also produce a chemical defence; synthesising anti-microbial compounds, including phenolics, alkaloids and terpenoids, to deter pathogen growth (Freeman and Beattie 2008). Antimicrobial compounds such as these can be important factors in the disease resistance of wheat (Gogoi et al., 2001). Other antimicrobial compounds, such as defensins are also often accumulated in defence responses, as well as wide range of other enzymes, aimed at disrupting the pathogen or in combating resultant stresses within the plant cell (Freeman and Beattie 2008).

In response to recognition of Z. tritici, wheat has been shown to display an increase in the cell wall degrading chitinase and beta-1,3 glucanse enzymes (Shetty et al., 2009). In response to Fusarium graminearum infection, the expression of many defence related wheat genes, including those involved in cell wall fortification, antioxidative stress and

the biosysnthesis of defence-related hormones and antimicrobial compounds, were differently regulated (Ding et al., 2011), suggesting that these are involved in the response of wheat to pathogens.

Pathogen Effectors

PTI is usually considered to be sufficient to prevent infection by most pathogens, whereas plants lacking PRRs or other components of PTI signalling are consequently more susceptible to pathogen attack (Zipfel et al., 2004; Miya et al., 2007; Zhang et al., 2010). As a result, in order to successfully infect a host, pathogens must evolve ways to circumvent or disrupt the PTI system, as well as other constitutive defence mechanisms. In order to do so, pathogens release proteins, called effectors, into the host, which perform a wide range of functions.

PTI is activated by binding of pathogen-derived PAMPs to receptors, and therefore can be avoided by preventing this recognition event. Many fungal pathogens achieve this through chitin-binding effectors, containing a LysM domain similar to that seen in the CERK1 receptor. These proteins prevent receptor binding by outcompeting PRRs, subsequently sequestering released chitin. Such mechanisms are often crucial to infection. (de Jonge et al., 2010; Marshall et al., 2011; Mentlak et al., 2012).

Whilst no such system has been documented for flagellin in bacteria, other mechanisms have appeared to fulfil a similar function. Polymorphisms in the flagellin-encoding sequence of some bacteria produce a protein, which is not recognised by FLS2 (Sun et al., 2006). Meanwhile the Pseudomonas syringae effector AvrPtoB, which is an ubiquitin E3 ligase, disrupts signalling of flagellin sensing by polyubiquitination of FLS2, which is then targeted for degradation (Gohre et al., 2008).

These effectors can be very specific, while others are more generalised, and can supress a number of different pathways. For example, the P. syringae effector AvrPto prevents recognition signalling by blocking the kinase domain of multiple PRRs, including FLS2, BAK1 and CERK1 (Shan et al., 2008; Xiang et al., 2008; Gimenez-Ibanez et al., 2009).

However, even if the recognition signal is received and successfully transmitted, other effectors can disrupt the signal further downstream. The AvrPphB effector is a cysteine protease, capable of cleaving a group of PBL1-like RLCKs, including BIK1, thus

preventing FLS2 signalling (Zhang et al. 2010). Other effectors can inhibit signalling by interacting with MAPKs, thereby disrupting the signalling cascade seen in a normal defence response (King et al., 2014).

Some effectors do not target the immune signalling pathway at all, instead directly affecting the plant responses. For example, the Ustilago maydis effector, ESSENTIAL DURING PENETRATION1 (PEP)1, interacts with a host peroxidase to prevent the creation of oxidative bursts, while another effector from the same pathogen, CHORISMATE MUTASE1 (CMU1), affects the accumulation of SA. Other pathogens have also been shown to impair the production of salicylic acid, in this case by hydrolysis of its precursor, isochromate (Djamei et al., 2011; Hemetsberger et al., 2012; Liu et al., 2014).

Many pathogens also produce effectors, which are able to directly regulate the transcription of some host genes, and are often referred to as Transcription Activator-Like Effectors (TALEs). TALEs target a variety of genes, often including membrane transporters, transcription factors and post-transcriptional modifiers and, while their targets are yet unknown, the Xanthomonas oryzae effectors TAL6 and TAL11a are crucial in the suppression of host defence (Ji et al., 2014; Boch et al., 2014).

Studies searching for Z. tritici effectors, which bring about the cell death response of the host, have found many putative effectors, but none which have any affect on virulence when deleted (Gohari et al., 2015, Rudd et al., 2015). LysM domain-containing effectors from Z. tritici have been shown to effect virulence on wheat, through the disruption of the CERK1 and CEBiP-mediated chitin recognition. However, these remain the only virulence-effecting Z. tritici effectors currently discovered.

1.2.3. Effector Triggered Immunity

Recognition

In order to contend with these infection strategies, plants have evolved another level of defence. Recognition of pathogen effector molecules by receptors, called R genes, through gene-for-gene interactions, leads to a defence response known as Effector-Triggered Immunity (ETI) (Flor 1971; Jones and Dangl 2006). Many of the currently identified R genes are defined according to their domain structure, as Nucleotide

Binding site Leucine-Rich Repeats (NB-LRRs), containing an NB domain, involved in ATP or GTP-binding, and LRR domains, which typically function in protein-protein interactions (Kobe and Deisenhofer 1994; Traut 1994).

A small number of R gene/effector pairs have shown a direct interaction (Jia et al., 2000; Deslandes et al., 2003). However, the 'Guard Hypothesis' (Van der Biezen and Jones 1998) suggests that many R genes indirectly detect effectors, through recognition of their targets or products. An example of this is the detection of the effector proteins AVRPTO and AVRPTOB, previously mentioned to disrupt chitin and flagellin-mediated signalling (Gohre et al., 2008; Giminez-Ibanez et al., 2009).

These effectors both interact directly with PTO and, in doing so, instigate an immune response. Rather than an NB LRR domain protein, PTO is a serine/threonine kinase, thought to be involved in immunity through triggering of a phosphorylation cascade. It is hypothesised that effector binding blocks this function, but the PTO/AVRPTO complex is recognised by the NB LRR protein PRF. PRF, which 'guards' the target PTO, then initiates the ETI response (Tang et al., 1996; Frederick et al., 1998; Van der Biezen and Jones 1998; Kim et al., 2002).

However, while AVRPTO contributes to virulence of wild type tomato and Arabidopsis plants, even in the absence of PTO, its contribution to virulence is not seen in plants lacking FLS2 (Chang *et al*., 2000; Xiang *et al*., 2008). This suggests that FLS2 is the direct target of AVRPTO, and has lead to the Decoy Theory (van der Hoorn and Kamoun 2008).

This theory proposes that, rather than having a direct effect in inducing pathogen defence, the decoy has evolved specifically for recognititon of the effector, by mimicking its target. In this example, PTO mimics FLS2, acting a decoy to compete for effector binding, while also triggering ETI through PRF. This theory porposed model is shown in Figure 1.3. (van der Hoorn and Kamoun 2008).

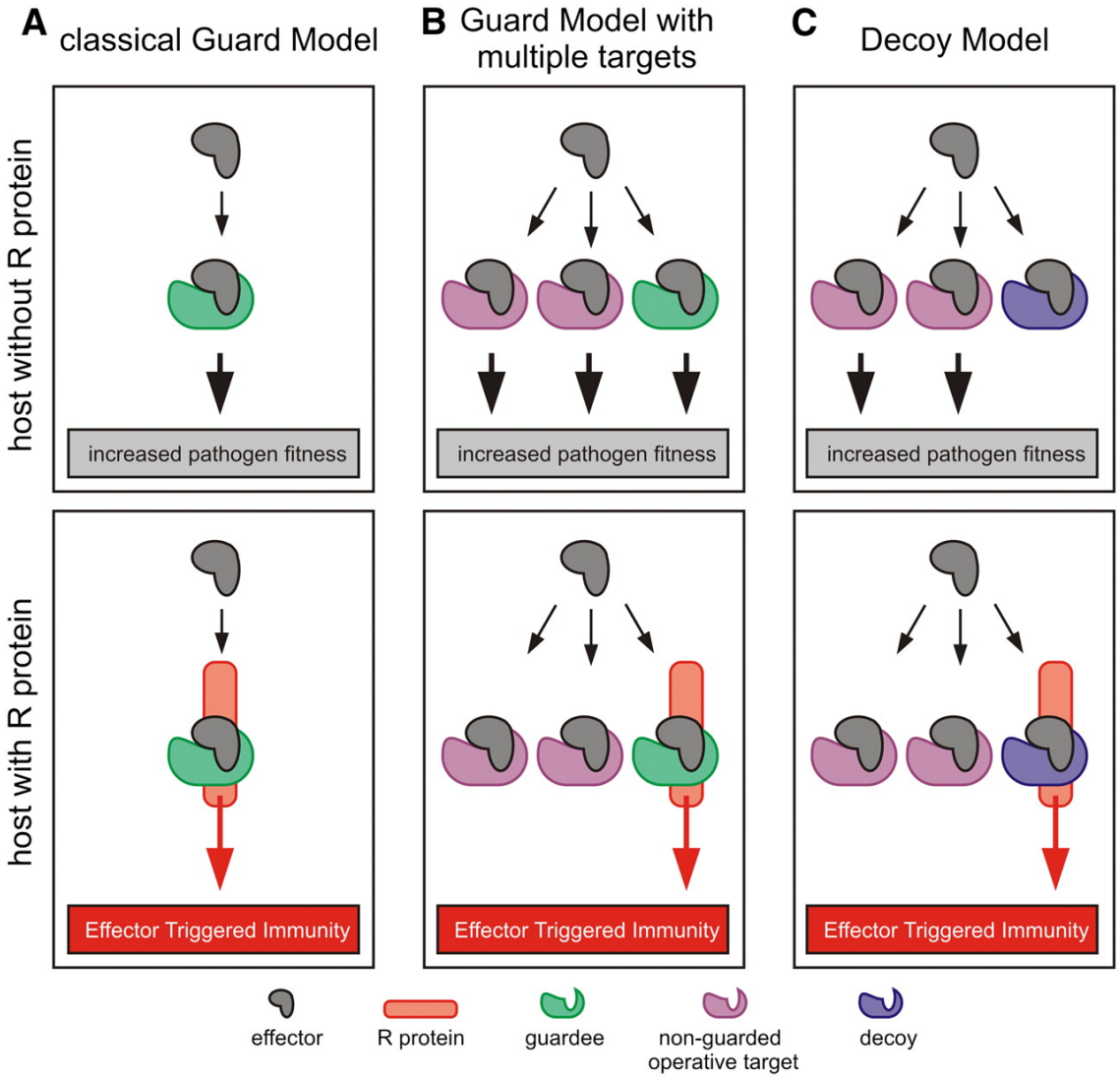

Figure 1.3. Comparisons of the Guard and Decoy Models. The classical Guard Model (A) is contrasted with a modified Guard Model in which the effector targets multiple plant proteins (B) and the Decoy Model (C). Effectors are depicted in gray, operative effector targets in purple, guardee in green, decoy in blue, and the R protein in orange (van der Hoorn and Kamoun 2008).

As mentioned above, the LysM domain effectors are the only currently discovered effectors involved in the wheat interaction with Z. tritici. Nothing is known of any plant response triggered by recognition of these and, therefore, nothing is currently known of ETI in this interaction.

Signalling

The downstream signalling components of R genes are less well established than those of PTI, but some components have been identified. Similarly to PTI, it appears that ETI signalling involves ROS bursts. In barley (Hordeum vulgare), ROS accumulation was shown to be downstream of the zinc-binding protein REQUIRED FOR MLA RESISTANCE1 (RAR1), which acts as a point of convergence for signalling from multiple R genes (Shirasu et al., 1999). RAR1 itself functions in a complex with Skp-cullin-F-box ubiquitination component SGT1, and the heat shock protein HSP90; the exclusion of either prevents any ETI response. This complex acts to stabilise NB LRR proteins, and is required for the accumulation of some R genes, including the Rx gene from potato (Austin et al., 2002; Azevedo et al., 2002; Hubert et al., 2003; Boter et al., 2007; Kadota et al., 2010).

As well as ROS, RAR1/SGT2 is also involved another common factor between PTI and ETI, MAPK signalling cascades. RAR1/SGT1 are vital to the function of NRC1, which acts downstream of the MAPK MEK2, in signalling pathways required for resistance to Cladosporium fulvum (Ekengren et al., 2003; Gabriels et al., 2007). As well as this, MAPKKKα and MAPKKKε are involved in the PTO/AVRPTO pathway mentioned above (Jin et al., 2002; del Pozo et al., 2004; Melech-Bonfil and Sessa 2010).

Response

Plant responses, as a result of ETI signalling, rely on large-scale transcriptional changes and, in particular, the involvement of WRKY transcription factors has often been implicated in this process (Shen et al., 2007, Pandey et al., 2010; Bhattacharjee et al., 2013). The ultimate conclusion of these ETI signalling pathways is the Hypersensitive Response and Programmed Cell Death (HR PCD), a localised cell death mechanism, intended to isolate pathogens and starve them of nutrition (Abramovich et al., 2006; Jones and Dangl 2006).

1.2.4. Necrotrophic Pathogens

Plant pathogens generally fall within two feeding styles: biotrophs, which feed on living tissue, and necrotrophs, which feed on dead tissue. While HR PCD is one the key factors in preventing infection by biotrophs, it actually assists in infection by necrotrophs. A third group of plant pathogens exist, called hemibiotrophs, which use both biotrophic and necrotrophic nutrition. Whilst the relative duration of these two nutritional phases varies from species to species, the biotrophic phase is commonly followed by a switch to necrotrophy. Although these pathogens, like necrotrophs, are capable of feeding on dead tissue, HR PCD has been associated with resistance to some hemibiotrophic pathogens (Jia et al., 2000; Vleeshouwers et al., 2000; Mengiste 2012). Therefore, plant defence responses can vary greatly between pathogens displaying these contrasting feeding mechanisms (Gilchrist 1998; Govrin and Levine 1999; Glazebrook 2005).

In order to promote infection, as well as PTI suppression as seen in biotrophs, necrotrophs also produce an array of other disease promoting chemicals, including cell wall degrading enzymes and toxins. Necrotrophs can be further defined as host-specific or broad host-range necrotrophs, as these effectors can either be target specific or have action against a wide range of species, respectively (Alfano and Collmer 1996; Walton 1996; van Kan 2006; Mengiste 2012).

As necrotrophic pathogens produce many of the same PAMPs as biotrophs, PTI does not vary much between the two. Other than this, however, responses by plants to necrotrophs are quite different, with only one known R gene implicated in providing immunity against necrotrophic pathogens (Staal et al., 2008). Rather than the ETI seen in biotroph interactions, the host-specific toxins can instead lead to a system known as effector-triggered susceptibility, where the gene-for-gene interaction, instead of promoting immunity, is required for successful infection (Wolpert et al., 2002; Oliver and Solomon 2010).

No toxins produced by Z. tritici have yet been identified. However, effector-triggered susceptibility has been shown previously in wheat, with the necrotrophic fungal pathogen Stagnospora nodorum toxin TOX3 induces symptoms through interaction with the host susceptibility factor SNN3 (Liu et al., 2009).

In the response of plants to necrotrophs, one clear difference to the biotrophic response is in the role of hormones. While SA is key in biotrophic immunity, the defence to necrotrophic pathogens instead relies on the Ethylene (ET) and Jasmonic Acid (JA), which work antagonistically to SA (Glazebrook 2005). JA signalling has also been implicated in the plant response to tissue damage other biotic stresses such as insect pests (McConn et al., 1997). JA-induced defence to necrotrophic pathogens relies on the transcription factor MYC2 (Lorenzo et al., 2004; Dombrecht et al., 2007).

A number of other important transcription factors have been identified in the response of plants to necrotrophic pathogens, amongst which is Arabidopsis WRKY33. WRKY33, which relies on MAPK cascade signalling, regulates the production of camalexin, an alkaloid anti-fungal compound, and in doing so is essential in defence against necrotrophic fungi (Qiu et al., 2008; Mao et al., 2011).

1.2.5. Crop Immunity

Pathogen defence has been widely studied in important crop species, such as rice, maize and wheat. The defence responses of these species are similar to those already described, with examples discovered of important PTI-related components, such as PRRs (Shimizu et al., 2010; Lee et al., 2014), RLCKs (Yamaguchi et al., 2013) and downstream elements including MAPKs, ROS production and defence-related transcription factors (Wong et al., 2007; Gao et al., 2011; Voitsik et al., 2013). Cultivated crops are also aided in defence against pathogens through the application of pesticidal chemicals, as well as the breeding of cultivars resistant to specific pathogens.

The large selection of genotypes displayed by these different crop cultivars exposes them to a wider array of pathotypes. Polymorphisms across a range of genes in the wheat yellow rust (Puccinia striiformis) population have been identified, which determine those cultivars that the individual pathotype is able or unable to establish infection on. Many of these genes were previously identified as likely effectors, and have since been confirmed as such through a bacterial injection system, suggesting that in addition to the presence or absence of certain effectors, individual polymorphisms within their respective sequences are also key to pathogen success (Cantu et al., 2013; Hubbard et al., 2015).

Much of the cereal immunity research is carried out in this area of identifying and testing candidate effectors of pathogens, and R genes in the host. For example, BLUMERIA EFFECTOR CANDIATE109 (BEC1019), a secreted effector, supresses cell death in the host and is crucial to the infection of Blumeria graminis, a disease for which the best established R gene is MLA6, an NB-LRR gene, which confers resistance in both wheat and barley (Halterman et al., 2001; Whigham et al., 2015).

1.3. The Importance of the Wheat-Zymoseptoria tritici Interaction

1.3.1. Wheat as a Crop

Wheat has been consistently amongst the most important cultivated crops worldwide for thousands of years (Kislev 1984). With more than 700 million tonnes harvested annually, wheat, along with rice and maize, is one of the most widely produced crops in the world, accounting for 20% of the protein and calorie intake for 4.5 million people, and, with the population set to continue to increase, wheat yield are predicted to require a 60% rise by 2050 to meet global food security demands. (FAO 2012; USDA 2015).

It is clear then that developing wheat production is vital to combating dangers to future global food security. With as much as 10% of global annual crop yields lost to disease, developing pathogen resistance and increasing yields despite the presence of biotic stresses will become an important global challenge (Strange and Scott 2005).

On a local scale, wheat production is also very important to the economy of the United Kingdom. The highest yielding UK cereal crop in tonnes per hectare, wheat accounts for 67% of the cereal production of the county (DEFRA 2015). Wheat pathogen resistance, therefore, will be an important part of the economic future of the country.

1.3.2. Septoria Leaf Blotch

Septoria leaf blotch (STB) is a foliar disease of wheat, caused by the hemibiotrophic fungal pathogen Zymoseptoria tritici. Wheat is grown worldwide, though STB is most prevalent in temperate climates. In particular, it is considered the most damaging disease of wheat in the UK, where it was found on up to 99% of surveyed plants (CropMonitor 2015). Infection, especially of the flag leaf, leads to chlorosis and necrosis, which diminish the photosynthetic capacity of the plant and, therefore, can reduce the ultimate yield produced by as much as 30-50%. Consequently, European yield losses to STB are an estimated $400 million annually, despite the high prices paid for fungicide treatment, of which approximately 70% is targeted towards Z. tritici (Ponomarenko et al., 2011; HGCA 2012).

The Z. tritici life cycle, as shown in Figure 1.2., begins with the germination of spores on the host leaf surface, usually having been dispersed by wind or rain splashes. These spores produce filamentous hyphae, which penetrate the leaf tissue through stomata. As a result of the stomatal entry system, Z. tritici is dependent on environmental conditions and stomatal opening. It is therefore considered that future Z. tritici control could be heavily influenced by the changing climate (Kema et al., 1996; Orton et al., 2011; Gouche et al., 2013).

Once inside the host tissue, hyphae continue to grow, feeding biotrophically, within the apoplastic space between mesophyll cells. No visible symptoms of infection are seen for an unusually long period, often lasting for 10-14 days (Kema et al., 1996). During this period, Z. tritici displays a greatly reduced set of cell wall degrading enzymes, as shown through analysis of both the genome and predicted secretome, instead possessing extended gene families of peptidases and alpha-amylases, which are suggested to allow the fungus greater access to less detectable apoplastic nutrient sources (Goodwin et al., 2011; Morais do Amaral et al., 2012). In addition to this, Z. tritici is capable of producing defence-supressing effectors, including lysM domain proteins, which prevent chitin recognition. This has lead to the concept of stealth pathogenesis by Z. tritici, evading host defences throughout this bitorophic phase (Goodwin et al., 2011; Marshall et al., 2011)

After this symptomless period, the pathogen switches to a phase of necrotrophic growth, which is associated with large-scale host cell death. This switch involves transcriptional change to thousands of host and pathogen genes, but little else is known of its causes. Some factors that appear to be involved include the PAMP-like recognition of β-1,3-glucans by an unknown receptor, and a host MAPK cascade, which may be hi-jacked by unknown fungal effectors (Keon et al., 2007; Rudd et al., 2008; Hammond-Kosack and Rudd 2008; Shetty et al., 2009; Deller et al., 2011; Yang et al., 2013).

Both asexual and sexual reproduction can occur in bodies produced within these lesions; asexual condiaspores are produced in structures called picnidia, while pseudothecia produce sexual ascospores. Due to its ability to reproduce sexually, with as much as 90% of global genetic variation found within each field, the evolutionary potential of Z. tritici is very high. This is especially the case when provided with selection pressures, such as fungicide or resistant cultivars, which makes the pathogen particularly difficult to control (Kema et al., 1996, Chen and McDonald 1996; Zhan et al., 2003; Dean et al., 2012).

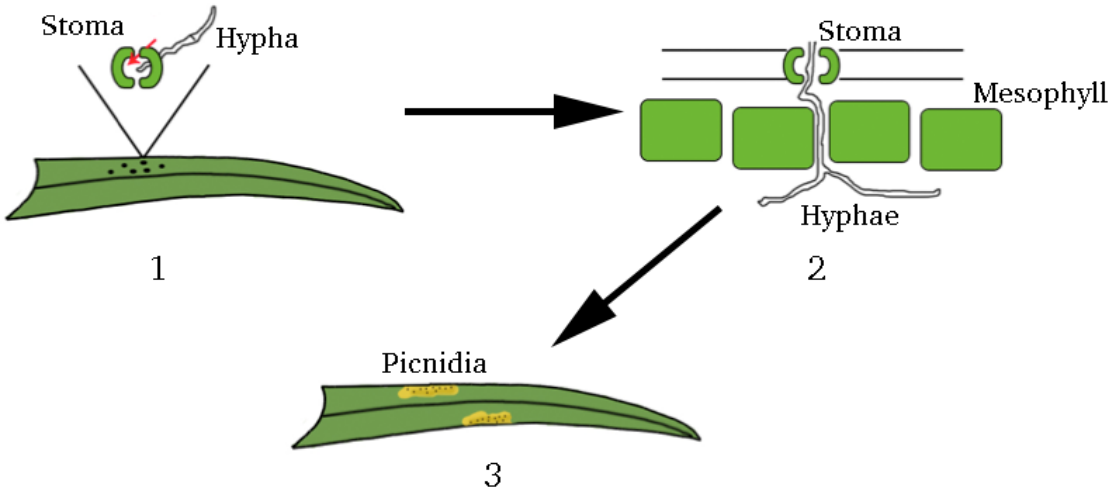

Figure 1.4. Zymoseptoria tritici Lifecycle. 1) Spores dispersed by wind or rain produce hyphae, which penetrate the leaf through the stomata 2) Hyphae spread throughout the mesophyll cells of the leaf, during a symptomless period which can last for two weeks 3) The pathogen switches to its necrotrophic phase and necrotic lesions appear on the leaf surface. Picnidia, in which further spores are produced, appear within these lesions.

While breeding is used to control STB in wheat, only 21 STB resistance genes have been identified, compared to over 50 resistance genes for each of Blumeria graminis and Puccinia striiformis, and most of these are effective against only a very narrow range of pathogen isolates (Mwale et al., 2014; Zhou et al., 2014; Brown et al., 2015). Considering the rapid evolutionary capacity of Z. tritici, this makes control through resistant breeding very challenging.

Instead, Z. tritici, is mainly controlled by application of fungicides, most often of the azole class. However, the fungus has also displayed the ability to develop rapid resistance to intensively used fungicides, and has acquired resistance to a number of azoles. Many strains now show multi-drug resistance having previously developed complete resistance to the strobilurin class of fungicides (Fraajie et al., 2005; Cools et al., 2011; Cools and Fraajie 2014; Omrane et al., 2015).

With these difficulties in disease management of such a devastating pathogen, and a crop disease that will become more and more important with the growth of the population and the unknown effects of climate change, increasing our understanding of the interaction between wheat and Z. tritici will be imperative for the future of global and local food security.

1.4. Post-Translational Modifications in Plant Immunity

1.4.1. Post-Translational Modification

Modifications to the structure of synthesised proteins, often by covalent modification by addition of functional groups to amino acid side-chains, known as post-translational modification (PTM), is a vital cellular process across all kingdoms of life. While phosphorylation is the most commonly seen PTM, many others are widely seen and studied, including acetylation, glycosylation, methylation, ubiquitination and hydroxylation (Karve and Cheema 2011; Khoury et al., 2011).

PTMs can regulate a wide variety of cellular processes, controlling many aspects of protein function, including stability and turnover (Vierstra 2009), cellular localisation (Sadler et al., 2013), enzyme activity (Berg et al., 2002) and altering protein-protein interactions (Karve and Cheema 2011). In plants, many PTMs are involved in

responding to stress, particularly in pathogen defence (Sadanandom et al., 2012; Piquerez et al., 2014). Below, ubiquitination and chromatin remodelling, often brought about through PTMs, will be discussed in relation to their roles in plant immunity.

1.4.2. The Ubiquitin-Proteasome System

Ubiquitination is the addition of a small molecule, ubiquitin (Ub), to free lysines of target proteins, through involvement of E1, E2 and E3 proteins. E1 ubiquitin activation enzymes catalyse the ATP-dependent activation of Ub molecules, forming a thioester bond between the two. This bond is then transferred to an E2 ubiquitin-conjugating enzyme, forming a high-energy intermediate. While there are just two known E1 genes, and less than 50 E2 genes identified in Arabidopsis, the majority of the target specificity of ubiquitination is thought to come from the E3 ubiquitin ligases, of which there are over 1400 known genes, across seven groups, based on their domains (Vierstra 1996; Hatfield et al., 1997; Ciechanover 1998; Vierstra 2009; Sadanandom et al., 2012).

Ub chains can form by addition of further molecules onto Ub lysine residues. The best-established of these is a chain linked at lysine 48, which signals the protein for degradation by the 26S proteasome (Hershko and Ciechanover 1998). While this was the first established and best-known role of ubiquitination, different chain topologies are capable of producing a diverse range of effects (Pickart and Fushman 2004).

In particular, this thesis will later focus on genes containing UBC or RING (Really Interesting New Gene) domains. UBC domains are key to the activity of E2 enzymes. RING domains interact with the E2, and the RING protein can act either independently or within a complex to form a bridge between E2 and substrate, allowing ubiquitination to occur (Sadanandom et al., 2012).

Ubiquitination has regularly been associated with all stages of plant pathogen interactions, from PAMP recognition to HR PCD. The function of the Arabidopsis PRR FLS2, which recognises bacterial flagellin, is attenuated by ubiquitination by the E3 ligases PUTATIVE U-BOX12 and 13 (PUB12 and 13) whereas three other E3 ligases, PUB22, 23 and 24 act as negative regulators of flagellin and chitin-induced PTI (Robatzek et al., 2006; Trujillo et al., 2008; Lu et al., 2011). Meanwhile, three

additional E3 ligases, ACRE74, 189 and 276 act as positive regulators of HR PCD, and are necessary in conferring resistance to Cladosporum fulvum (Gonzalez-Lamonthe et al., 2006; Yang et al., 2006; van den Burg et al., 2008).

As many as 30 E3 ligases show transcriptional responses to chitin recognition in Arabidopsis (Libault et al., 2007), but the role of ubiquitination in immunity is by no means restrained to Arabidopsis pathogen responses. Instead, it has been implicated in a huge range of plant immune responses, such as the wheat-Blumeria graminis, rice-Magnaporthe oryzae and tomato-Phytophthora infestans interactions amongst many others (Ni et al., 2010; Zhang et al., 2012; Liu et al., 2015).

However, due to its central role in plant immune signalling, the ubiquitin system has also emerged as an important target for disruption by pathogen effectors. For example, the M. oryzae effector AvrPiz-t increases host susceptibility through suppression of APIP6, a host E3 ligase, required for ROS production and pathogen induced gene expression on flagellin recognition (Park et al., 2012). Pathogens are also known to produce their own ubiquitin-related effectors to disrupt plant immunity. One such example of this is the previously mentioned P. syringae effector AvrPtoB, which ubiquitinates FLS2 and CERK1, targeting them for degradation and preventing flagellin and chitin sensing (Gohre et al. 2008; Giminez-Ibanez et al. 2009). The role of ubiquitination in plant defence is further summarised in Figure 1.5.

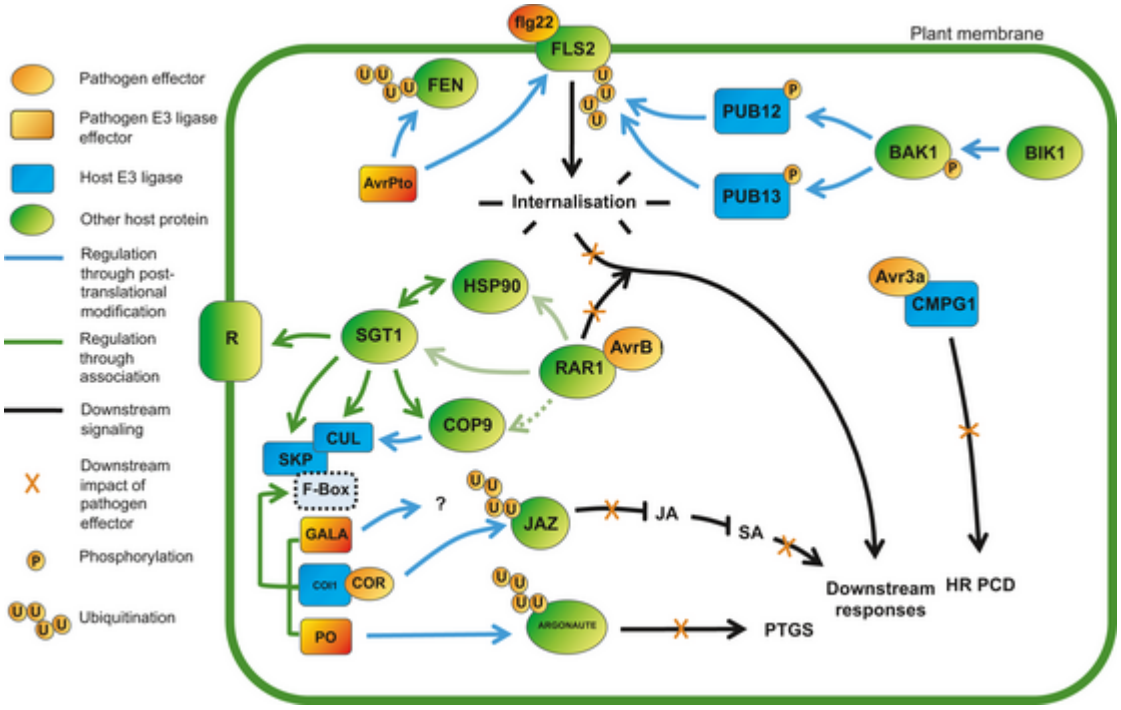

Figure 1.5. Ubiquitination in Plant Defence. Pathogen-associated molecular pattern (PAMP) and effector-triggered immune pathways are targeted by pathogens to overcome host defence responses. FLS2 flagellin perception is targeted by the AvrPto effector with E3 ligase activity. Pathogen encoded F-box motifs are present in GALA and PO effectors which bind to host Skp1-Cullin-F-box (SCF) ubiquitin ligase subunits. SCFPO has been shown to target host component ARGONAUTE to proteasomal degradation blocking post-transcriptional gene silencing of viral factors. Bacterial coronatine mimics active jasmonic acid (JA) and promotes the degradation of the JAZ transcriptional repressors, activating the JA pathway which antagonizes the salicylic acid (SA) mediated systemic acquired resistance (SAR) response. AvrB targets RAR1 blocking PAMP triggered immune responses in susceptible interactions Oomycete effector Avr3a binds to CMPG1 suppressing effector-triggered hypersensitive response programmed cell death. Figure and legend from Sadanandom *et al.*, 2012.

1.4.3. Chromatin Remodelling

Chromatin remodelling is a means of bringing about modifications to the structure and arrangement of nucleosomes in relation to DNA. Such modifications are known to affect the accessibility of the transcriptional machinery to this DNA and consequently, the expression of these genes (Whitehouse et al., 2007; Henikoff 2008). This is achieved through two main functions; the ATP-dependent complexes, which directly alter the nucleosome-DNA interaction or relocate nucleosomes in relation to DNA, and the post-

translational modification of the nucleosome-forming histone proteins, which this section will focus on (Bannister and Kouzarides 2011; Hargreaves and Crabtree 2011).

Histones can be post-translationally modified in a number of ways, the most widely studied of which is acetylation (Allfrey et al., 1964; Kouzarides 2000). Histone Acetyl Transferases (HATs) catalyse the addition of an acetyl group to lysine side-chains of histones. This modification weakens the positive charge of the lysine, and so lessens its binding affinity to DNA. Reduced binding leads to easier access to the DNA, and so increased expression of those genes. In turn, histone deacetylases (HDACs) remove the acetylations, thus compacting the chromatin and supressing transcription (Hong et al. 1993; Yang and Seto 2007; Teif and Rippe 2009; Bannister and Kouzarides 2011).

As mentioned previously, phosphorylation is the most common form of PTM and is unsurprisingly seen on histones. Whilst the roles of the kinases and phosphatases that control the modification seemingly poorly understood, phosphorylation is thought to act similarly to acetylation, with the addition of a significant negative charge (Oki et al., 2007; Bannister and Kouzarides 2011.)

Histone methylation, as with acetylation, is well-established, and while it can modify similar lysines, it is not thought to alter the positive charge and DNA affinity. Nonetheless, histone methylation has been linked with transcriptional regulation (Chen et al., 1999; Rea et al., 2000). Instead, it has been hypothesised to act a ‘code’, which is read by other chromatin modifying or transcription-related proteins (Stahl and Allis 2000).

One example of this is the modifier HETEROCHROMATIN-ASSOCIATED PROTEIN1 (HP1), which is key to repressing transcription through the formation of tightly packed heterochromatin. HP1 binds exclusively to Histone 3, methylated on lysine 9 (H3k9me) (James and Elgin 1986; Bannister et al., 2001; Lachner et al., 2001; Nakayama et al., 2001). Conversely, methylation, and particularly tri-methylation on lysine 4 of the same Histone 3 (H3k4me3), is considered to be a marker of actively transcribed genes. While the mechanism for this is not certain, such a histone modification was seen to correlate with enriched acetylation (Stahl et al., 1999; Bernstein et al., 2002; Santos-Rosa et al., 2002).

Histones can be modified in many other ways, including the aforementioned ubiquitin system. However, rather than proteasomal, which is degradation most often seen with ubiquitination, this modification appears to act by altering the action of the histones (Wang et al., 2004; Kim et al., 2009). The Small Ubiquitin-like Modifier (SUMO) also acts as a histone modifier, although usually by preventing other modifications, such as acetylation, to the same side chain (Shiio and Eisenman 2003; Nathan et al., 2006).

Much like the ubiquitin system, both of these methods of chromatin remodelling; ATP-dependent and histone-modifying, and in particular HDACs, have shown to be associated with the plant immune response (Zhou et al., 2005; Kim et al., 2008; Walley et al., 2008; Wang et al., 2010). While these responses are more likely a direct interaction affecting transcriptional access, WRKY70 mediated pathogen defence requires H3k4 methylation by ARABIDOPSIS TRITHORAX-LIKE1 (ATX1) (Alvarez-Venegas et al., 2007).

However, much like many other important aspects of plant immune responses, chromatin remodelling is targeted for disruption by pathogens. This includes the crop pathogens Altenaria brassicicola and Cochliobolus carbonum, which produce toxins to specifically inhibit HDAC function, presumably to disrupt the transcription of pathogen associated genes (Privalsky 1998; Walton 2006).

In particular, this thesis will focus on the role of PHD (Plant Homeodomain) domain containing proteins, and their role in histone modification. PHD domains are zinc finger domains, which are conserved across eukaryotes (Aasland et al. 1995). They were initially classified due to their homology to the Arabidopsis PHD domain protein HISTONE ACETYL TRANSFERASE3 (HAT3) to HOMEOBOX1a (HOX1a), a maize homeodomain protein, and are often characterised by a conserved, regularly spaced motif of eight cysteine/histidine residues involved in zinc binding (Schindler et al. 1993). In this way it is very structurally similar to the RING E3 ligase domain (Bienz 2006). However, despite some suggestion that they may act similarly, there is no evidence that PHD domains act as ubiquitin ligases (Scheel and Hoffman 2003).

A study to identify predicted PHD domain proteins in Arabidopsis (Lee et al. 2009) found that many had a high NucPred score. NucPred (Brameier et al. 2007) is sequence-analysis software, predicting the nuclear localisation of proteins, suggesting the proteins

would localise to the nucleus. Many of these same sequences were also found on ChromDB (ChromDB, http://www. chromdb.org/) a chromatin database, listing proteins predicted to be involved in chromatin regulation.

PHD domain proteins are regularly associated with protein-protein interactions in the nucleus (Bienz 2006) and, in particular, have often been shown to bind to Histone 3 specifically modified by di- or trimethylation on lysine 4 (H3k4me3) (Shi et al. 2006; Taverna et al. 2006; Wysocka et al. 2006; Lee et al. 2009), through a conserved sequence of residues predicted to form an aromatic cage important in target binding (Lee et al. 2009). Disruption of this cage prevents binding. However, binding to otherwise modified Histone 3 (Mansfield et al. 2011), or other targets such as phosphatidylinositol phosphates (Gozani et al. 2003) has also been shown.

As a result of this histone binding capacity, PHD domains have been linked with maintenance of chromatin structure or chromatin remodelling (Bochar et al. 2000; Gaetani et al. 2012). In fact, in many cases it has been seen that PHD domains bring about changes to histone or chromatin structure through interactions with other proteins or complexes (De Lucia et al. 2008; Molitor et al. 2014). With the ability of the PHD domain to bind to specific methylations, it can be assumed that its most likely role is to target the complex by 'reading' modification markers (Mellor 2003). A group of proteins called INHIBITOR OF GROWTH (ING) domain proteins, which contain PHD domains only, are important factors in histone acetylation and deacetylation by chromatin remodelling complexes (Soliman and Riabowol 2007).

This often results in transcriptional changes (Shi et al. 2006; Taverna et al. 2006; Wysocka et al. 2006) and PHD domain proteins are generally associated with bringing about changes to transcription (Wilson et al., 2001). Therefore, a PHD domain linked to pathogen defence could play a role in the large-scale host transcriptional changes seen on Z. tritici infection of wheat (Rudd et al. 2015).

However, Lee et al. (2009) also discovered a large number of Arabidopsis proteins, which, despite containing a PHD domain, did not bind to the histone modification marker that many others did. Included amongst these was a protein called ALFIN1-LIKE3 (AL3), with strong homology to six other Alfin1-like proteins, which were all proven or predicted to bind to this sequence. Further to this, these proteins were

identified by homology to ALFIN1 of Alfalfa (Medicago sativa), which contains a canonical PHD domain, but has displayed a DNA binding-function, rather than protein binding, and has been theorised to be a transcription factor or transcription co-activator (Bastola et al. 1998; Winicov and Bastola 1999; Winicov 2000). Similarly, AL5, predicted to bind H3k4me3, is a positive regulator of plant abiotic stress through direct interaction with promoter regions, suppressing negative stress regulators (Wei et al., 2015).

While there are a large number of possible interactors for a PHD domain in complex, and a very large number of potential downstream targets, it was noted that many PHD domain proteins linked with chromatin remodelling achieved this through an association with Histone Acetyl Transferase (HAT) or Histone DeACetylase (HDAC) proteins (Schindler et al, 1993; Shi et al., 2006; Taverna et al., 2006; Li et al., 2007.), which add and remove acetylations from histones respectively.

1.5. Virus-Induced Gene Silencing

In order to study the involvement of these processes in the interaction between wheat and Z. tritici, a system called VIGS will be used to create plant transiently silenced for specifically targeted genes. Any possible role of these genes in the interaction can then be ascertained by infection of these plants and comparison of the infection with that seen in wild type plants.

VIGS is based on the principle of post-transcriptional gene silencing in the plant in response to the recognition of viral infection. Upon detection of viral double-stranded RNA (dsRNA), Dicer-like proteins, small family of multi-domain ribonucleases found in plants (Liu et al. 2009) process this dsRNA into small interfering RNA (siRNA) of around 21 nucleotides in length. siRNAs are then used to target the RNA-induced silencing complex (RISC) onto viral mRNA, which it subsequently degrades (Baulcombe 2004). Inserting fragments of sequence from a plant gene of interest into a viral vector, and infecting the plant with this virus, will then lead to not only silencing of the viral genes, but also the plant gene from which the fragments were taken.

Initial experiments in VIGS were carried out Nicotiana benthamiana using Tobacco Mosaic Virus (Kumagai et al. 1995) and Potato Virus X (Ruiz et al. 1998) to silence the carotenoid biosynthesis gene PHYTOENE DESATURASE (PDS). Silencing PDS disrupts the production of carotenoid pigments, which protect the plant from photo-bleaching. As a result, PDS silenced plants show a distinct white leaf phenotype. Since this initial work, many other viruses have been employed, most notably the Tobacco rattle virus (Ratcliff et al. 2001), which has been shown to silence multiple plant species, including Solanum lycopersicum (Liu et al. 2002), Solanum tuberosum (Brigneti et al. 2004) and Arabidopsis thaliana (Burch-Smith et al. 2006).

For silencing in wheat, this project will utilise the Barley Stripe Mosaic Virus (BSMV), a tripartite RNA virus of the Hordevirus genus (Palomar et al 1977). The genome consists of RNAα, encoding the methyltransferase/helicase subunit of the RNA-dependent RNA polymerase (RdRp) (Jackson et al. 2009), RNAβ, encoding the coat protein and three essential movement proteins (Jackson et al. 2009) and RNAγ encoding the polymerase subunit of the RdRp and the γb protein, which has multiple functions involved in pathogenicity, movement and suppression of silencing defences (Donald and Jackson 1994; Bragg and Jackson 2004; Jackson et al. 2009). Though it's primary host its barley, it has been found naturally in other cereals (Najar et al. 2000).

BSMV was adapted for use in VIGS, initially in Barley (Holzburg et al. 2002) and later for Wheat (Scofield et al. 2005). A high-throughput method was developed (Yuan et al. 2011), in which individual α, β and γ cDNA vectors were produced with the double 35S promoter of Tobacco ringspot virus. A ligation-independent cloning site was also added to the BSMVγ vector, to allow silencing fragments to be cloned into the vector more easily. The vectors used are summarised in Figure 1.6. A system of infection using Agrobacterium tumefaciens was also developed. Using this system, in 2011 Yuan et al. were able to reproduce the white leaf phenotype of effective PDS silencing, and also analyse the role of TaPMR5 in resistance to powdery mildew (Blumeria graminis). As a result, we will use this high-throughput system to screen a number of target genes for their involvement in the interaction with Z. tritici.

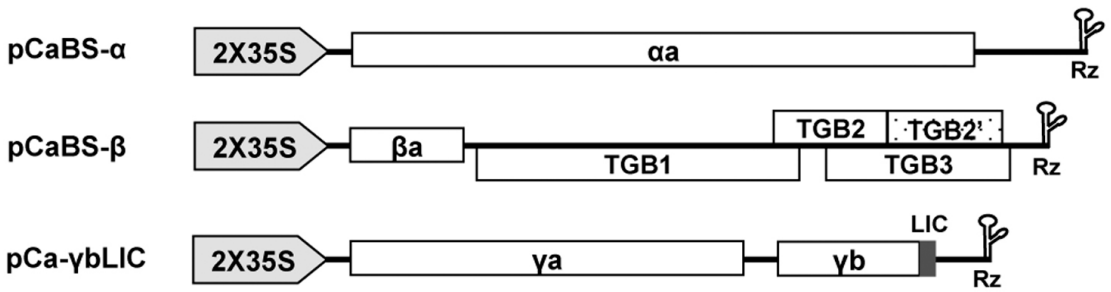

Figure 1.6. BSMV Vector Map. A map of the BSMV vectors used for VIGS in this study, showing the α, β and γ vectors. The γ vector contains the shown LIC cloning site, with which targets genes are incorporated into the vector. Adapted from Yuan et al., 2011.

1.6. Study Objectives

Many of the underlying processes involved in plant innate immunity in general are well understood, but how these relate specifically to the wheat Z. tritici is in most cases still unknown. In particular, the ubiquitin system, and other post-translational modifications have often been implicated in plant defence, yet nothing at all is known about their involvement here. As a consequence, this project will aim to identify components of these systems involved in the plant defence response.

In order to do so, the VIGS system previously outlined will be used. Firstly, as in many previous VIGS projects, PDS silencing will be attempted first, with the visible phenotype of PDS silencing used as a positive control for a functional system.

Once this has been established, a list of target genes, identified as potentially linked to the ubiquitin system and to the wheat Z. tritici interaction will be silenced. Plants silenced for these genes will then be infected and compared to the wild type, to examine any involvement of these genes in this plant-pathogen interaction.

Once genes involved in the interaction have been found, their function within the immune response will be examined. In vitro and in vivo protein-protein assays will be used to identify possible targets or interactors, while qPCR will be used to both verify effective gene silencing and to examine how transcription of these genes is affected during infection.

Chapter 2

Materials and Methods

2.1. Materials

2.1.1. Chemicals

Unless otherwise stated, all chemicals were purchased from Sigma-Aldrich (St. Louis, USA).

2.1.2. Vectors

Table 2.1. List of vectors used

Name	Resistance	Use	Supplier
pENTR D-TOPO	Kan	Gateway entry vector	Life Technologies
pDEST 15	Amp	N-terminal GST tag E. coli expression	Life Technologies
pDEST 17	Amp	N-terminal HIS tag E. coli expression	Life Technologies
pEarleygate 104	Kan	N-terminal YFP tag plant expression	Earley *et al.,* 2006
pEarleygate 201	Kan	N-terminal HA tag plant expression	Earley *et al.,* 2006
pK7WGR2	Kan	N-terminal RFP tag plant expression	Karimi *et al*., 2005
BSMVα	Kan	Virus Induced Gene Silencing	Yuan *et al*., 2011
BSMVβ	Kan	Virus Induced Gene Silencing	Yuan *et al*., 2011
BSMVγ	Kan	Virus Induced Gene Silencing	Yuan *et al*., 2011

2.1.3. Bacterial and Fungal Strains

Table 2.2. List of Bacterial and Fungal Strains

Organism	Strain	Resistance	Use	Supplier
E. coli	DH5α	n/a	Plasmid maintenance and propagation	Fisher
E. coli	BL21	n/a	Protein expression	Fisher
Agrobacterium tumafaciens	GV3101:pMP90	Rif, gent	Plant transient transformation	Koncz and Schell 1986
Zymoseptoria tritici	IPO323	n/a	Plant infection	Koncz and Schell 1986

2.1.4. Plants

The wheat used in this work was Avalon variety, provided by Rothamsted Research and Fielder variety, provided by the National Institute of Agricultural Biology (NIAB, Cambridge UK). Transgenic wheat was Fielder variety, provided by NIAB. *Nicotiana benthamina* plants were supplied internally by Durham University.

2.2. RNA Extraction

Leaf tissue was frozen in liquid nitrogen on collection. 75 mg tissue was ground to a powder and 750 µl of trizol (Zymo Research, Irvine, USA) added and mixed in a vortex (Vortex-Genie 2, Scientific Industries). This mixture was centrifuged (Eppendorf 5417R Microcentrifuge) at 15,000 *g* for 10 minutes at 4 °C. RNA was extracted using Direct-zol™ RNA miniprep kit (Zymo Research) including the in-column DNase I digestion and eluted in 30 µl DNase/RNase-free water. RNA concentration was measured by Nanodrop spectrophotometer (Nanodrop ND-1000 Labtech, Uckfield, England) and stored at -80 °C.

2.3. cDNA Synthesis

Where possible, 2 µg total RNA was brought up to a total volume of 10 µl with water. If RNA was too dilute to permit this, all samples within an individual experiment would be standardised to the concentration of the weakest sample. 1 µl 10 mM oligo dT (VWR,

Radnor, USA) was added to the RNA mixture, heated at 65 °C for 5 minutes and placed on ice. 8 μl containing 1x first strand buffer (Invitrogen, Grand Island, USA), 25 μM DTT (Invitrogen), 2 mM dNTPs (0.5 mM each) (VWR) and 12.5% RNase OUT Ribonuclease Inhibitor (Invitrogen) was added. This was heated to 42 °C for 2 minutes, 1 μl Superscript II Reverse Transcriptase (Invitrogen) added and then heated at 42 °C for 50 minutes then 70 °C for 15 minutes. The cDNA was stored at -20 °C.

2.4. Polymerase Chain Reaction (PCR)

2.4.1 Primers

Information on all primers used is listed in the appendix. All primers were ordered from Eurofins (Luxembourg) and used at a concentration of 10 pmol/ml.

2.4.2. Taq Polymerase PCR

20 μl PCR reactions at a final concentration of 1x ReddyMix (containing 0.625 units ThermoPrime Taq DNA polymerase) (Thermo Scientific), 5 mM forward primer, 5 mM reverse primer, 5 mM template cDNA in sterile distilled water were run in a heat cycler (TC-3000G Techne machine) using a variation of the following standard conditions:

95 °C for 5 minutes, then 30 cycles of 95 °C 15 seconds, annealing temperature* for 30 seconds, 72 °C 1 minute per 1 kb of expected product, followed by 5 minutes at 72 °C.

*Annealing temperature depended on melting temperature of primers. New primers were tested by a gradient PCR with a range of annealing temperatures.

The PCR products were run on an agarose gel (see 2.5 Gel Electrophoresis) to see the results.

2.4.3. Q5 Polymerase Proof-Reading PCR

50 μl PCR reactions at a final concentration of 1x Q5 reaction buffer (NEB, Ipswich, USA), 200 μM dNTPs (50 μM each), 5 mM forward primer, 5 mM reverse primer, 5 mM template cDNA, 1 unit Q5 high-fidelity DNA polymerase (NEB) in sterile distilled water

were run in a heat cycler (TC-3000G Techne machine) using a variation of the following standard conditions:

98 °C for 2 minutes, then 30 cycles of 98 °C 15 seconds, annealing temperature* for 30 seconds, 72 °C 30 seconds per 1 kb of expected product, followed by 5 minutes at 72 °C.

*Annealing temperature depended on melting temperature of primers.

5 µl 10x DNA loading dye was added to PCR products, which were run on an agarose gel (see 2.5 Gel Electrophoresis) to see the results.

2.4.4. Colony PCR

Colony PCR used the same conditions as in Taq polymerase PCR. However, instead of cDNA, individual colonies were picked and suspended in 20 µl sterile distilled water. 1 µl of this was used in each reaction.

2.4.5. Site-Directed Mutagenesis

50 µl PCR reactions at a final concentration of 1x Q5 reaction buffer, 200 µM dNTPs (50 µM each), 5 mM forward primer, 5 mM reverse primer, 3 mM plasmid DNA, 1 unit Q5 high-fidelity DNA polymerase (NEB) in sterile distilled water were run in a heat cycler (TC-3000G Techne machine) using a variation of the following standard conditions:

98 °C for 2 minutes, then 18 cycles of 98 °C 15 seconds, annealing temperature* for 30 seconds, 72 °C 30 seconds per 1 kb of expected product, followed by 5 minutes at 72 °C.

*Annealing temperature depended on melting temperature of primers.

DNA template was then digested by addition of 1.25 µl DpnI (NEB) directly to PCR product and incubated at 37 °C for 2 hours. The enzyme was then deactivated by heating at 80 °C for 20 minutes and the DNA was transformed into competent DH5α *E. coli* cells (see 2.8. Transformation).

2.4.6. Quantitative Real Time PCR (qPCR)

20 μl reactions at a final concentration of 1x SYBR Green JumpStart Taq ReadyMix (Sigma), 5 mM forward primer, 5 mM reverse primer, 5 mM template cDNA, 2.5% ROX reference dye in sterile distilled water were run in a StepOnePlus Real-Time PCR System (Applied Biosystems) using a variation of the following standard conditions:

95 °C for 20 seconds, then 40 cycles of 95 °C for 3 seconds and annealing temperature* 30 seconds.

*Annealing temperature depended on melting temperature of primers.

3 technical replicates were used for each sample and were normalised against a reference gene and compared using the $\Delta\Delta C_T$ method (http://www6.appliedbiosystems.com/support/tutorials/pdf/performing_rq_gene_exp_rtpcr.pdf).

2.5. Gel Electrophoresis

Gels between 0.8-1.2% agarose (Melford, Ipswich, UK) were made, depending on the size of the product to be visualised, using 1x TAE buffer (OmegaBio-Tek, Norcross, USA), with a final concentration of 0.5 μg/ml ethidium bromide (Fischer Scientific, Waltham, USA). Electrophoresis was carried out at 80-100 V in a tank of 1x TAE. 10 μl of each sample were run, along with 5 μl of either 50 bp or 1 kb hyperladder (Bioline). DNA was visualized under UV using a Gene Flash machine and Quantity One software.

2.6. Gel Extraction

DNA was extracted from excised bands of gel (from 2.5. Gel Electrophoresis), using the **QI**Aquick gel extraction kit (Qiagen, Limburg, Netherlands) and eluted into 30 μl sterile distilled water.

2.7. Cloning

2.7.1. Gateway Cloning

1 µl pENTR/D-TOPO entry vector (Invitrogen) was added to 5 µl of PCR product (produced via 2.4.3 Q5 polymerase proof reading PCR, 2.5 Gel Electrophoresis and 2.6. Gel Extraction), mixed and incubated at room temperature for 30 minutes before transformation into competent DH5α *Escherichia coli* cells (see 2.8. Transformation).

2.7.2. Destination Vector Recombination

0.5 µl donor vector (50-150 ng), 0.5 µl destination vector (150 ng) and 6 µl TE buffer pH 8 were mixed and 0.5 µl LR Clonase II Enzyme (Invitrogen) was added, before incubating at 25 °C for 1 hour. 0.5 µl of Proteinase K Solution (Invitrogen) was added to stop the reaction by incubating at 37 °C for 10 minutes. The product was transformed into competent DH5α *E. coli* cells (see 2.8. Transformation).

If the donor and destination vector shared the same antibiotic resistance, the donor was pre-digested by incubation for 1 hour at 37 °C in a 25 µl mixture including 2.5 µl 10 CutSmart Buffer (NEB), 0.5 µl PVUII-HF enzyme (NEB) 5 µl donor vector (up to 500 ng) and 17 µl sterile distilled water. This product was then extracted before use (2.5. Gel Electrophoresis and 2.6. Gel Extraction).

2.7.3. Ligation-Independent Cloning (LIC)

PCR products were cloned into the LIC site of the BSMVγ vector.

BSMVγ was first digested with ApaI (Promega, Madison, USA) by incubating a 20 µl mixture at a final concentration of 1x Buffer A (Promega), 0.1x acetylated BSA (Promega), 50 µg/ml BSMVγ, 2.5% ApaI in sterile distilled water at 37 °C for 4 hours and then 65 °C for 15 minutes.

4 µl of this mixture was then added to 16 µl of a reaction mixture to create a 20 µl mixture (Mix A) at a final concentration of 5 mM dTTP, 0.1x BSA, 1x T4 buffer (NEB), 2% T4 DNA Polymerase (NEB) in sterile distilled water.

Simultaneously, a 10 μl reaction (Mix B) was made to a final concentration of 5% PCR product, 5 mM dATP, 0.1x BSA, 1x T4 buffer (NEB), 2% T4 DNA Polymerase (NEB) in sterile distilled water.

Both mix A and mix B were incubated at room temperature for 30 minutes and then 75 °C for 15 minutes. 2 μl of mix A was then added to mix B and incubated at 65 °C for 2 minutes then room temperature for 10 minutes, before transforming into competent DH5α *E. coli* cells (see 2.8. Transformation).

2.8. Transformation

2.8.1. Competent *E. coli* Production

Bacteria were streaked onto a LB plate with no antibiotic and incubated overnight at 37 °C. 10ml of liquid medium was then inoculated with a single colony and grown overnight at 37 °C with shaking. This was then added to 250ml LB, which was grown at 18 °C with shaking, until an OD600 of 0.6 was reached. The liquid medium was then cooled on ice and centrifuged at 2000 g and 4 °C for 10 minutes. The pellet was resuspended in 80 ml ice-cold TB buffer (10mM PIPES pH 6.7, 55mM $MgCl_2$, 15mM $CaCl_2$, 250mM KCl) and incubated on ice for 10 minutes. The cells were centrifuged as before and then resuspended in 20 ml TB and 1.5 ml DMSO was added. 100 μl aliquots were frozen at -80°C for later use.

2.8.2. *E. coli* Transformation

Two different strains of *E.coli* were used; DH5α, for storage and production of plasmid DNA, and BL21, for protein expression. The same transformation protocol was used for both.

100 μl of chemically competent cells were thawed on ice before the addition of 2 μl of vector. The cells were then heat shocked at 42 °C for 30 seconds before returning to ice. 800 ml of S.O.C. medium (Super Optimal broth with Catabolite repression) was added and incubated with shaking at 37 °C for 1 hour. The cells were then spread onto LB agar plates containing the appropriate antibiotic for the vector and left overnight to incubate at 37 °C.

For long-term storage, single colonies were taken from plates and suspended in 10 ml liquid LB (Melford) media with appropriate antibiotics (Melford) and grown overnight at 37 °C with shaking. After growth, 0.375 ml 60% glycerol (Fisher) was added to 1.125 ml liquid culture, mixed by vortex and frozen in liquid nitrogen. Glycerol stocks were kept at -80 °C.

2.8.2. Competent Agrobacterium Production

Bacteria were streaked onto a LB plate with Rifampicin and Gentamicin at 28 °C for 48 hours. 10ml of liquid medium was then inoculated with a single colony and incubated at 28 °C with shaking for 24 hours. This was then added to 250ml LB, which was grown at 18 °C with shaking for 18 hours. The liquid medium was then cooled on ice and centrifuged at 2000 g and 4 °C for 10 minutes. The pellet was resuspended in 20 ml ice-cold TE buffer (10mM Tris pH 8, 1mM EDTA) and incubated on ice for 10 minutes. The cells were centrifuged as before and then resuspended in 20 ml ice-cold liquid LB. 100 μl aliquots were frozen at -80°C for later use.

2.8.2. Agrobacterium Transformation

The agrobacterium strains GV3:101, PMP90 was used for all transformations.

200 ml of chemically competent cells were thawed on ice before the addition of 2 μl of vector. This was then incubated for 5 minutes on ice, liquid nitrogen for 5 minutes and then 37 °C for 5 minutes. To this mixture 800 ml of LB was added before being incubated for 2 hours at 28 °C with shaking. The cells were then spread out onto LB agar plates containing the appropriate antibiotic for the vector, as well as 25 μg/ml rifampicin and 25 μg/ml gentamycin, and left to incubate for 48 hours at 28 °C.

For long-term storage, single colonies were taken from plates and suspended in 10 ml liquid LB media with appropriate antibiotics and grown overnight at 28 °C with shaking. After growth, 0.375 ml 60% glycerol (Fisher) was added to 1.125 ml liquid culture, mixed by vortex and frozen in liquid nitrogen. Glycerol stocks were kept at -80 °C.

2.9. Plasmid Purification

E. coli with the desired plasmid was grown overnight at 37 °C with shaking in 10 ml of LB with appropriate antibiotic, then centrifuged for 10 minutes at 2000 g and the supernatant removed. The plasmid was then isolated using QIAprep Spin Miniprep kit (Qiagen) eluting in 30 ml of DNase free water and stored at -20 °C.

2.10 Protein Analysis

2.10.1. SDS PAGE

Acrylamide gels for electrophoresis were cast and run using the Min-Protean Tetra Cell system (Bio-Rad, Hercules, USA). Stacking gels were prepared as 5% acrylamide, 0.125 M Tris pH 6.8, 0.1% SDS, 0.1% ammonium persulphate and 0.01% TEMED. Resolving gels ranged from 10-15% acrylamide, depending on expected protein size, and were 0.375 M Tris pH 8.8, 0.1% SDS, 0.1% ammonium persulphate and 0.04% TEMED.

All samples were diluted 3:1 before running with 4x SDS PAGE loading buffer (40% glycerol, 8% SDS, 200 mM Tris pH 6.8, 0.1% bromophenol blue, 1% beta-mercaptoethanol).

Electrophoresis was carried out at 80-100V in a tank containing 1x Running Buffer (25 mM Tris, 192 mM glycine, 0.1% SDS).

2.10.2. Coomassie Blue Staining

Gels were stained for 20 minutes in Coomassie Blue Stain (0.25% Brilliant Blue, 50% methanol, 10% glacial acetic acid) and destained for an hour in Destain (10% methanol, 10% glacial acetic acid).

2.10.3. Western Blotting

Proteins for Western Blotting were first transferred from the gel onto Porablot PVDF membrane (Fisher) using the Mini-Protean Tetra Cell System. Transfer was carried out overnight at 20V in transfer buffer (25 mM Tris, 192 mM glycine, 10% methanol) at 4 °C.

Conditions for probing varied greatly depending on the combination of antibodies used and the protein being probed for. However, the standard protocol, from which they were all adapted, is shown below. All blocking, probing and washing was carried out in 1x TBST (50 mM Tris pH 7.4, 150 mM NaCl, 0.1% TWEEN 20) with gentle shaking:

5% milk for 1 hour

1:10,000 primary antibody (abcam) for 2 hours

Wash with 1x TBST for 5 minutes (x3)

1:20,000 secondary antibody (abcam) for 1 hour

Wash with 1 x TBST for 10 minutes (x5)

After probing, ECL solution 1 (2.5 mM luminol, 0.4 mM p-coumaric acid, 100 mM Tris pH 8.5) and 2 (0.02% hydrogen peroxide, 100 mM Tris pH 8.5) were mixed 1:1 and added to the membrane. This was incubated for 1 minute before visualising by exposing it to a Fujifilm X-ray film (Fisher).

2.11. Protein Expression

All constructs to be expressed as protein were transformed into *E. coli* strain BL21 (2.8. Transformation). 10 ml cultures were grown overnight in liquid LB medium with appropriate antibiotics at 37 °C with shaking. 0.5 ml of this culture was added to 50 ml fresh LB medium with appropriate antibiotics and grown at 37 °C with shaking. The optical density at a wavelength of 600 nm (OD600) of the culture was checked regularly using a GeneQuant 1300 Spectrophotometer (GE Healthcare). Once the OD600 reached 0.6, two pre-induction samples were taken and IPTG (Fisher Scientific) was added to a final concentration of 1 mM. Post induction samples were then taken at regular time points. Before each sample, the OD600 was measured, and the volume sampled reduced, so that the same number of cells could be expected to be in each sample.

All samples were centrifuged for 2 minutes at 12,000 *g*. For each time point, 1 sample was taken as the total protein extract, and the pellet was resuspended in 60 μl water

and 20 μl 4x SDS PAGE loading buffer (see 2.10.1. SDS PAGE). The second sample was resuspended in 60 μl BugBuster (Novagen, Billerica, USA) and left to shake for 15 minutes. This was again centrifuged for 2 minutes at 12,000 *g*. The supernatant was kept decanted to a new tube, as the soluble protein fraction, and 20 μl 4x SDS PAGE loading buffer added. The pellet was kept as the insoluble fraction, and resuspended in 60 μl water and 4x SDS PAGE loading buffer. All samples were heated to 95 °C for 5 minutes before long-term storage at -20 °C or immediate analysis (2.10.) to determine if expression was successful.

2.12 Protein Purification

Once a construct was proven to express the correct sized protein (2.11. Protein Expression and 2.10. Protein Analysis) protein expression was repeated (as in 2.11.) with a larger volume of culture. The final volume from this was centrifuged for 10 minutes at 2000 *g*. As all proteins to be purified were shown to be expressed in the soluble fraction, the pellet was then resuspended in BugBuster (5 ml/g of pellet), with 1 tablet of cOmplete™ Mini EDTA-Free Protease Inhibitor Tablets (Roche, Indianapolis, USA) and incubated for 20 minutes. Protein was then purified with His-Bind Resin (Novagen) using the following procedure:

200 μl His-Bind slurry was added to a microcentrifuge tube and centrifuged for 1 minute at 500 *g* and the supernatant removed. The remaining pellet was then washed twice with 200 μl sterile distilled water, 3 times with 200 μl Charge Buffer (50 mM $NiSO_4$) and twice with 200 μl Binding Buffer (5 mM imidazole, 0.5 M NaCl, 20 mM Tris-HCl pH 7.9) to charge and equilibrate the resin. 1 ml of cell extract was then added and incubated, rocking, for 10 minutes, then centrifuged as before and the supernatant discarded. This was repeated until all extract was used. The resin was then washed 3 times with 300 μl Binding Buffer and twice with 300 μl Wash Buffer (60 mM imidazole, 0.5 M NaCl, 20 mM Tris-HCl pH 7.9). Protein was then eluted twice by mixing the resin with 300 μl Elute Buffer (1 M imidazole, 0.5M NaCl, 20 mM Tris-HCl pH 7.9), centrifuging and collecting the supernatant.

2.13. *In Vitro* Histone Binding Assay

Lyophilised histone peptide-biotin conjugates were purchased (Merck-Millipore, Darmstadt, Germany): Histone 3 (H3), Histone 3 monomethylated on lysine 4 (H3k4me1), Histone 3 dimethylated on lysine 4 (H3k4me2), Histone 3 trimethylated on lysine 4 (H3k4me3) and Histone 3 trimethylated on lysine 27. These were dissolved at 0.5 mg/ml in Histone Binding Buffer (HBB) (50 mM Tris pH 7.5, 300 mM NaCl, 1 mM PMSF, 0.1% IGEPAL. Purified GST-tagged protein (2.12.) was diluted to 0.5 mg/ml for use in the assay.

10 μl of purified protein was added to 20 μl of each histone peptide, plus a control containing only HBB. 10 μl of GST protein (0.5 ml/ml) was then added to a separate set of peptides. 970 μl of HBB was added to each, and they were incubated overnight, rocking end over end at 4 °C.

Streptavidin beads (Millipore) were then prepared for the assay from a 50% slurry by centrifuging at 1 °C for 30 seconds at 500 *g*, removing the supernatant and washing with 500 μl HBB 3 times. After the final wash the beads were resuspended in another 500 μl HBB.

60 μl of the resulting bead mixture was then added to each overnight incubation and incubated at 4 °C with end over end rocking for 1 hour. After this, all reactions were centrifuged at 1 °C for 30 seconds at 500 *g* and the supernatant removed. These were then washed with 500 μl of HBB 8 times. After the final wash the 90 μl HBB was added to the 60 μl of beads. 50 μl 4x SDS PAGE loading buffer was added and the assay analysed by SDS PAGE (10.10.).

2.14. Antibody Purification

Anti-TaR1 antibody was purified using the Immuno-Link Plus Immobilization Kit (Thermo Scientific), using the following protocol:

Firstly the TaR1 column was prepared by suspending Amino-Link Plus resin in a column with 2 ml pH 7.2 Coupling Buffer (0.1 M phosphate, 0.15 M NaCl, pH 7.2) and the liquid allowed to run through by gravity. A further 2 ml pH 7.2 Coupling Buffer was

added and mixed, then allowed to run through. 3 ml purified His-TaR1 at 1 ml/ml in pH 7.2 Coupling Buffer with a final concentration of 50 mM $NaCNBH_3$ was added to the resin and mixed end-over-end overnight at 4 °C.

The liquid was then again allowed to flow through and the resin washed twice with 2 ml Quenching Buffer (1 M Tris-HCl 0.05% NaN3, pH 7.4). 2 ml Quenching Buffer with NaCNBH3 added to a final concentration of 50 mM was then added to the resin and incubated for 30 minutes end-over-end. This was again allowed to run through and the resin washed five times with 2 ml Wash Solution (1 M NaCl, 0.05% NaN3). The column was then equilibrated with 6 ml Phosphate Buffered Saline (PBS).

Meanwhile a concentrated antibody solution was prepared by adding 6.67 ml saturated ammonium sulphate solution to 20 ml anti-TaR1 and incubating on ice for two hours, then centrifuging for 30 minutes at 4000 *g* at at 4 °C. The supernatant was removed and the remaining pellet resuspended in in 4 ml PBS.

2 ml of the concentrated antibody solution was added to the column resin and incubated end-over-end at room temperature for 1 hour, then allowed to flow through. This was then repeated with the remaining antibody solution. The column was then washed 5 times with 2 ml PBS.

2 ml Elution Buffer (0.1 M glycine pH 3) was added to the resin to elute into 1 ml fractions, to which 100 μl Neutralization Buffer (1 M Tris-HCl pH 8.5) was added. This was repeated twice, producing six fractions, to be analysed by western blotting (2.10.3.)

2.15. Plant Growth Conditions

Nicotiana benthamiana plants were grown in environmentally controlled cabinets at 24 °C with 16 hour light and 8 hour dark cycles. *Triticum aestivum* cv. Avalon and Fielder plants were grown in an environmentally controlled room at 20 °C with 16hr light and 8 hr dark cycles. However, in order to aid viral growth for VIGS, the growth temperature was increased to 24 °C. All samples for RNA (2.2.) and protein extraction (2.17) were collected 8 hours into the 16-hour light cycle.

2.16. Agrobacterium Infiltration

Agrobacterium was grown overnight at 28 °C with shaking in 10 ml liquid LB with rifampicin, gentamycin and the appropriate antibiotic for the construct. This culture was then centrifuged at 2000 *g* for 10 minutes. The resulting pellet was resuspended in 10 mM $MgCl_2$ to an OD600 of 0.2*. Acetosyringone (39 mg/ml in DMSO) was added 1:1000 and incubated for 3 hours. The underside of a *N. benthamiana* leaf was then infiltrated with this mixture with a 1 ml syringe (Fisher Scientific).

*Where 2 constructs were co-infiltrated, both agrobacterium lines were diluted to OD600 0.4 and mixed 1:1.

2.17. Plant Total Protein Extraction

Plant material was collected, frozen in liquid nitrogen, and then ground to a fine powder in pestle and mortar. 100 mg of powder was transferred to a micro-centrifuge tube with 1 ml chilled protein extraction buffer (50 mM Tris-HCl pH 8, 100 mM NaCl, 5 mM EDTA, 10 mM Dithreothritol (DTT), 5% glycerol, 0,1% Triton X-100, with one cOmplete Mini EDTA-Free Protease Inhibitor Tablets (Roche) per 10 ml) and vortexed until homogenous. The resulting mixture was centrifuged at 4 °C for 10 minutes at 12000 *g*. The supernatant was transferred to a new tube and mixed in a 3:1 ratio with 4x SDS PAGE loading buffer, before freezing or analysing by SDS PAGE.

2.18. Immunoprecipitation

Immunoprecipitation was carried out with the µMACS GFP Isolation Kit (Miltenyi Biotec) using the following procedure:

Plant tissue was frozen in liquid nitrogen and ground to a fine powder. 1 ml Lysis Buffer (25 mM Tris-HCl pH 7.5, 150 mM NaCl, 1 mM EDTA, 10% glycerol, 5 mM DTT, 0.1% Triton X-100, with one cOmplete Mini EDTA-Free Protease Inhibitor Tablets per 10 ml) was added per gram of tissue and vortexed until homogenous. The resulting mixture was centrifuged at 4 °C for 10 minutes at 12000 *g*, and the supernatant retained

30 µl Anti-GFP beads were added to 1970 µl lysate and incubated on ice for 1 hour. Meanwhile, a µMACS column was placed into a magnetic µMACS Separator and washed with 200 µl Lysis Buffer. The lysate was then allowed to flow through the column. The column was then washed 4 times with 200 µl Lysis Buffer. 20 µl Elution Buffer (50 mM Tris-HCl pH 6.8, 50 mM DTT, 1% SDS, 1 mM EDTA, 0.005% bromphenol blue, 10% glycerol) at 95 °C was then added to column and incubated for 5 minutes. A further 60 µl Elution Buffer was then added and the elution collected for SDS PAGE analysis (2.10.)

2.19. Plant Nuclear Isolation

Plant nuclei were isolated with a percoll/sucrose density gradient. Firstly, 5 g of leaf tissue was finely chopped and treated with 10 ml ice-cold diethyl ether, then rinsed with 10 ml Nuclear Isolation Buffer (NIB) (10 mM MES-KOH pH 5.4, 10 mM KCl, 2.5 mM EDTA, 250 mM sucrose, 0.1 mM spermine, 0.5 mM spermidine, 1 mM DTT). The tissue was then ground in 5 ml NIB until homogenous and decanted through 2 layers of Miracloth (Millipore). 10% Triton X-100 was then added drop-wise to a final concentration of 0.5% and the solution gently mixed for 20 minutes at 4 °C.

5 ml 2.5 M sucrose was poured into a cold falcon tube and 5 ml 60% Percoll carefully overlaid. The tissue extract mixture was then carefully overlaid above this layer and the tube centrifuged at 1000 *g* for 30 minutes at 4 °C. This middle layer of the resultant mixture was then extracted and centrifuged at 12000 *g* for 10 minutes at 4 °C. The pellet was resuspended in 200 µl protein extraction buffer (2.17. Plant Total Protein Extraction) and centrifuged again. The resulting supernatant was then analysed by SDS PAGE (2.10.).

2.20. Virus Induced Gene Silencing

Three agrobacterium strains, containing the BSMVα, β and γ cDNAs were co-infiltrated using the method shown previously (2.16.), except each strain was resuspended to an OD600 of 1.5 and all three constructs co-infiltrated. These plants were then left to grow

for 5 days, after which the infiltrated leaves were ground in pestle mortar with water (1 ml of water per g leaf tissue) until homogenised.

Leaves of 2-week-old wheat plants were lightly dusted with carborundum powder (Fisher). The homogenised sap of the infiltrated *N. benthamiana* leaves was then rubbed into the leaves. The plants were left in low light conditions for 2 days and then returned to normal growth conditions.

2.21. *Zymoseptoria tritici* Infection

2.21.1. Infection

Prior to infection, *Z. tritici* strain IPO323 spores were grown on a Yeast Extract Peptone Dextrose (YEPD) plate (2% peptone, 1% yeast extract, 2% dextrose, 1.2% agar) at 18 °C for 7 days.

Two weeks after silencing (2.20.) plants were trimmed so that only the 3rd leaf remained. These leaves were then taped down to a flat surface. Spores were harvested from the plate and suspended in sterile distilled water. The concentration of spores was measured by haemocytometer Axkiospop microscope at x20 magnification and diluted to 0.75x10^{6} spores/ml. Tween 20 was then added to a final concentration of 0.1%. Each leaf was then infected by rubbing spores onto the surface with a sterile cotton bud. Plants were kept in a growth cabinet at 20 °C with 16 hours light and 90% humidity. Lids were kept on the plants to increase the humidity as much as possible for the first 3 days. At the end of the infection cycle, the lids were returned to promote picnidia and spore production.

2.21.2. Scoring

Photographs were taken regularly during infection so that the development of symptoms could be scored visually. Photographs were also taken at the end of infection so that picnidia could be counted. Leaves were then cut and were placed 3 a time in falcon tubes with 10 ml of sterile distilled water, vortexed for 1 minute and left for 1 hour. Tubes were then vortexed for another minute, and a sample taken. The

concentration of spores in that sample was then counted by haemocytometer, as in 2.21.1.

2.22. Plant Tissue Culture

Seeds were sterilised by washing with 70% ethanol for 5 minutes and then 30 minutes in 2% sodium hypochlorite with shaking. They were then washed 3 times with sterile distilled water before transferring to plates.

Plates were ½ Murashige and Skoog (MS) medium (Duchefa) with 0.8% agar. For selection of kanamycin resistant transgenic plants, a final concentration of 200 μg/ml was used.

2.23. Genomic DNA Extraction

1 cm^2 leaf sections were ground with a micropestle in a microcentrifuge tube with 20 μl 1 M NaOH. 10 μl of the resulting mixture was then diluted with 90 μl 100 mM Tris-HCl pH 8 and heated to 98 °C for 5 minutes, before use as a template for PCR (2.4.).

2.22. Confocal Microscopy

2.22.1. DAPI Staining

Leaves to be stained were infiltrated with 10 μg/ml 4′6-Diamidino-2-phenylindole (DAPI) in 10 mM $MgCl_2$ 20 minutes before imaging.

2.22.2. Microscopy

Samples were prepared for microscopy by suspending in water on glass slides and were imaged using a Leica SP5 confocal laser scanning microscope (Leica, Berlin, Germany) with x63 objective lenses. DAPI was excited at 405 nm and detected between 420-470 nm. All constructs used for fluorescence microscopy contained either the Yellow

Fluorescent Protein (YFP) or Red Fluorescent Protein (RFP). YFP was excited at 415 nm and detected at 555-700 nm. RFP was excited at 560 nm and detected at 580-650 nm.

2.23. Sequence Analysis

DNA and protein sequences were analysed using NCBI BLAST (Camacho *et al*., 2008) and the NCBI Conserved Domain Database (Marchler-Bauer *et al*., 2015). Mulitple sequence allignments and phylogenetic trees were created using Clustal Omega 1.2.0 or 1.2.1 (Sivers *et al*., 2011).

Chapter 3

Using Virus Induced Gene Silencing to Identify Genes Involved in the Interaction Between Wheat and *Zymoseptoria tritici*

3.1 Introduction

Virus-Induced Gene Silencing (VIGS) is a tool that can quickly generate knockdowns of individual genes, in order to study their function. These knockdowns are produced without the need for transformation. This is particularly useful in wheat, which is hexaploid and has a significantly longer life cycle than most model plants, making the production of transgenic plants more difficult and time-consuming to produce.

A high-throughput VIGS method, designed for silencing in wheat using the Barley Stripe Mosaic Virus (BSMV) was recently developed (Yuan *et al*. 2011). This method was tested using the historically widely used marker for VIGS function, *Phytoene desaturase* (*PDS*). *PDS*-silenced plants show a clear white-leaf phenotype (Kumagai *et al.* 1995; Ruiz *et al.* 1998). BSMV VIGS was also utilised to find genes involved in the interaction between wheat and *Blumeria graminis* (Yuan *et al*., 2011). This system will be used to screen for involvement of genes in the wheat-*Z. tritici* interaction, by silencing target genes and infecting silenced plants.

The Ubiquitin Proteasome System (UPS) (reviewed by Sadanandom *et al*. 2012) is involved throughout plant cell signalling, in a wide array of processes. However, it has particularly been associated with plant-pathogen interactions, and a number of reviews have been written in this area (Trujillo and Shirasu 2010; Marino *et al.* 2012; Duplan and Rivas 2014).

The UPS has been shown to be involved in all stages of pathogen defence from perception (Wang *et al.* 2006) to both positive (Yu *et al.* 2013) and negative (Trujillo *et al.* 2008) roles in downstream signalling. The above reviews also show the UPS to be involved in a huge range of plant and pathogen systems. However, very little is known about any possible role it may play in the wheat-*Z. tritici* interaction. As such, it was decided to begin by identifying UPS-related targets to silence.

Based on the above, the initial aim of this chapter was to determine that silencing of the wheat *PDS* gene could be achieved, to be used as a positive control for silencing efficiency. Once this had been achieved, further aims include the selection of target genes, associated with ubiquitin-mediated degradation, whose expression was changed upon pathogen infection. These genes would then be silenced, their silencing efficiency confirmed by qPCR, and the infection phenotypes of silenced plants by infecting with *Z. tritici* and taking a spore count.

3.2 Silencing *PDS* to Determine VIGS Efficiency

As we began by establishing the existing VIGS protocol in a new facility, which had not been previously proven to silence genes using this system in wheat, the first aim was to show that this result could be repeated with the tools and growth facilities available (as described in chapter 2). Many investigations, including Yuan *et al*. 2011, on which our technique was based, have used *PDS* as a visible marker of effective silencing. As such, in order to test our conditions, we received a BSMVγ vector, containing a 185 bp sequence from *TaPDS* (figure 3.1.) from Dr. Kostya Kanyuka at Rothamsted Research. Avalon variety wheat plants were then inoculated. Initial attempts at silencing, carried out at a temperature of 20 °C proved unsuccessful. However, it was considered that the cause might be that BSMV required a higher growth temperature, and so this was increased to 24 °C. This proved sufficient to allow the virus to grow and the plants to produce the white leaf phenotype (figure 3.2.).

PCR carried out on silenced and mock-silenced plants, infected with an empty BSMVγ vector (figure 3.2), showed that *PDS* was present at a far higher level in mock silenced plants. While this result shows no *PDS* expression, VIGS is expected to create knockdowns rather than knockouts, and some residual expression should be expected.

ATGGATACCAGCTGCCTATCATCTATGAACATAGCTGGAGCGAAGCAAGTAAGATCTTTTGCTGGACAACTTCATACGCAGAGGTGTT
TCACAAGTAGCAGCGTCCAGGCACTAAAAACTAGTCATCGTACGACCTCCCTTGGCTTAAGGAATAAAGTAAAAGGATCACGTCATGG
ACTTCGTGCTCTGCAGGTTGTTTGCCAAGATTTTCCAAGGCCTCCACTAGAGAACACGATTAACTATTTGGAAGCTGGCCAGCTTTCT
TCGTCGTTTAGAAGCAGTGAACGCCCCAGTAAACCATTACAGGTCGTGATTGCTGGTGCAGGACTGGCTGGTCTATCAACTGCAAAAT
ACCTGGCAGACGCTGGCCACAAACCCATAGTGCTTGAGGCAAGAGATGTGTTGGGCGGAAAGTTAGCTGCATGGAAGGATGAAGATGG
TGATTGGTACGAGACTGGCCTTCATATTTTTTTTGGAGCTTATCCCAATGTACAGAATTTGTTTGCTGAGCTTGGTATTAGTGATCGC
TTGCAATGGAAGGAACACTCCATGATATTTGCCATGCCAAACAAACCAGGAGAATACAGCCGTTTTGATTTCCCAGAGACTTTGCCGG
CGCCCTTAAATGGAGTGTGGGCCATACTGAAAAACAATGAAATGCTTACTTGGCCGGAGAAGGTGAAGTTTGCTATTGGGCTTCTACC
AGCAATGCTTGGTGGCCAAGCTTACGTTGAAGCTCAAGATGGCTTAACTGTTTCCGAATGGATGGAAAAGCAGGGTGTTCCTGATCGA
GTCAACGACGAGGTTTTTATTGCAATGTCCAAGGCACTGAATTTCATAAACCCTGACGAGTTATCCATGCAGTGCATTCTGATTGCTC
TAAACAGATTTCTCCAGGAGAAGCATGGCTCGAAAATGGCATTCTTGGATGGTAATCCTCCTGAAAGGCTATGCATGCCTATTGTTAA
CCACATTCAGTCTTTGGGTGGTGAGGTCCGGCTGAATTCTCGTATTCAGAAAATTGAACTGAACCCTGACGGAACAGTGAAGCACTTT
GCACTTACTGATGGGACTCAAATAACTGGAGATGCATATGTTTTTGCAGCACCAGTTGATATCTTCAAGCTTCTTGTACCACAAGAGT
GGAGAGAGATCTCTTATTTCAAAAGGCTGGATAAGTTGGTGGGAGCTCCTGTCATCAATGTTCATATATGGTTTGACAGAAAACTGAA
GAACACGTATGACCACCTTCTTTTCAGCAGGAGTTCACTTTTAAGCGTTTATGCAGACATGTCTTTAGCGTGCAAGGAGTACTATGAT
CCAAACCGTTCAATGCTGGAGCTGGTCTTTGCTCCAGCAGAGGAATGGATCGGGCGGAGTGACACCGAAATCATCGAAGCAACTATGC
TAGAGCTAGCCAAGTTGTTTCCTGATGAAATCGCTGCTGACCAGAGTAAAGCAAAGATTCTTAAATACCATGTTGTGAAGACACCGAG
GTCCGTTTACAAGACTGTCCCGAACTGCGAACCTTGCCGACCCCTGCAACGATCACCGATCGAAGGGTTCTATCTGGCCGGCGATTAC
ACAAAGCAGAAATACCTGGCTTCCATGGAGGGTGCGGTTTTGTCAGGGAAGTTTTGTGCTCAGTCCATAGTGCAGGATTCTAAGATGC
TGTCCCGCAGGAGCCAGGAGAGCCTGCAATCCGAAGCCCCGGTCGCCTCCAAGTTGTAG

Figure 3.1. *TaPDS* Sequence. Sequence of *TaPDS* with the silencing fragment highlighted in blue. Start and Stop codons are in red.

Figure 3.2. *TaPDS* Silencing. Upper panels show the normal, green colour of leaves mock silenced with empty BSMV vector (left) and the white leaf effect of *TaPDS* silenced leaves after infection BSMV:PDS (right). Lower panels show result of 30 cycles of RT PCR using primers specific to *TaPDS* with mock silenced showing strong expression (left) compared to silenced (right). The cDNA used for this experiment was taken from different leaves to those shown in the top panel, but which showed the same visible phenotype.

3.3 Target Gene Selection

Collaborators at Rothamsted Research (Rothamsted Research, West Common, Harpenden) and Syngenta (Jealott's Hill, Bracknell) conducted transcriptomics on plant and fungal material at various stages that they considered to be key points in the infection process (Rudd *et al* 2015). The first timepoint was one day post infection (dpi) when the fungal spores begin to germinate on the leaf surface. The next was four dpi, by which time hyphal growth has begun, and hyphae have penetrated the leaf and started to grow in intracellular space. The third timepoint was nine dpi, defined as an increased fungal growth rate, and the first signs of visible symptoms, followed by 14 dpi, which is associated with an acceleration in host cell death and a large increase in fungal biomass. The final stage was 21 dpi at the onset of asexual sporulation in necrotic leaf tissue. From this, a database of genes, which changed in expression between any of these stages, was generated.

In order to generate a list of genes to target with VIGS, the database of wheat-only genes was interrogated with sequences of F-box, BTB, UBC and RING domains, all of which are associated with the UPS (Sadanandom *et al.* 2012). A large list of sequences was generated, and it was decided to further narrow this down. Firstly, sequences showing homology to the UBC and RING domains (Kraft *et al*. 2005) only were focussed on, as they predominantly function individually, rather than requiring a complex and, therefore, their individual function would be easier to discover. Secondly, as the leaf tissue in the day 14 and 21 samples was mostly necrotic, it was decided to consider only genes showing expression changes from day one-four and four-nine. From this, 10 genes were selected and named based on their domain homology: five genes appearing to posses UBC domains named *Triticum aestivum UBC1-5* (*TaU1-5*) and five appearing to posses RING domains (*Triticum aestivum RING1-5* (*TaR1-5*).

The expression patterns of these genes are seen in Figure 3.3. While these genes were initially discovered based on the DNA sequence, the translated protein sequences were also compared with proteins known to contain these domains. Figure 3.4. shows an alignment of the full protein sequences of TaU1-5 and the Arabidopsis UBC domain proteins TaUBC1-3. Conserved residues are highlighted, including the important active site cysteine (Sadanadom *et al*., 2012). Figure 3.5. shows an alignment of areas of protein sequences of TaR1-5 and the Arabidopsis RING domain proteins At1g14260,

At1g02860 and At1g12760, showing strongly homology. This sequence contains the RING domain of each protein and conserved residues, forming the cysteine-histidine zinc-binding backbone of the RING domain are highlighted.

In order to begin silencing these genes, fragments were of the sequence were obtained by PCR and cloned into the BSMV vector. It has previously been shown that, using this vector system, fragments 200-400 bp in length are the most effective for silencing (Yuan *et al* 2011). It was also decided that, in order to reduce the possibility of off-site silencing causing any phenotype seen, two separate, non-overlapping fragments were designed for each gene. In this way, if a consistent phenotype was seen when both constructs were used for silencing there could be higher confidence that this was caused by silencing of the intended gene. Due to the limitations of the length of the genes targeted, it was decided to create 200 bp fragments for *UBC1-5* and 250 bp fragments for *TaR1-5*. These fragments are shown in Figure 3.6. and 3.7.

Table 3.1. Target genes chosen based on UPS-related domains and expression changes on infection

Gene Name	UPS-related Domain	Expression Change Day 1-4	Expression Change Day 4-9
TaU1	UBC	Increase	Decrease
TaU2	UBC	Increase	Decrease
TaU3	UBC	Increase	Decrease
TaU4	UBC	Increase	Decrease
TaU5	UBC	Decrease	Decrease
TaR1	RING	Increase	Increase
TaR2	RING	Decrease	Decrease
TaR3	RING	Decrease	Decrease
TaR4	RING	Decrease	Decrease
TaR5	RING	Decrease	Decrease

3.4 Preliminary Infection Experiments

Once two fragments had been designed for each gene, cloning of each into the BSMV vector was attempted. Due to the high GC content of some regions of DNA sequence, particularly in the RING domain homologous sequences, some fragments proved particularly difficult to amplify. However, once both fragments of six genes were cloned and transformed into Agrobacterium, the process of silencing and screening for infection phenotypes was initiated. The first six genes to have two fragments cloned were *TaU1*, *TaU2*, *TaU3*, *TaU5*, *TaR1* and *TaR3*.

Plants were silenced with each of these constructs, and infected with *Z. tritici* strain IPO323. Along with these plants, two other lines were included the infection: a non-silenced line, which had undergone the same physical disruption as the silenced lines, but had not been inoculated with virus, and a mock silenced line, which was inoculated with the empty BSMV vector (BSMV:00).

A full 28-day infection cycle was allowed to take place and, at the end, infected leaves were harvested and a spore wash and count was used to determine the level of *Z. tritici* infection. From this, the average concentration of spores on leaves of each line were calculated and compared, relative to the non-silenced line. The results of this are shown in figure 3.8.

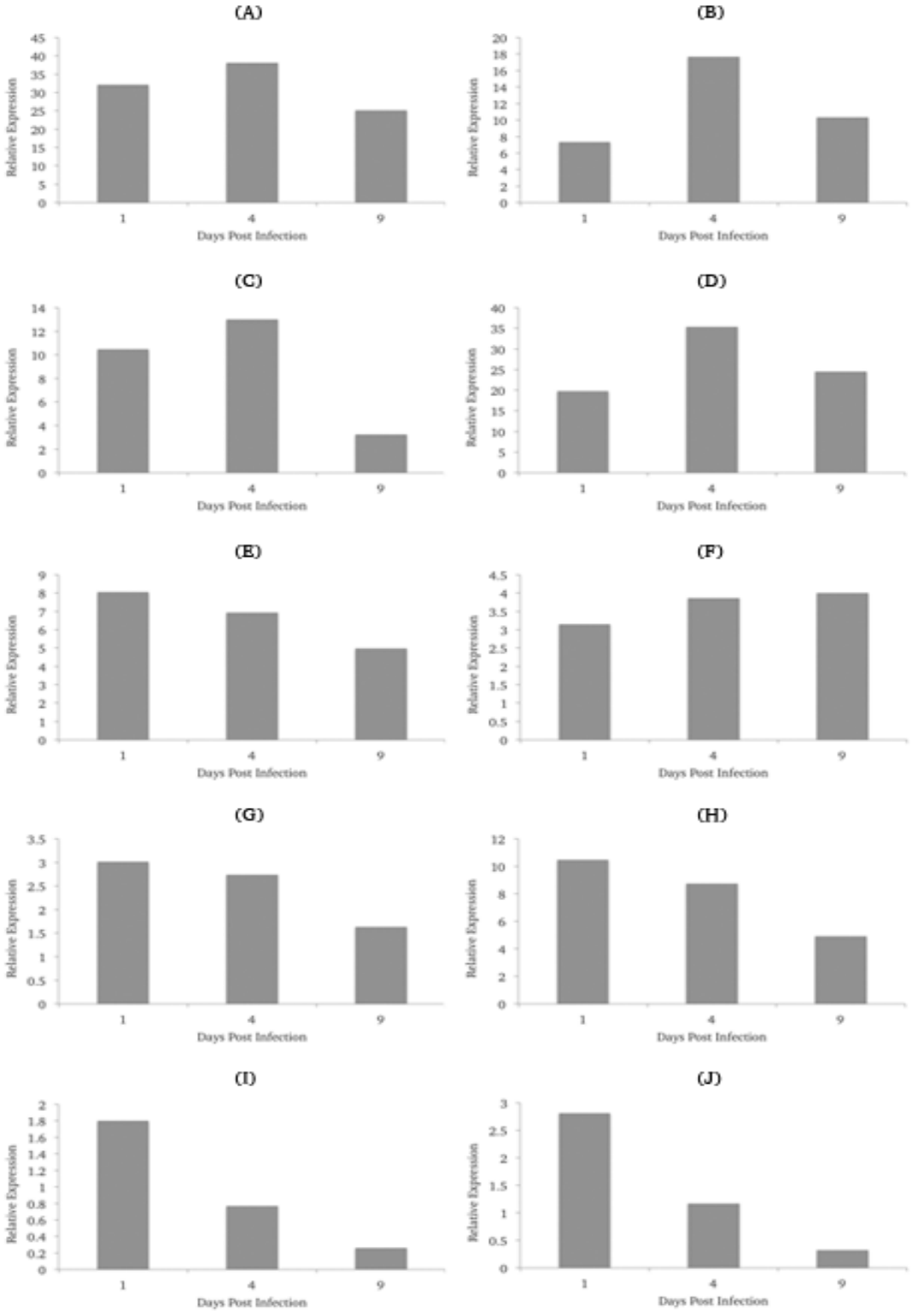

Figure 3.3. Expression profiles of *TaU1-5* and *TaR1-5* after *Z. tritici* infection. Graphs showing the change in expression between, days 1,4 and 9 in wheat leaves infected with *Z. tritici*, of (A) *TaU1*, (B) *TaU2*, (C) *TaU3*, (D) *TaU4*, (E) *TaU5*, (F) *TaR1*, (G) *TaR2*, (H) *TaR3*, (I) *TaR4*, (J) *TaR5*. Relative expression is equal to number of reads from transcriptomic data/10,000. Extracted from data provided by Rothamstead Reaseach.

```
TaU5      MSSPSKRREMDLMKLMMSDYKVEM----VNDGMQEFFVEFRGPTESIYQGGVWKVRVELP
TaU3      -------------------------------MFHWQATIMGPSDSPYSGGVFLVTIHFP
TaU1      ---MASKRILKELKDLQKDPPTSCSAGPSGEDMFHWQATIMGPPDSPYAGGVFLVNIHFP
TaU2      ---MASKRILKELKDLQKDPPTSCSAGPAGEDMFHWQATIMGPPDGPYAGGVFLVNIHFP
TaUBC3    MTTPAKKRLMWDFKRLQKDPPVGISGAPQDNNIMHWNALIFGPEDTPWDGGTFKLTLHFT
TaU4      MSTPSRKRLMRDFKRLMQDPPAGISGAPQDNNIMLWNAVIFGPDDSPWDGGTFKLTLQFN
TaUBC1    MSTPARKRLMRDFKRLQQDPPAGISGAPQDNNIMLWNAVIFGPDDTPWDGGTFKLSLQFS
TaUBC2    MSTPARKRLMRDFKRLQQDPPAGISGAPQDNNIMLWNAVIFGPDDTPWDGGTFKLSLQFS

TaU5      DAYPYKSPSIGFINKIYHPNVDEMSGSVCLDVINQTWSPMFDLVNVFEVFLPQLLLYPNP
TaU3      PDYPFKPPKVAFRTKVFHPNIN-SNGSICLDILKDQWSPALTISKVLLS-ICSLLCDPNP
TaU1      PDYPFKPPKVSFKTKVFHPNIN-SNGSICLDILKEQWSPALTISKVLLS-ICSLLTDPNP
TaU2      PDYPFKPPKVSFKTKVFHPNIN-SNGSICLDILKEQWSPALTISKVLLS-ICSLLTDPNP
TaUBC3    EDYPNKPPIVRFVSRMFHPNIY-ADGSICLDILQNQWSPIYDVAAVLTS-IQSLLCDPNP
TaU4      EEYPNKPPTVRFISRMFHPNIY-ADGSICLDILQNQWSPIYDVAAILTS-IQSLLCDPNP
TaUBC1    EDYPNKPPTVRFVSRMFHPNIY-ADGSICLDILQNQWSPIYDVAAILTS-IQSLLCDPNP
TaUBC2    EDYPNKPPTVRFVSRMFHPNIY-ADGSICLDILQNQWSPIYDVAAILTS-IQSLLCDPNP

TaU5      SDPLNGEAAALMMRDRPAYEQKVKEFCEKYVKP-EDAGITPEDKSSDEEELSDEDDSGDE
TaU3      DDPLVPEIAHMYKTDRHKYESTAR-----TWTQRYAM----------------------
TaU1      DDPLVPEIAHMYKTDRSKYETTAR-----SWTQKYAMG---------------------
TaU2      DDPLVPEIAHMYKTDRSKYETTAR-----SWTQKYAMG---------------------
TaUBC3    DSPANAEAARLFSENKREYNRKVIEIVEQSYV----------------------------
TaU4      NSPANSEAARMFSENKREYNRKVREIVEQSWTAD--------------------------
TaUBC1    NSPANSEAARMYSESKREYNRRVRDVVEQSWTAD--------------------------
TaUBC2    NSPANSEAARMFSESKREYNRRVREVVEQSWTAD--------------------------
```

Figure 3.4. UBC Protein Sequence Alignment. A multiple sequence alignment of the available protein sequence of *TaU1-5* and the Arabidopsis UBC genes *AtUBC1-3*. The alignment was produced using Clustal Omega (1.2.0). Colour was added to show strongly conserved residues in red and the active site cysteine in blue.

```
At1g1426  --------------------------------MSNHHTVVYVNGLVRP----------VL
At1G02860 ------LINAVAIRKILKKYDKI-HESRQGQAFKTQVQKMRIEILQSPWLCELMAFHINL
At1g12760 LPCIIAVLYAVADQEGASK-----EDIEQLTKFKFR----------------------KL
TaR       LPTVYEVISGMRQSKERDRSGGIDNSGRN----------------------------KL
TaR4      LPTIFDVVSGKSKTQAPTHNNHSNSKSKSNNKMKTSEPR------------------AKQ
TaR5      LPTIFDVVSGKSKTKAPTNNNHSNSKSKSNNKMKTSEPR------------------AKQ
TaR2      LPTIFEVVTGAAKKQIKEKAPNSTHKSNNKPSMKTY----------------------SK
TaR3      LPTIYEVVTGTAKKQVKEKHPKSSSKINK-SGTKPS----------------------RQ

At1g14260 AEAE--YSMRTESPADNAIDIYDGDTTE-----------NEEEDSLISSAECRICQDECD
At1G02860 KESKKESGATITSPPPPVHALFDGCALTFDDGKPLLSCELSDSVKVDIDLTCSICLDTV-
At1g12760 GDAN--KH--TNDEA--Q-GTTEGIMTECGTDSP------IEHTLLQEDAECCICLSAYE
TaR1      PSKH-----TVEAPPPPR-AENNARD---ADEGY------DEDDGDHSETLCRTCGGIYS
TaR4      PKPQL-KEEDHEDEAPDA-GEDGG-----GAAGG------GGGGEEHGDTLCGACGDNYG
TaR5      PKPQL-KEEDHEDEAPDA-GEDGG-----GAAGG------GGGGEEHGDTLCGACGDNYG
TaR2      PESQS-KA--PKIAAPPK-DEDES-----GEDYG------EEEEEERDNTLCGTCGTNDG
TaR3      PEPNS-RG--PKMPPPPK-DEDDS-----GGEE--------EEGEEHEKALCGACNDNYG

At1g14260 IKNLESPCACNGSLKYAHRKCVQRWCNE-------KGNTICEICHQPYQAGYTSPPPPPQ
At1G02860 ---FDPISLTCGHIYCYMCACSAASVNVVDGLKTAEATEKCPLCREDGVYKGAV-----H
At1g12760 DGT-ELRELPCGHHF--HCSCVDKWL---------YINATCPLCKYNILKSSNL-----D
TaR1      AQEFWIGCHVCERWY--HGKCVKITPAK----AESIKQYKCPSCSSKRPRQ---------
TaR4      QDEFWIGCDMCEKWF--HGKCVKITPAK----AEHIKQYKCPSCMGANGGGSGS-----N
TaR5      QDEFWIGCDMCEKWF--HGKCVKITPAK----AEHIKQYKCPSCMGANGGGSGS-----N
TaR2      KDEFWICCDNCERWY--HGKCVKITPAR----AEHIKHYKCPDCSNKRARA---------
TaR3      QDEFWICCDACETWF--HGKCVKITPAK----AEHIKHYKCPNCSSSSKRARA-------
```

Figure 3.5. RING Protein Sequence Alignment. A multiple sequence alignment of an area of homology between *TaR1-5* and the Arabidopsis RING proteins At1g12760, AT1G02860 and At1g14260. The alignment was produced using Clustal Omega (1.2.0). The conserved Cysteine and Histidine residues which are required for the zinc-binding function of the RING domain are highlighted in red.

TaU1

GCGAAGAAAAGGAGCTTATCATGGCTTCAAAACGTATCCTGAAGGAACTGAAGGACTTGCAGAAAGATCCTCCGACATCATGCAGTGC
AGGTCCTTCTGGTGAGGATATGTTCCATTGGCAGGCAACCATTATGGGTCCTCCTGATAGTCCCTATGCTGGAGGTGTTTTCTTAGTG
AATATCCATTTCCCCCCGGACTACCCCTTCAAGCCGCCGAAGGTATCGTTCAAGACAAAGGTCTTCCATCCGAACATCAATAGCAATG
GAAGCATATGCCTTGACATTCTGAAGGAGCAATGGAGTCCTGCTTTGACAATCTCTAAGGTTCTGCTTTCAATCTGCTCGCTGCTTAC
CGACCCTAACCCGGACGACCCTCTCGTCCCCGAGATTGCCCACATGTACAAGACGGATCGGTCCAAGTATGAGACGACAGCCCGCAGC
TGGACGCAGAAGTATGCCATGGGATGA

TaU2

ATGGCATCAAAGCGCATCCTCAAGGAACTCAAGGACCTGCAGAAGGACCCGCCCACATCATGCAGTGCAGGTCCTGCTGGTGAGGACA
TGTTTCATTGGCAAGCAACAATTATGGGACCCCCTGACGGTCCCTATGCCGGCGGTGTTTTCTTAGTGAACATTCATTTCCCTCCGGA
TTACCCCTTCAAGCCACCAAAGGTATCTTTTAAGACAAAGGTCTTCCATCCTAATATCAACAGCAATGGAAGCATATGCCTTGATATT
CTTAAGGAGCAGTGGAGCCCTGCTTTGACGATCTCTAAGGTCTTGCTCTCTATCTGTTCCCTGCTGACCGATCCCAACCCGGATGATC
CCCTTGTTCCCGAGATTGCCCACATGTACAAGACGGACCGGTCAAAGTATGAGACGACAGCCCGCAGCTGGACGCAGAAGTACGCCAT
GGGTTGA

TaU3

AGCGGAAGCAGGAGGCAGAGAGGAGATCAGGCCAGAGGAGGGCGAGGGAGGGCGCGATGGCGTCCAAGAGGATACAGAAGGAGCTCAA
GGATCTGCAGAAGGATCCCCCCCACCTCATGCAGCGCAGGCCCTGTGGGTGAAGATATGTTCCATTGGCAGGCAACAATAATGGGCCC
ATCTGACAGCCCATATTCCGGTGGAGTTTTCCTAGTTACTATCCACTTCCCTCCTGATTATCCTTTCAAACCACCAAAGGTGGCATTC
CGCACCAAGGTGTTCCATCCAAACATCAACAGCAACGGGAGCATTTGTCTGGACATCCTCAAGGACCAATGGAGCCCCGCTCTGACCA
TTTCCAAGGTGCTGCTGTCCATCTGCTCCCTGCTGTGTGACCCAAACCCTGACGATCCTCTGGTTCCTGAGATCGCTCACATGTACAA
GACGGACCGGCACAAGTATGAGAGCACCGCCAGGACCTGGACGCAAAGGTATGCCATGTAA

TaU4

CGCCCAGGCCGACCTAAAGCCGTCCATTCCGTCGTCTCCATGCTCTAGGACAACGAGCACGCGGAGCCCACGTCTCCACCCCCACCGC
CGGCCGCATCTCAGAGAATTTCGAGGATGTCGACTCCTTCAAGGAAGAGGCTGATGAGGGACTTCAAGCGGCTGATGCAGGACCCTCC
TGCGGGCATAAGCGGGGCGCCGCAGGACAACAACATAATGCTGTGGAATGCTGTGATTTTTGGCCCTGACGATAGCCCGTGGGATGGA
GGCACGTTTAAGCTGACTCTCCAGTTTAATGAAGAATATCCTAATAAGCCACCAACAGTTCGGTTTATTTCTCGGATGTTTCACCCTA
ACATTTATGCTGATGGAAGCATATGCTTAGATATTCTACAGAATCAGTGGAGCCCAATATATGATGTAGCTGCTATACTTACATCTAT
CCAGTCGCTGCTGTGTGATCCTAACCCAAATTCGCCTGCTAACTCAGAAGCTGCCCGCATGTTCAGTGAGAACAAGCGAGAGTACAAC
CGCAAAGTGCGGGAGATTGTTGAGCAGAGCTGGACGGCAGACTAA

TaU5

AGGAGGAAGGGAAGATTTCATCTTTTTTGCCCCCAAGATGTCCTCCCCAAGCAAGCGCCGCGAGATGGACCTCATGAAGCTGATGATG
AGTGACTATAAGGTGGAGATGGTGAACGATGGGATGCAAGAATTCTTCGTGGAATTCCGAGGGCCTACTGAAAGTATTTATCAAGGTG
GTGTCTGGAAGGTTAGAGTAGAACTGCCTGATGCATATCCTTACAAATCTCCGTCAATTGGGTTCATTAATAAGATTTATCACCCAAA
TGTGGATGAAATGTCTGGTTCCGTATGTTTAGATGTTATCAACCAGACATGGAGCCCAATGTTTGATCTAGTAAATGTGTTCGAAGTC
TTCCTTCCACAACTTCTGTTGTACCCAAATCCGTCTGATCCATTAAATGGAGAGGCTGCTGCACTTATGATGCGAGATCGCCCTGCTT
ATGAACAAAAAGTGAAAGAATTTTGTGAAAAATATGTGAAACCAGAGGATGCTGGCATAACCCCAGAAGACAAGTCCAGTGATGAAGA
GGAGCTTAGCGACGAAGATGACTCCGGCGATGAGGATATAGTGGGCAAACCAGATCCTTAG

Figure 3.6. Nucleotide sequences of *TaU1-5*. The nucleotide sequences of *TaU1-5* are shown. Fragment A for each is highlighted in blue, while Fragment B is green. Start and Stop codons are in red.

TaR1

ATCACGAGAGGCGGCGCCCCCATCCCCGCGATGGACGCCTCCTACCGCCGCTCAGGTGCGGGCGGTGGCGGCGGCTCAGCCCCCCGCA
CCGTCGAGGACATCTTCAAGGACTACCGCGCCCGCCGCAACGCCATCCACCGCGCCCTCACCCACGACGTCGAGGAGTTCTACGCGCA
GTGCGATCCAGAGAAGGAGAACCTGTGCCTGTACGGGTACGCTAACGAGGCGTGGGAGGTGGCGCTGCCCGCGGAGGAGGTGCCCACC
GAGCTGCCGGAGCCGGCGCTCGGGATCAACTTTGCGCGCGACGGGATGAAGCGCAGCGACTGGCTCGCGCTCGTCGCCGTCCACTCCG
ATTCGTGGCTTGTCTCCGTAGCTTTCTACTATGCCGCGCGGCTCACCCGCAACGACCGGAAGCGTTTATTTGGAATGATGAATGATTT
GCCAACCGTGTATGAAGTCATCTCAGGTATGAGACAATCGAAGGAGAGGGACAGATCAGGTGGTATTGACAACAGCGGTAGAAACAAG
CTGCCATCAAAGCATACAGTCGAGGCGCCGCCACCACCACGTGCAGAAAATAATGCCAGGGATGCCGATGAAGGCTACGATGAAGATG
ACGGCGACCACAGCGAGACCTTATGCCGAACGTGTGGTGGCATATACAGCGCCCAGGAATTCTGGATTGGGTGCCACGTGTGCGAGAG
GTGGTACCATGGCAAGTGCGTGAAGATAACTCCGGCGAAGGCGGAGAGCATAAAGCAGTACAAATGCCCAAGCTGCAGCTCCAAGAGA
CCTAGGCAGTAG

TaR2

ACACCCTTCTCGCCGCCGCCGCCGCCCCCTCGCCGGAACCCTAAATGGACGCCGGCGCCGGCGCCGGCGCTGGCGCGCCCTACGCCTC
CCGCACGGCGGAGGAGGTCTTCCGCGACTTCCGCGGCCGCCGCGCCGGCATGATCAAGGCCCTCACCCAAGAAGTGGACAAGTTCTAC
CAGCTCTGCGACCCCGAAAAGGAGGACTTGTGCCTTTATGGGTACCCTAATGAAACATGGGAAGTGACGTTGCCTGCTGAGGAAGTTC
CCCCAGAGATTCCTGAACCAGCACTTGGAATCAACTTTGCTAGGGATGGCATGAACGAGAAGGATTGGTTGGCACTAGTTGCTGTTCA
CAGTGATTCCTGGTTGTTGGCTGTTTCATTCTACTTCGCGGCACGGTTTGGATTTGACAAAGAGGCAAGGAGGCGACTCTTCAACATG
ATAAATAACCTGCCTACAATATTTGAAGTCGTGACTGGGGCTGCAAAGAAGCAGATCAAGGAGAAGGCCCCCAACAGTACGCACAAGA
GCAATAATAAGCCAAGCATGAAAACTTATTCAAAGCCTGAGTCCCAATCAAAGGCCCCAAAGATAGCAGCGCCCCCAAAGGATGAAGA
TGAGAGCGGCGAGGACTATGGAGAAGAAGAGGAGGAAGAGCGCGACAACACCTTGTGTGGTACCTGTGGAACAAACGACGGCAAGGAC
GAGTTCTGGATCTGCTGCGACAACTGCGAGCGGTGGTATCATGGGAAATGCGTCAAGATCACGCCTGCTCGAGCCGAGCATATCAAGC
ACTACAAGTGCCCAGACTGCAGCAACAAGAGGGCGAGGGCGTAA

TaR3

ATGGACGGGGGAGGCACGCATCGCACGCCGGAGGACGTGTTCAGGGATTTCCGCGCGCGGCGGGCCGGCATGATTAAGGCGCTCACCA
CCGATGTGGAGAAGTTCTACCAGCAGTGCGACCCAGAGAAAGAGAATCTATGTCTGTATGGTCTTCCCAATGAAACATGGGAAGTGAA
CTTGCCTGCAGAGGAGGTTCCCCCAGAACTTCCAGAGCCGGCACTGGGAATTAATTTTGCTCGGGATGGGATGGATGAGAAAGATTGG
TTGTCACTTGTTGCGGTGCACAGTGATGCCTGGTTGCTAGCAGTAGCCTTCTACTTTGGAGCAAGATTCGGGTTTGACAAAGAATCCA
GGAAGCGGCTTTTTAGCATGATAAACAACCTCCCCACCATATATGAGGTTGTCACCGGAACTGCGAAGAAGCAGGTCAAAGAAAAACA
CCCCAAAAGCAGCAGCAAGATAAATAAATCTGGCACTAAGCCATCTCGCCAGCCAGAACCTAACTCAAGGGGTCCAAAGATGCCACCA
CCTCCGAAGGATGAGGACGACAGTGGAGGCGAGGAAGAAGAGGGAGAAGAACATGAAAAGGCATTATGTGGTGCGTGTAACGATAACT
ATGGACAGGATGAATTCTGGATCTGCTGTGATGCTTGTGAGACATGGTTCCACGGTAAGTGTGTGAAGATCACCCCTGCCAAAGCTGA
GCACATCAAGCACTACAAATGCCCGAATTGCAGCAGCAGTAGCAAGAGGGCCAGAGCATGA

TaR4

TCGAATCCTCTGCGGTTAACAATGGACGCGCAGTACAACCCCAGGACGGTGGAGGAGGTCTTCCGGGATTACAAGGGCCGCCGCAACG
GCCTCGCCCGCGCGCTCACCACCGATGTGGAGGAATTCTTCCGGCAATGCGACCCGGAAAAAGAAAATTTGTGCCTTTATGGGTTTCC
CAATGAGCATTGGGAAGTAAACTTACCTGCTGAAGAAGTGCCACCTGAGCTCCCAGAGCCAGCATTGGGCATCAACTTTGCACGAGAT
GGAATGCAGGAAAAAGATTGGCTATCCATGGTTGCAGTACACAGCGACGCATGGTTACTATCTGTTGCATTCTACTTTGGTGCTCGAT
TCGGATTTGATAAAAGTGACAGGAAGCGCCTGTNTGGTATGATTAATGAGCTTCCCACGATTTTTGATGTTGTTAGTGGGAAGAGTAA
AACCCAGGCTCCGACCCACAATAACCACAGCAATAGCAAATCCAAGTCCAACAATAAAATGAAAACCTCGGAGCCTCGGGCGAAGCAG
CCCAAGCCCCAGCTGAAGGAGGAAGATCATGAGGACGAAGCCCCGGATGCGGGCGAGGATGGTGGAGGCGCCGCCGGCGGTGGCGGTG
GCGGGGAAGAGCACGGCGATACGCTGTGCGGCGCGTGTGGGGACAACTACGGGCAGGACGAGTTCTGGATCGGCTGCGACATGTGCGA
GAAGTGGTTCCACGGCAAGTGTGTCAAGATCACGCCGGCCAAGGCGGAGCACATCAAGCAGTACAAGTGCCCGTCGTGCATGGGCGCC
AACGGCGGCGGCAGCGGCAGCAACAAGCGGGCGCGCCCGTCCTCCTAA

TaR5

ATGGACGCGCAGTACAACCCCAGGACGGTGGAGGAGGTCTTCCGGGACTACAAGGGCCGCCGCAACGGCCTCGCCCGCGCGCTCACCA
CCGATGTGGAGGAGTTCTTCCGGCAATGCGACCCGGAAAAAGAAAATTTGTGCCTTTATGGGTTTCCCAATGAGCATTGGGAAGTAAA
CTTACCTGCTGAAGAAGTGCCACCTGAGCTCCCAGAGCCAGCATTGGGCATCAACTTTGCACGAGATGGAATGCAGGAAAAAGATTGG
CTATCCATGGTTGCAGTACACAGCGACGCATGGTTACTATCTGTTGCATTCTACTTTGGTGCTCGATTCGGATTTGATAAAAGTGACA
GGAAGCGCCTGTTTGGTATGATTAATGAGCTTCCCACGATTTTTGATGTTGTTAGTGGGAAGAGTAAAACCAAGGCTCCGACCAACAA
TAACCACAGCAATAGCAAATCCAAGTCCAACAATAAAATGAAAACCTCGGAGCCTCGGGCGAAGCAGCCCAAGCCCCAGCTGAAGGAG
GAAGATCACGAGGACGAAGCCCCTGATGCGGGCGAGGATGGTGGAGGCGCCGCTGGTGGTGGTGGTGGCGGAGAAGAGCACGGCGATA
CGCTGTGCGGCGCGTGTGGGGACAACTACGGGCAGGACGAGTTCTGGATCGGCTGCGACATGTGCGAGAAGTGGTTCCACGGCAAGTG
TGTCAAGATCACGCCGGCCAAGGCGGAGCACATCAAGCAGTACAAGTGCCCGTCGTGCATGGGCGCCAACGGCGGCGGCAGCGGCAGC
AACAAGCGGGCGCGCCCGTCCTCCTAA

Figure 3.7. Nucleotide sequences of *TaR1-5*. The nucleotide sequences of *TaR1-5* are shown. Fragment A for each is highlighted in blue, while Fragment B is green. Start and Stop codons are in red.

3.5 Target Gene Silencing

From the preliminary spore count (Figure 3.8.) it was noted that in multiple lines the spore count showed significant difference compared to the mock. However, this trend is only seen from one *TaU3_B* silencing, and not *TaU3_A*, while there was also a large difference between *TaU2_A* and *B*, and *TaU5_A* and *B*. While *TaR3_A* and *B* showed the same trend, the difference to the mock was much lower in these lines. As such, it was decided to focus on *TaU1* and *TaR1*, allowing a more in-depth analysis to be conducted on these genes. This started by verifying that the genes targeted were being silenced.

While *TaPDS* silencing had been verified by RT-PCR (Figure 3.2.), it was decided that the greater accuracy of real-time quantitative PCR (qPCR) would be required to establish target gene silencing. VIGS typically produces knockdowns rather than knockouts, so a conclusion as clear as that seen in Figure 3.2. is unlikely, and in the case of an uncertain result, *TaU1* and *TaR1* knockdowns lack the clear physical phenotype of *TaPDS*.

To conduct qPCR, distinct qPCR primers, with a T_m of 60°C and product size of ~100bp, were ordered for all target genes. Primers were also ordered to *TaUb* (ubiquitin) to use as a reference gene. In order to verify that qPCR was adequately quanitifying silencing, *TaPDS* primers were also included, allowing qPCR results to be obtained from *TaPDS* silenced cDNA. To verify that these primers were functioning correctly, they were used in a PCR reaction at standard qPCR conditions and visualised on an agarose gel, to confirm that only one product was present. This is shown in figure 3.9.

Once this had been confirmed, qPCR was carried out on *TaPDS* silenced cDNA. Figure 3.10. indicates that qPCR does show *TaPDS* to be silenced, compared to the BSMV:00 control. While the error make this result less convincing, it was not repeated as the white leaf phenotype of the leaves was considered strong enough evidence of silencing.

RNA was then extracted from *TaU1* and *TaR1* silenced tissue. qPCR for *TaU1* and *TaR1* respectively was then carried out on the cDNA generated from each. The result of this (Figure 3.10.) confirmed that *TaU1* and *TaR*1 were being silenced compared to the BSMV:00 control. Although the extent of gene knockdown does vary (65-85% efficiency), all lines are showing consistently lower expression of the intended target gene.

3.6 *TaR1* Silencing Affects *Z. tritici* Spore Production

After confirmation that *TaU1* and *TaR1* were both effectively silenced by both fragment A and B of each, two individual biological repeats of all four lines were, along with the BSMV:00 control, subjected to repeats of *Z. tritici* infection and spore washes and counts. The results from both were averaged and are shown in Figure 3.11. From this, it can be seen that across the two biological replicates, plants silenced with both the BSMV:TaR1_A and BSMV:TaR1_B constructs maintain the reduced *Z. tritici* sporulation phenotype seen in the initial experiment. This is confirmed by a Student's t-Test, which shows the average of TaR1_A (p value = $3.39x10^{-8}$) and TaR1_B (p value = $5.35x10^{8}$) both differ significantly from the BSMV:00 control.

However, the lines silenced by BSMV:TaU1_A and BSMV:TaU1_B shows a very different infection phenotype to the initial experiment. While the TaU1_B line still results in slightly lower spore prediction, TaU1_A plants show a slightly higher sporulation, and neither TaU1_A (p value = 0.06) nor TaU1_B (p value = 0.14) differ significantly from the BSMV:00 control, according to the Student's t-Test.

While spore counts alone are not a perfect measure of the pathogen infection, further methods of infection scoring will be introduced in Chapter 4.

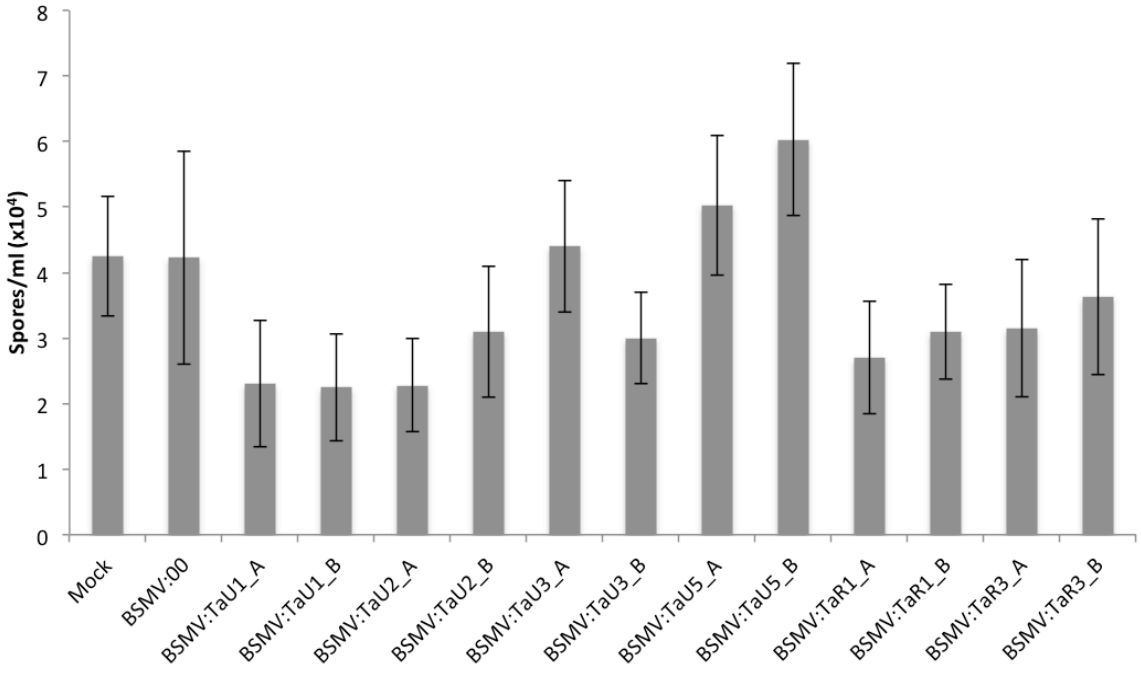

Figure 3.8. Preliminary spore count experiment. A graph showing the number of spores washed off mock lines (no BSMV infection), empty vector infected lines (BSMV:00) and lines silenced in *TaU1,2,3,5* and *TaR1* and *TaR3* in spores x10^4/ml Error bars represent standard error of the mean over five technical replicates.

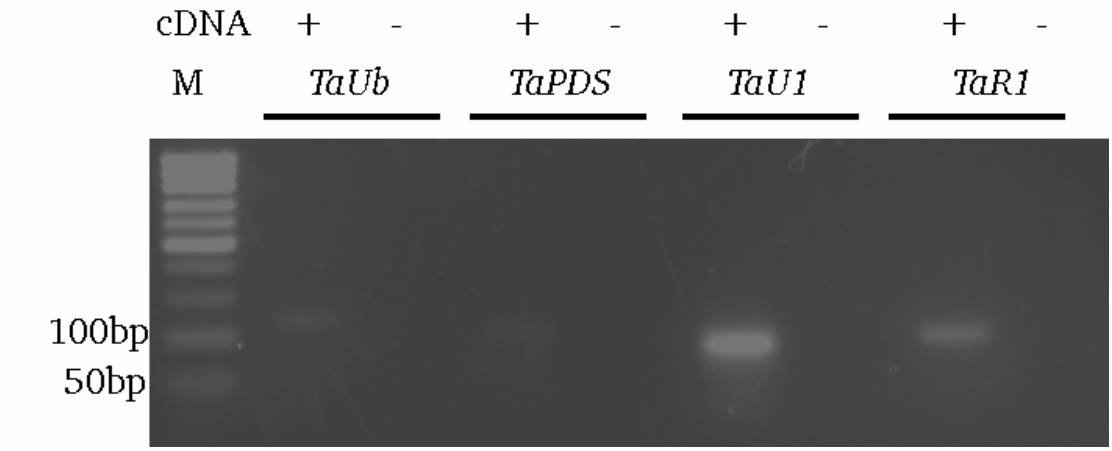

Figure 3.9. qPCR primer products. qPCR products of *TaUb (expected size 118bp), TaPDS* (92bp), *TaU1* (93bp) and *TaR1* (95bp) visualised on a 2% agarose gel.

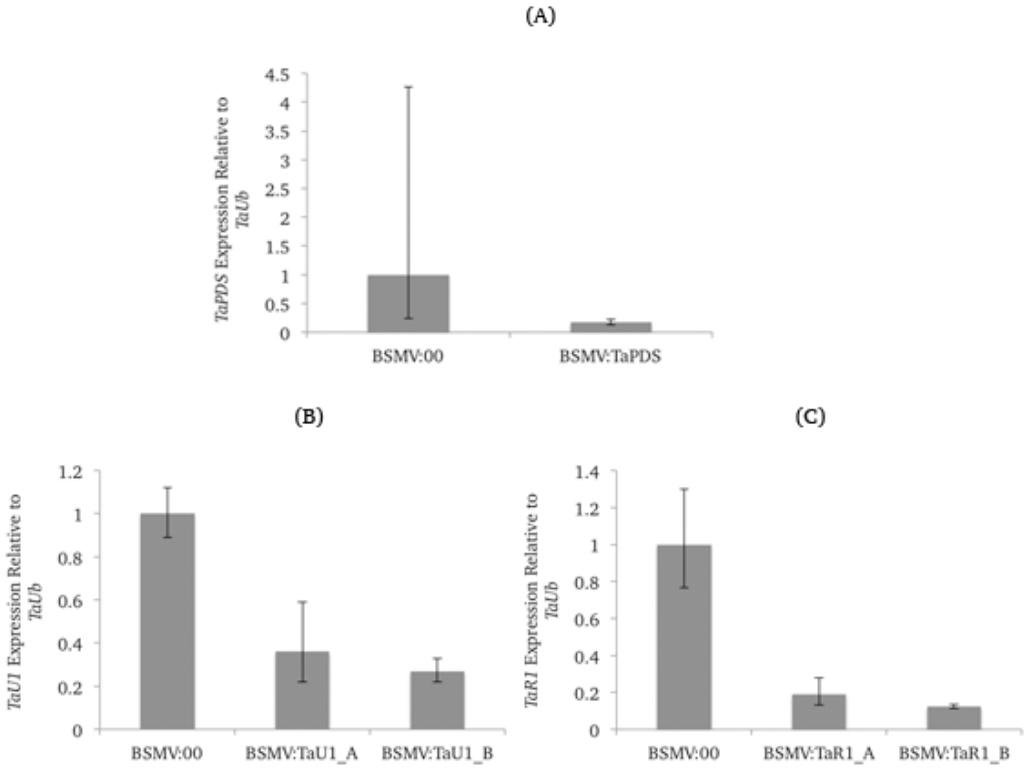

Figure 3.10. Silencing qPCR. Graphs showing the relative levels of (A) *TaPDS*, (B) *TaU1* and (C) *TaR1*, standardised to the *TaUb* reference gene, in silenced lines compared to the mock-silenced control.

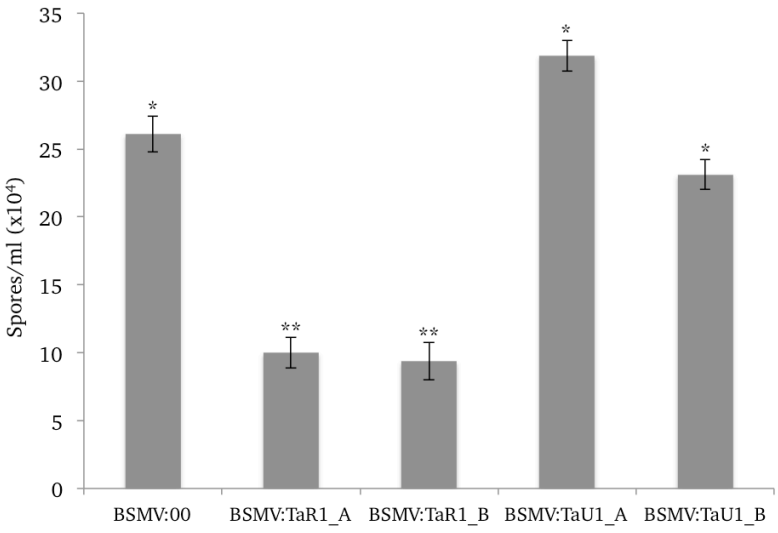

Figure 3.11. *TaR1* and *TaU1*-silenced spore count data. Graph showing the spores/ml washed off mock silenced (BSMV:00), *TaR1*-silenced (BSMV:TaR1_A, BSMV:TaR1_B) and *TaU1*-silenced (BSMV:TaU1_A, BSMV:TaU1_B) plants.

3.7 TaR1 Domain Clarification

Translated protein sequences for each of the selected target genes were all confirmed to contain UPS related domains. This was achieved by inputting the sequence into the NCBI Conserved Domain Database (CDD) (Marchler-Bauer *et al.* 2015). As can be seen in Figure 3.10., at this first point in time, TaR1 was shown to contain a RING domain. However, this search was repeated at a later date following a database update, resulting in TaR1 being reclassified as possessing a Plant Homeodomain (PHD) domain, as is again shown in Figure 3.12.

A phylogenetic tree, based on an alignment of the full sequence of a number of RING and PHD domain proteins (Figure 3.13.) was created using Clustal Omega (Sievers *et al*. 2011) and shows that this confusion is created by a very close homology between RING and PHD domain sequences, to the extent that there is a group of variant RING domains, which are listed as RING, but are less closely related to other RING domains than the PHD domains are. Nonetheless, the tree does show that TaR1 domain is most closely related to other PHD domains, than it is to RING domains. This suggests that the second CDD search provided the most accurate classification, and that TaR1 does contain a PHD domain, as opposed to a RING domain.

The difference between these domains, and further clarification of important PHD domain motifs and residues within the TaR1 sequence, will be further discussed in Chapter 4.

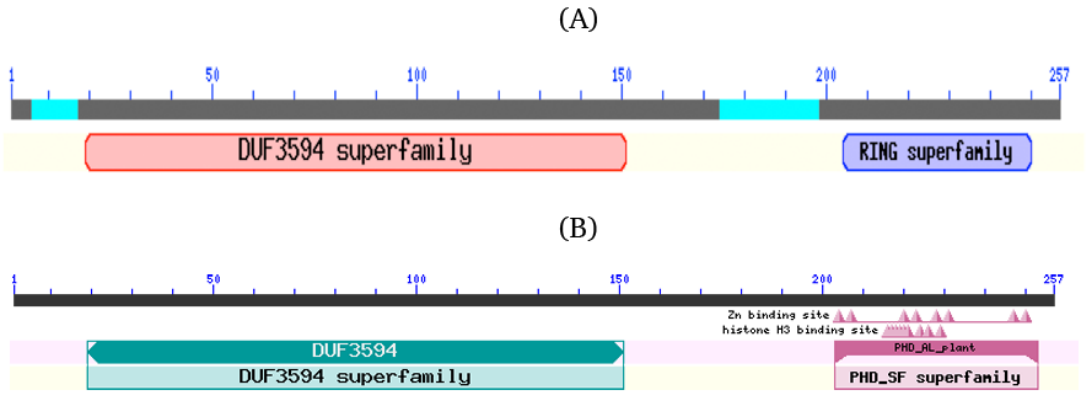

Figure 3.12 Conserved Domain Database search results for TaR1. Results from two separate CDD searches with the TaR1 sequence show (A) a RING domain and (B) a PHD domain.

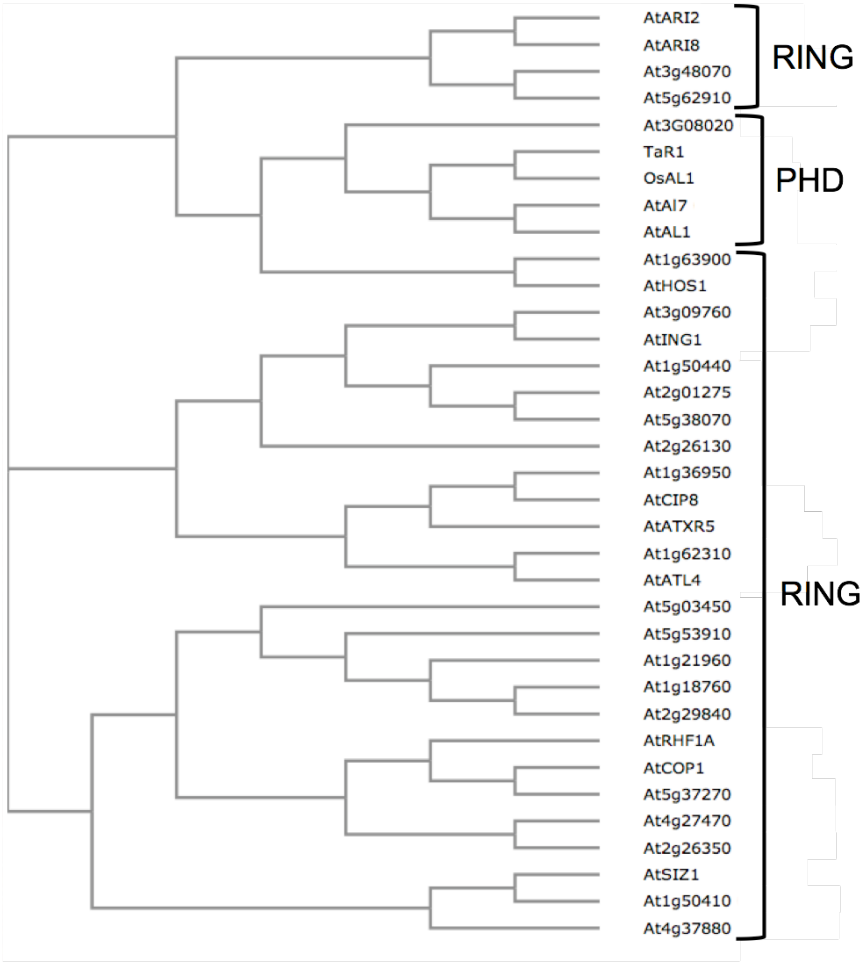

Figure 3.13. Phylogeny of RING and PHD domain proteins. A phylogenetic tree showing that the sequence of some RING domain proteins is closer to that of some PHD domain proteins than it is to other RING domains.

3.8 Conclusions

In order to use VIGS as a method of determining which wheat genes are involved in the plant-pathogen interaction with *Z. tritici*, it was first important to ascertain that this is a viable method of creating gene knockdowns in the conditions available to us. From the results obtained in this chapter, in particular those shown in Figure 3.2. and 3.10., it can be concluded that this is indeed the case. These results have also proven that the silencing of *TaPDS* is an effective marker for whether or not VIGS is functioning. While this is hardly an unexpected occurrence, given that the silencing of *PDS* genes has historically been an effective marker across all species (Kumagai *et al.* 1995; Ruiz *et al.* 1998), including wheat (Yuan *et al*. 2011), it is nonetheless useful information for a newly established VIGS facility. Given that environmental conditions had originally caused silencing to not function, it was decided to include a *TaPDS* silencing control along with all other silencing attempts. This would indicate to us whether the conditions were correct for silencing, without necessity for unnecessary molecular testing.

Once the visible symptoms of *TaPDS* silencing have shown that the VIGS system is functioning, however, it is still necessary to determine the silencing of gene with no visible phenotype. In these cases, it was determined, first by confirmation through *TaPDS*, and then with *TaU1* and *TaR1*, that qPCR was a good measure of silencing efficacy (Figure 3.10.).

Our initial testing also verified that the system of using two separate silencing fragments for each gene is essential. In particular, it can be seen from Figure 3.8. that plants silenced using more than one fragment do not always produce the same result. Confirming that two fragments are each creating the same phenotype when used for silencing is, therefore, a useful screen when selecting genes to target. The method of spore washing and counting also appears to be a useful method of screening genes for involvement in the interaction in as quick a manner as possible, given the necessary 28-day infection cycle.

Using a combination of these methods we were able to narrow down our target list and focus on only one gene. While the more rigorous infection testing appears to have ruled out an involvement of *TaU1* in this plant pathogen interaction, this is actually a helpful

result. In order to be more certain that any genes identified are genuinely affecting the process, it must be known that the VIGS process itself is not the cause. Figure 3.11. shows that mock silenced plants are infected in a very similar manner to plants untouched by the BSMV and, therefore, it is not the presence of the virus causing any infection phenotype seen. Similarly, a lack of infection phenotype in *TaU1*-silenced plants suggests that any differences seen can be concluded to be specifically brought about by the silencing of the target gene, rather than an artefact of a general disruption to the system by silencing unrelated genes.

Based on this, it can then be said that the method used is effective for determining genes involved in the interaction of wheat with *Z. tritici*. In a relatively short time period, *TaR1* was identified as a gene which, when silenced, does alter the infection process (Figure 3.11.), and is worth studying more closely.

It is noteworthy, however, that, while there was ultimately some effect of the target gene, selection based on homology to existing UPS sequences was not entirely successful. The main target derived from these results, *TaR1*, was shown not contain the domain expected, but instead a PHD domain. While *TaR1* remains a good candidate, it will first be necessary to determine its function, before any suggestion could be made into the role it is performing in the wheat *Z. tritici* interaction. Results of the investigation into the function of TaR1, and the role it plays in pathogen defence will be presented in Chapter 4.

Chapter 4

Characterisation of TaR1 and its Role in *Zymoseptoria tritici* Infection

4.1. Introduction

From the results in chapter 3, we have seen that TaR1 is an interesting target protein to study in the wheat *Z. tritici* interaction, as silencing *TaR1* leads to an altered infection phenotype. In order to better understand the role of TaR1 in this interaction, further study will be required into the effects caused by *TaR1* silencing. While the results obtained thus far are a good indicator of an overall effect, they only show the end result of infection, and so a more in depth examination of the onset of disease will be necessary.

In addition to this, a repeat of the RNA sequencing, mentioned in Chapter 3, which initially identified *TaR1* as increasing in expression in the leaves over the course of *Z. tritici* infection, suggested that there was no significant change in *TaR1* expression at any stage of infection (Rudd *et al*., 2015). Therefore, it was necessary to conduct our own time course and test *TaR1* expression over this. It was considered that a more frequent sampling would increase the accuracy of this search, by giving an understanding of changes in expression that may be transient. This was, in fact, proven to be the case (Lee *et al*. 2015). *TaR1* transcript was upregulated in wheat leaves infected with *Z. tritici*, but the peak at day nine lasted for only one time point (samples collected every two days) and levels rarely exceeded the 2x threshold. Therefore it is entirely possible that this increase in expression is real, but was missed by the second RNA-sequencing experiment. Of equal interest is that, while expression initially rises, it appears to drop to lower than pre-infection levels just at the point symptoms begin to appear.

Finally, while it was identified in a screen for targets related to the Ubiquitin Proteasome System (UPS), further analysis suggested that this incorrect, and that TaR1

in fact possesses a plant homeodomain (PHD) domain. Thus, in order to fully understand the role played by TaR1 in the infection interaction, it will first be necessary to ascertain and test its molecular function. The first step of this process is to confirm the existence of the PHD domain and investigate the role of proteins possessing similar domains.

4.2. TaR1 Domain Analysis

In order to determine a more specific like function of TaR1, the protein sequence of the PHD domain of TaR1 (amino acid 203-253) aligned with the PHD domains of several other known PHD domain proteins (Figure 4.1A). This shows that the cysteine-histidine zinc-binding motif is well conserved throughout PHD domains, including TaR1. Further to this, TaR1 also contains the residues required for the aromatic cage and Histone 3 argenine 2 binding site, previously highlighted by Lee *et al.* (2009). The mutation of these residues was shown to prevent histone binding.

A phylogenetic tree developed with Clustal Omega (Sievers *et al*. 2011) from this alignment (Figure 4.1B) suggests that TaR1 is most similar to a group of Alfin-like proteins, in particular the rice protein OsAL1, with which it shares 98.15% homology. These proteins all also contain a C-terminal domain of unknown function (amino acid 19-151 in TaR1), here called an Alfin-like (AL) domain. An alignment (Figure 4.2A) and phylogenetic tree (Figure 4.2B) of these C-terminal domains, along with that of the original Alfin1 from alfalfa (Bastola *et al.* 1998) show that, while TaR1 is again most similar to OsAL1, this region is strongly conserved between all of these proteins.

The Alfin-like proteins included in these alignments (AtAL1, AtAL7 and OsAL1) are the same as those included in Figure 3.11., in which TaR1 appeared to form a clade of close homology with these proteins, separate from other PHD domain proteins. Together these all suggest that TaR1 shows a strong homology to all Alfin1-like proteins at the full protein and domain levels. Therefore, the results in figures 4.1. and 4.2. suggest that TaR1 may have a similar function to these other proteins, and that, as they appear to have a conserved function (Lee *et al*., 2009), this should be investigated in TaR1.

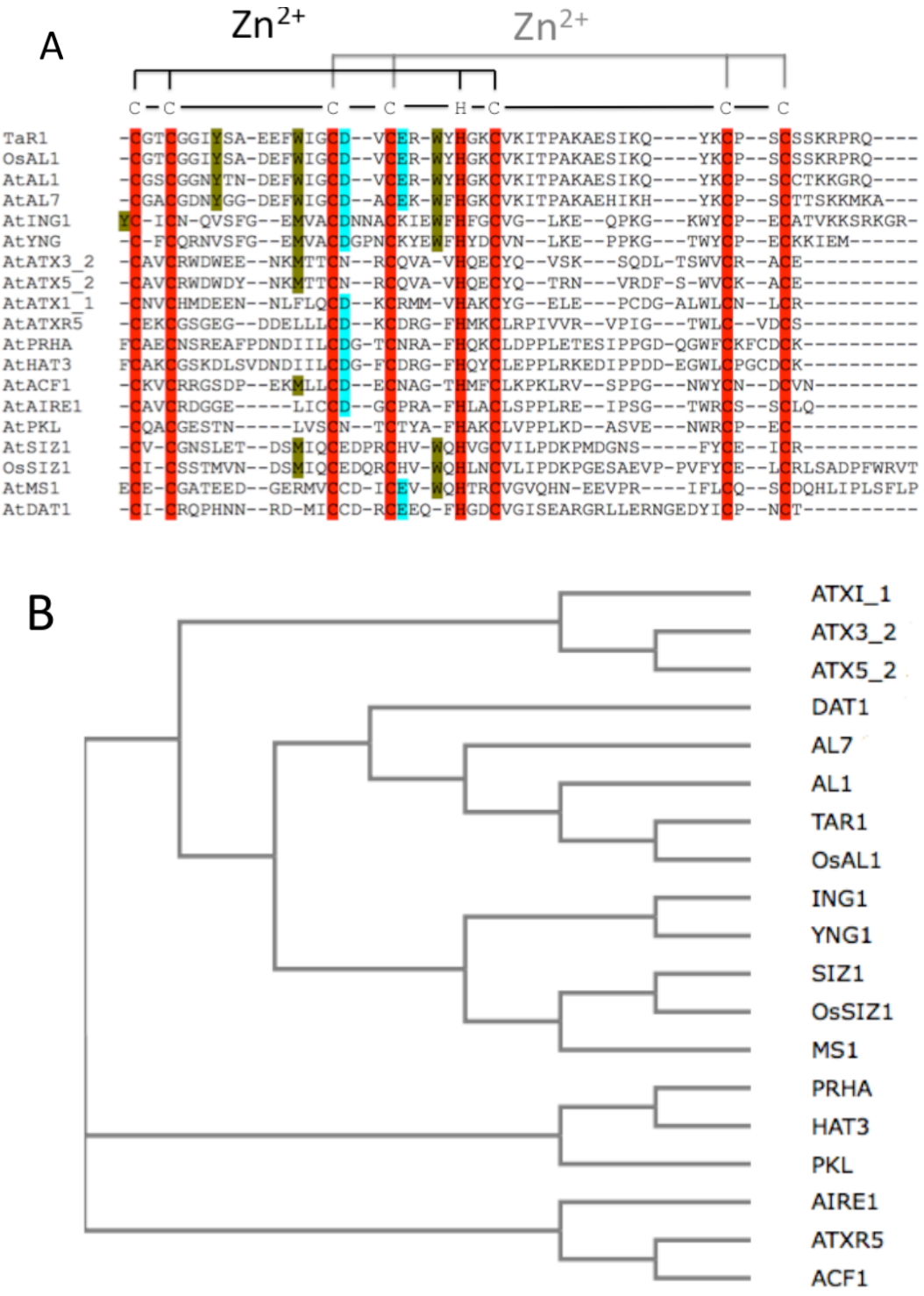

Figure 4.1. TaR1 PHD Domain Alignment and Phylogenetic Tree. (A) A multiple sequence alignment of PHD domains from TaR1 and other plant PHD domain proteins. The alignment was produced using Clustal Omega (1.2.0), then re-coloured. The zinc-binding cysteine-histidine backbone is shown in red. Residues indicated by Lee et al. (2009) as important for formation of an aromatic cage (gold) and for Histone 3 Arginine 2 recognition (blue) are also indicated. (B) Phylogenetic tree illustrating the grouping of PHD domain of TaR1 amongst other PHD domain proteins. The phylogenetic tree was created using Clustal Omega(1.2.0).

A

```
TaR1       RTVEDIFKDYRARRNAIHRALTHDVEEFYAQCDPEKENLCLYGY
OsAL1      RSVEDIFKDFRARRTAILRALTHDVEDFYAQCDPEKENLCLYGY
AtAL1      RTVEEIFKDFSGRRSGFLRALSVDVDKFYSLCDPEMENLCLYGH
AtAL7      RSAEDVFRDFRARRAGIVKALTTDVEKFYRQCDPEMENLCLYGL
MsAlfin1   RTVEEVFSDYKGRRAGLIKALTTDVEKFYQLVDPEMENLCLYGF

TaR1       ANEAWEVALPAEEVPTELPEPALGINFARDGMKRSDWLALVAVH
OsAL1      ANEAWQVALPAEEVPTELPEPALGINFARDGMNRRDWLALVAVH
AtAL1      PNGTWEVNLPAEEVPTELPEPALGINFARDGMQRKDWLSLVAVH
AtAL7      PNETWDVTLPAEEVPTELPEPALGINFARDGMIEKDWLSLVAVH
MsAlfin1   PNETWEVNLPVEEVPTELPEPALGINFARDGMQEKDWLSLVAVH

TaR1       SDSWLVSVAFYYAARL--TRNDRKRLFGMMNDLPTVYEVISG--
OsAL1      SDSWLVSVAFYYAARL--NRNDRKRLFGMMNDLPTVYEVVS---
AtAL1      SDCWLLSVSSYFGARL--NRNERKRLFSLINDLPTVFEVVTGRK
AtAL7      SDAWLLSVAFYFGARFGFDKEARRRLFTMINGLPTVYEVVTGIA
MsAlfin1   SDSWLLAVAFYFGARFGFGKNDRKRLFQMINDLPTVFELATG--
```

B

Figure 4.2. TaR1 AL Domain Analysis. (A) Multiple sequence alignment of the AL domain of TaR1, Alfin1 and Alfin1-like proteins from Arabidopsis and rice. Conserved residues are highlighted in red. The alignment was produced using Clustal Omega (1.2.0), then re-coloured. (B) Phylogenetic tree illustrating the grouping of AL domain of TaR1, Alfin1 and Alfin1-like proteins from Arabidopsis and rice. The phylogenetic tree was created using Clustal Omega(1.2.0).

4.3. TaR1 is Nuclear-Localised

The majority of PHD domain proteins, including those to which TaR1 is most closely related, are nuclear-localised and associated with chromatin interactions, therefore the subcellular localisation of TaR1 was tested. This was achieved by cloning the full-length coding sequence of *TaR1* into the N-terminal Yellow Fluorescent Protein (YFP) fusion vector pEARLYGATE104. This construct was transformed into agrobacterium, which was infiltrated into *Nicotiana benthamiana* leaves, in order to transiently express the TaR1-YFP construct.

The presence and localisation of YFP in this transiently transformed leaf was then detected by confocal microscopy (Figure 4.3.). In this figure, TaR1-YFP (panel Ai) is shown to localise specifically to the nucleus, which is confirmed by over-laying with DAPI staining (panel Aiii, Aiv). This is in contrast to the YFP-only control (Figure 4.3B.), which is seen to mark the entire cell. Alongside the confocal microscopy, protein was also extracted from the TaR1-YFP leaves and analysed. Figure 4.4. shows that when the total protein was extracted and probed with an αGFP antibody, a band of the correct size appears for both TaR1-YFP and YFP only, suggesting that the correct fusions have been made and imaged.

However, due to the nature and, in particular, the size, of the YFP protein, it very easily enters the nucleus, and so the YFP-only control is seen here as well. In order to combat this a second infiltration and confocal microscopy imaging was carried out, this time using *TaR1* in the N-terminal Red Fluorescent Protein (RFP) fusion vector pK7WGR2. In this case (Figure 4.5.) it can be seen that the RFP only control (panel B) marks the cytoplasm but not the nucleus. TaR1-RFP (panel A) also shows some expression outside the nucleus in this case. However, it is also expressed inside the nucleus, showing that TaR1-RFP can enter the nucleus, while RFP alone cannot.

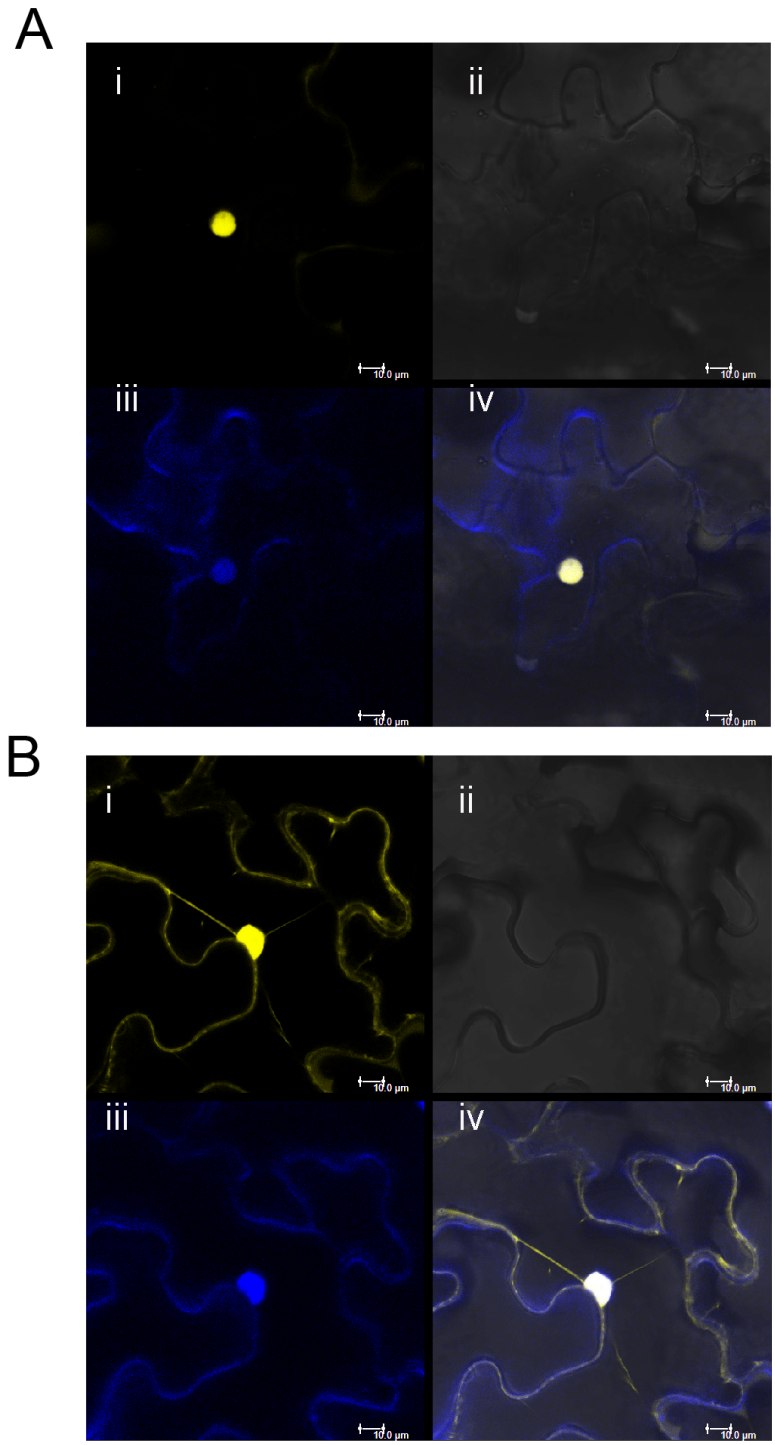

Figure 4.3. YFP-TaR1 Confocal Microscopy. (A) Confocal microscopy of *N. benthamiana* cells infiltrated with the pEARLYGATE104:*TaR1* construct showing (i) YFP-TaR1 detected at 555-700nm (ii) white light (iii) DAPI detected at 420-470nm (iv) i-iii overlaid. (B) Confocal microscopy of *N. benthamiana* cells infiltrated with the pEARLYGATE104:00 construct showing (i) YFP detected at 555-700nm (ii) white light (iii) DAPI detected at 420-470nm (iv) i-iii overlayed.

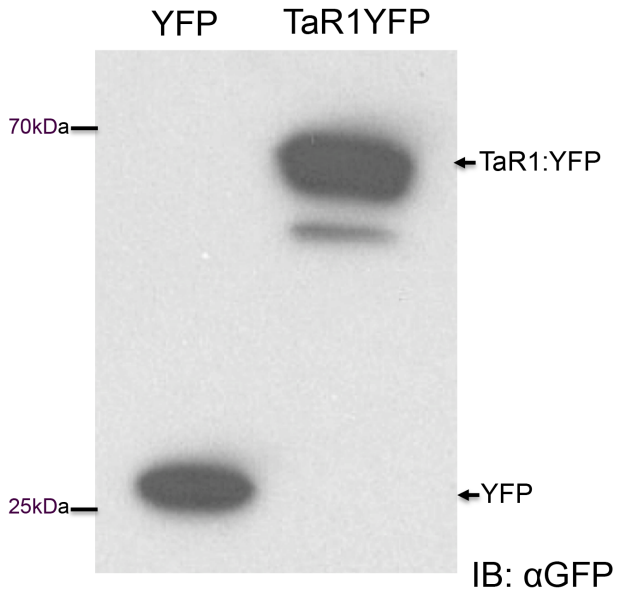

Figure 4.4. Western Blotting of Infiltrated *N. benthamiana*. Western blotting with anti-GFP antibody, which recognizes YFP, shows presence of YFP and YFP-TaR1 in infiltrated N. benthamiana.

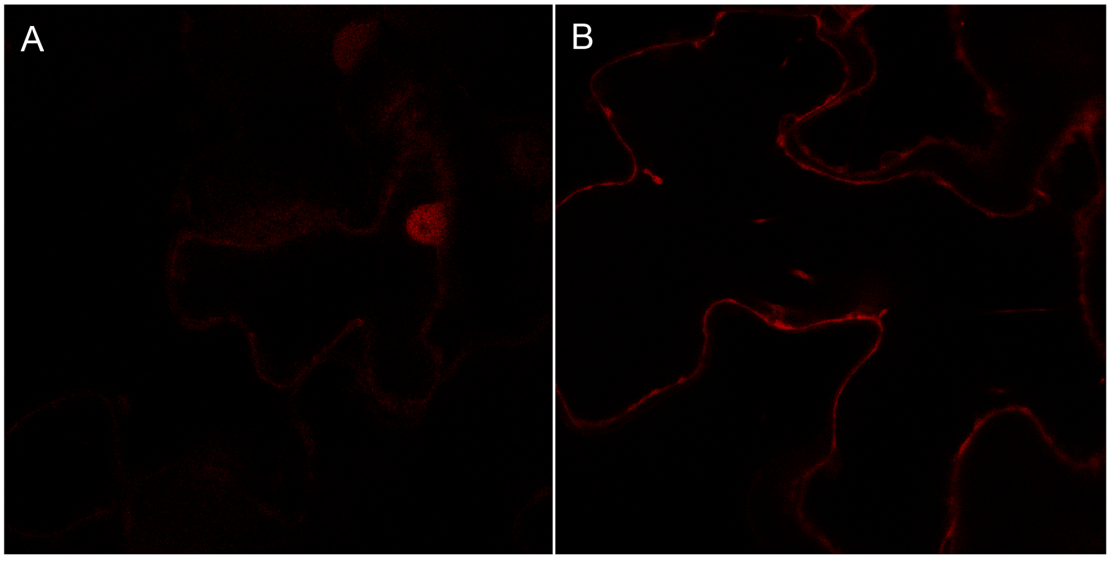

Figure 4.5. RFP-TaR1 Confocal Microscopy. Confocal microscopy detected at 580-650nm of *N. benthamiana* infiltrated with (A) pK7WGR2-TaR1 and (B) pK7WGR2.

4.4. TaR1 Binds to Specifically Modified Histones

The Arabidopsis AL proteins, to which TaR1 is so closely related, show the commonly seen PHD domain function of binding to histones. In particular, they bind specifically to modified Histone 3 di- or trimethylated on lysine 4 (H3k4me2/3) (Lee *et al.* 2009). As a result of this, it was decided to test the histone binding capacity of TaR1.

Firstly, the ability of TaR1 to bind Histone 3 of wheat (TaH3) was tested *in planta* with a co-immunoprecipitation assay. The full sequence of *TaH3* was obtained, cloned and inserted into N-terminal HA fusion vector pEARLYGATE201. This was then co-infiltrated into *N. benthamiana* leaves with the TaR1-YFP construct used previously, along with a repeat with the YFP-only control. The total protein from these leaves was extracted and, from this extract, any YFP or YFP-associated protein was immunoprecipitated (IP) using magnetic GFP beads, which also bind YFP due to its high sequence similarity. This YFP IP fraction was then examined by gel electrophoresis and probed with both αGFP and αHA antibodies. The result of this (Figure 4.6.) is that a band of the size expected for HA-TaH3 is visible in the input lanes for both YFP-TaR1 and YFP only, but only appears in the IP lane of YFP-TaR1.

This suggests that HA-TaH3 is able to bind to YFP-TaR1, but not to YFP, suggesting that TaR1, and not the YFP is responsible for the binding. However, to ensure that the binding is not between TaR1 and the HA tag, the co-IP assay was repeated, with the tags reversed (HA-TaR1 and YFP-TaH3). This can be seen in Figure 4.7. The result produced is the same; that HA-TaR1 binds to YFP-TaH3, but not to YFP only.

This experiment was repeated and probed with an antibody specific to modified H3k4me3. The results (Figure 4.6) suggest that at least some of the HA-TaH3 bound by YFP-TaR1 had been modified with the specific methylation signal to which it is predicted that TaR1 will bind.

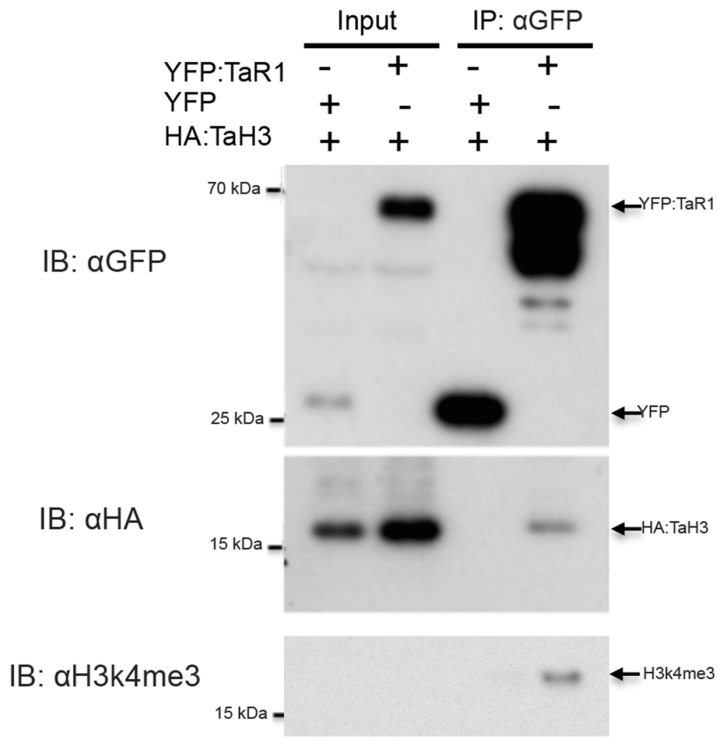

Figure 4.6. Co-immunoprecipitation of YFP-TaR1 and HA-H3. GFP pulldown of protein from *N. benthamiana* tissue co-infiltrated with HA-TaH3 and either YFP-TaR1 or YFP. αGFP Western blot shows presence of YFP-TaR1 and YFP in both, αHA Western blot shows HA-TaH3 is present in the input of both, but is pulled down by YFP-TaR1 and not by YFP. αH3k4me3 Western blot shows that some pulled down Histone 3 is trimethylated on lysine 4.

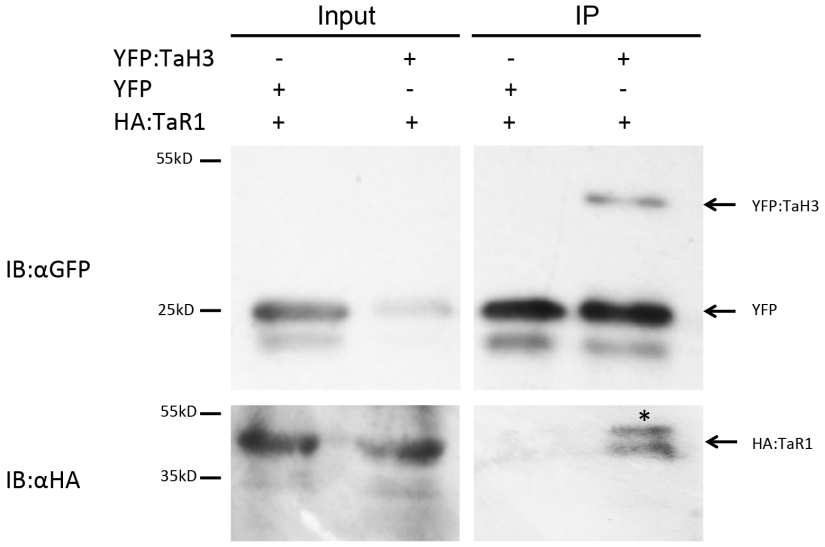

Figure 4.7. Co-immunoprecipitation of HA-TaR1 and YFP-TaH3. GFP pulldown of protein from *N. benthamiana* tissue co-infiltrated with HA-TaR1 and either YFP-TaH3 or YFP. αGFP Western blot shows presence of YFP-TaH3 and YFP in both, αHA Western blot shows HA-TaR1 is present in the input of both, but is pulled down by YFP-TaH3 and not by YFP.

As a consequence of this, an assay was designed to test *in vitro* whether TaR1 was specifically binding to histones with this methylation signal. Firstly, the full length *TaR1* sequence was recombined into the pDEST17 N-terminal His-fusion *Escherichia coli* expression vector. This vector was used to express and purify the His-TaR1 protein (Figure 4.8). Site-directed mutagenesis was used to produce a mutated *TaR1* sequence with the Aspartic Acid residue at position 221 substituted for an Asparagine (TaR1ΔD221N). Lee *et al.* (2009) had shown this Aspartic Acid to be an important residue in histone recognition and binding, while the Aspragine is not predicted to bind. This was purified using the same system.

These purified proteins, along with purified His-TaU1 as a control, were incubated with a series of biotinylated histone peptides with various methylation signals (H3 – Histone 3 unmethylated, H3k4me1 – Histone 3 methylated on Lysine 4, H3k4me2 Histone 3 dimethylated on Lysine 4, H3k4me3 - Histone 3 trimethylated on Lysine 4 and H3k9me3 Histone 3 trimethylated on Lysine 9) as well as a no peptide control. Streptavidin-agarose beads were then used to pull down the biotinylated peptides from the mixture. The product of this was then probed with an αHis antibody, to see which peptides had pulled His-tagged proteins down with them. The result of this, as seen in Figure 4.9., is that His-TaR1 bound only to H3k4me2 and H3k4me3 modified peptides, while neither His-TaU1 or His-TaR1ΔD221N were able to bind any peptides.

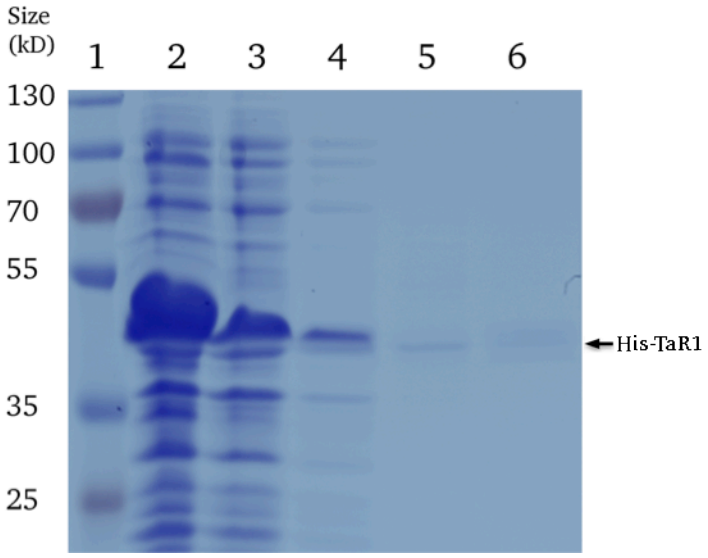

4.8. Purification of His-TaR1. A Coomassie Blue stained gel showing stages from the purification of His-TaR1. Lane 2 – total protein extract of *E. coli* expressing pDEST17-TaR1. Lane 3 – Run off after incubation with His-Bind beads. Lane 4 – Flow-through after washing with wash buffer. Lane 5 – His-TaR1 1st elution. Lane 6 – His-TaR1 2nd elution.

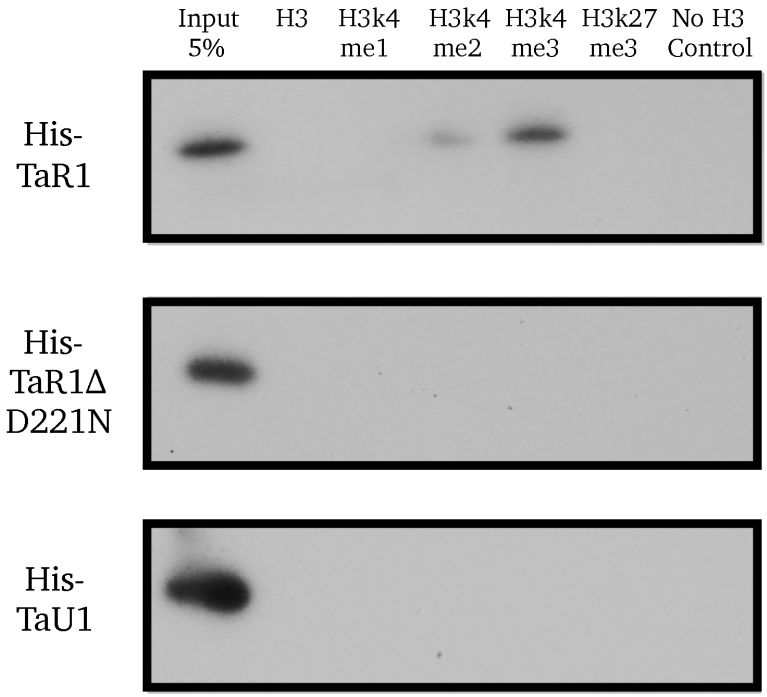

Figure 4.9. Histone Peptide Pulldown Assay. Purified His-TaR1, His-TaR1ΔD221N and His-TaU1 were incubated with biotinylated Histone peptides with no methylation (H3), monomethylated lysine 4 (H3K4me1), dimethylated lysine 4 (H3K4me2), trimethylated lysine 4 (H3K4me3) or trimethylated lysine 27 (H3K27me3), which were pulled down with streptavidin beads. Western blotting with αHis shows TaR1 to bind specifically to Histone 3 peptides, with lysine 4 methylated and particularly to trimethylated lysine 4 (H3K4me3).

4.5. *TaR1* Silencing Reduces *Z. tritici* Reproduction by Disrupting the Timing of the Life Cycle.

In order to gain a better understanding into the role of TaR1 in *Z. tritici* infection and to how silencing *TaR1* influences infection, a more detailed study of the development of the disease in silenced and non silenced plants was carried out by taking daily photographs of the infected plants, and tracking the spread of symptoms on a daily basis.

Figure 4.10. shows a representative image of each of the line infected over time. From this it can be seen that the earliest symptoms of disease appear two days earlier in *TaR1* silenced lines than they do in the non-silenced control. This finding is supported by a graph that was produced, showing the reduction in relative green leaf area in each line over the course of the infection (Figure 4.11). This graph suggests that green area disappears faster in the *TaR1* silenced lines, meaning that the necrotic symptoms of the disease are appearing earlier.

Finally, a repeat of the spore counting experiment from Chapter 3 was carried out. However, before this, the number of picnidia, the spore producing bodies of *Z. tritici*, produced on each leaf was also counted. The results from both of these are shown in Figure 4.12. and suggest that in *TaR1* silenced plants, the number of picnidia and spores produced by *Z. tritici* are halved.

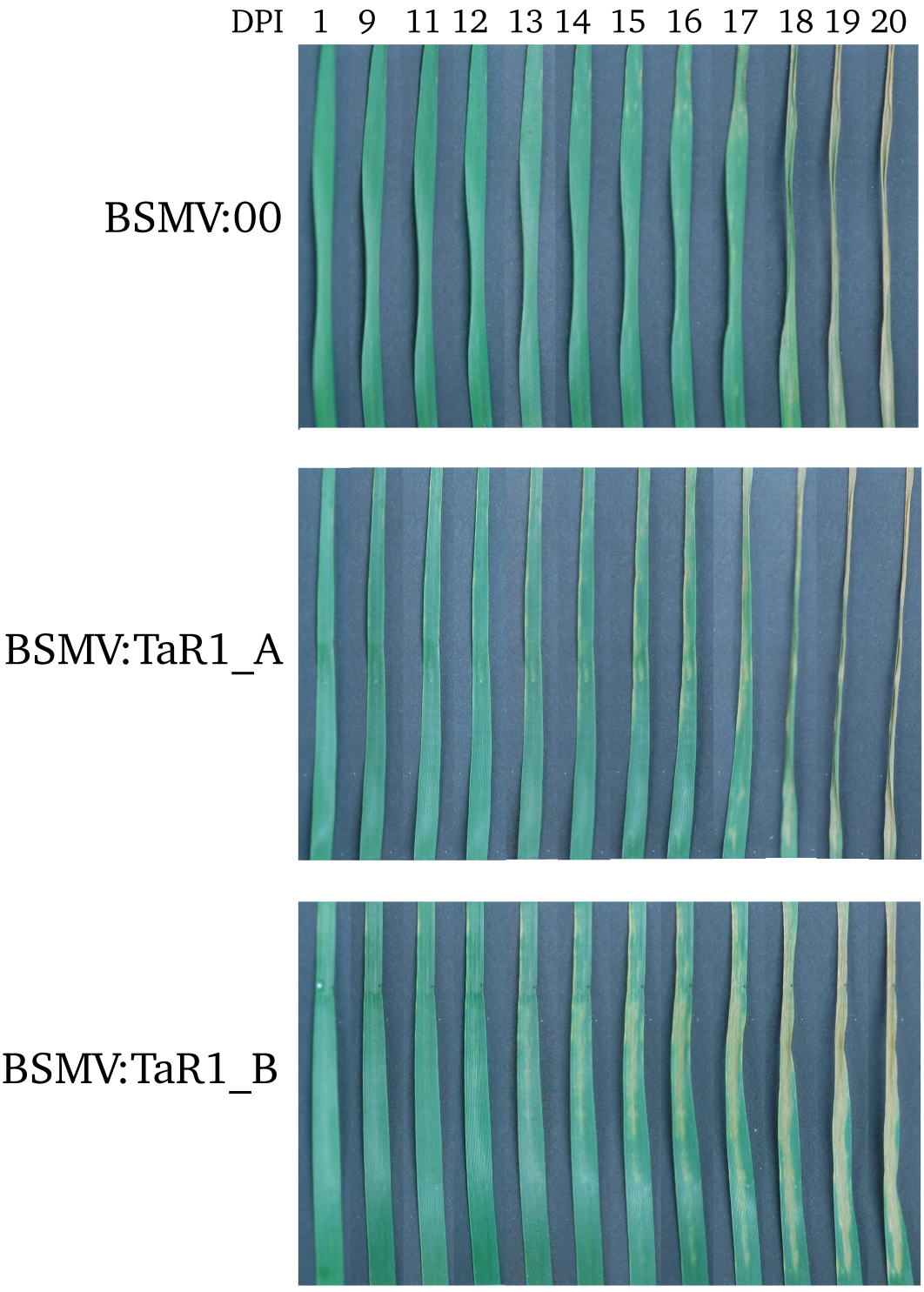

Figure 4.10. Infection Phenotype of *TaR1*-Silenced Plants. A representative image of plants either mock silenced (BSMV:00) or *TaR1* silenced (BSMV:TaR1_A BSMV:TaR1_B) plants over the course of *Z. tritici* infection. Visible disease symptoms appear earlier when *TaR1* is silenced.

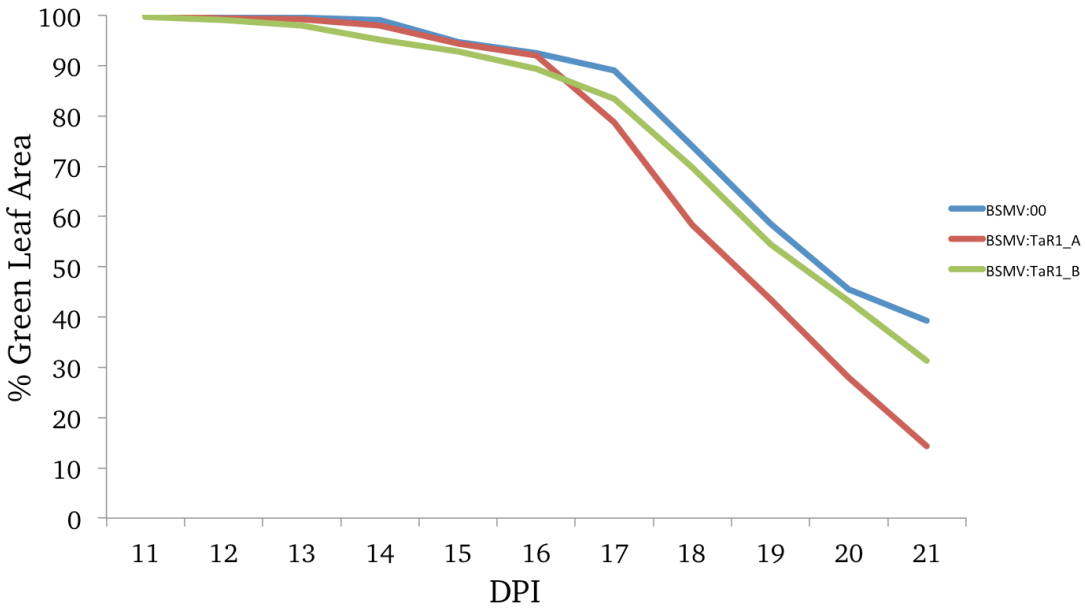

Figure 4.11. Green area percentage of *Z. tritici* infected leaves. A graph showing the percentage area of silenced (BSMV:TaR1_A, BSMV:TaR1_B) or mock silenced(BSMV:00) leaves, infected with *Z. tritici*, which remain green over time.

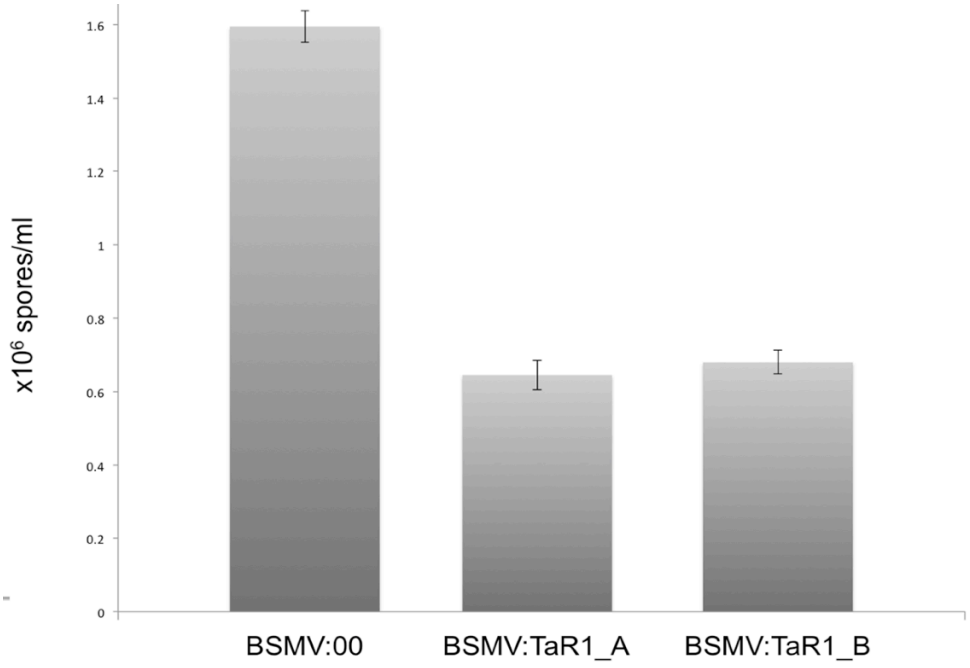

Figure 4.12. Repeated *TaR1*-Silenced Spore Count. A graph of the concentration of spores washed off mock silenced (BSMV:00) and *TaR1* silenced (BSMV:TaR1_A and BSMV:TaR1_B) 28 days after infection with *Z. tritici*.

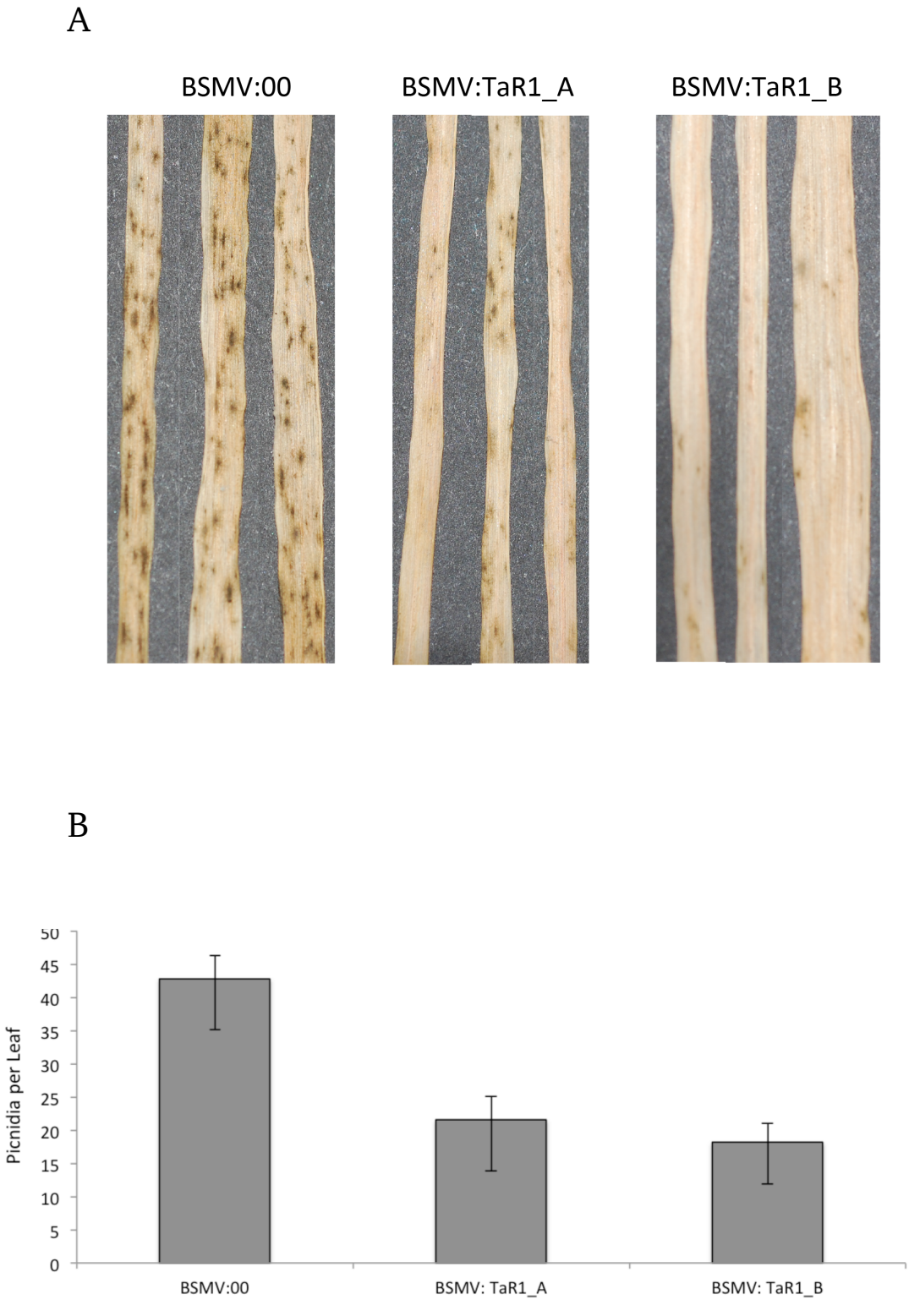

Figure 4.13. *TaR1*-Silenced Picnidia Count. Total numbers of picnidia found on mock silenced (BSMV:00) and *TaR1* silenced (BSMV:TaR1_A and BSMV:TaR1_B) leaves 28 days after infection with *Z. tritici* represented by (A) a representative image of an individual leaf from each line and (B) a graph showing the average picnidia per leaf over a sample of 12 leaves per line.

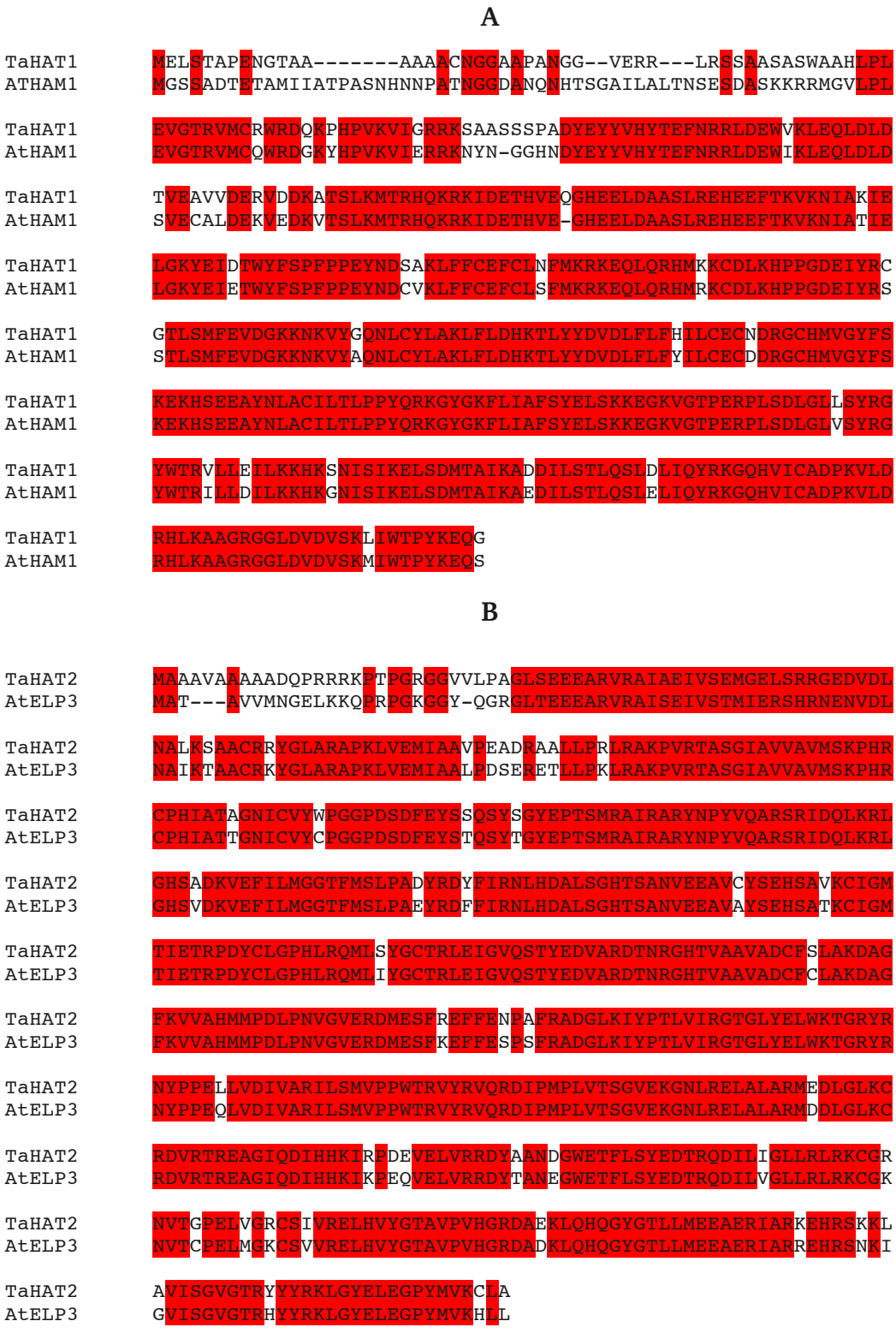

Figure 4.14. Histone Acetyl Transferase Multiple Sequence Alignments. Multiple sequence alignments showing homology between A) the wheat HAT TaHAT1 and Arabidopsis HAT AtHAM1 and B) the wheat HAT TaHAT2 and Arabidopsis HAT AtELP3. Created using Clustal Omega (1.2.1) with identical residues highlighted in red.

A

```
TaHD1       MAASGEGASLPSPAGGEDSRRRRVSYFYEPTIGDYYYGQGHPMKPHRIRMAHSLVIHYGL
AtHDA6      MEADESGISLPS---GPDGRKRRVSYFYEPTIGDYYYGQGHPMKPHRIRMAHSLIIHYHL

TaHD1       HRLLELSRPFPASEADISRFHSDEYVSFLASATGNP--TILDPRAVKRFNVGEDCPVFDG
AtHDA6      HRRLEISRPSLADASDIGRFHSPEYVDFLASVSPESMGDPSAARNLRRFNVGEDCPVFDG

TaHD1       LFPFCQASAGGSIGAAVKLNRGDADITVNWAGGLHHAKKGEASGFCYVNDIVLAILELLK
AtHDA6      LFDFCRASAGGSIGAAVKLNRQDADIAINWGGGLHHAKKSEASGFCYVNDIVLGILELLK

TaHD1       FHRRVLYVDIDVHHGDGVEEAFFTTNRVMTVSFHKYGDFFPGTGHITDVGAGEGKHYAVN
AtHDA6      MFKRVLYIDIDVHHGDGVEEAFYTTDRVMTVSFHKFGDFFPGTGHIRDVGAEKGKYYALN

TaHD1       VPLSDGIDDDTFRDLFQCIIKRVMEVYQPEVVVLQCGADSLAGNRLGCFNLSVKGHADCL
AtHDA6      VPLNDGMDDESFRSLFRPLIQKVMEVYQPEAVVLQCGADSLSGDRLGCFNLSVKGHADCL

TaHD1       RFLRSFNIPMMVLGGGGYTIRNVARCWCYETAVAVGVEPDNKLPYNDYYEYFGPDYNLHI
AtHDA6      RFLRSYNVPLMVLGGGGYTIRNVARCWCYETAVAVGVEPDNKLPYNEYFEYFGPDYTLHV

TaHD1       QPRIVENLNTTKDLENIKNMILDHLSKLEHVPNAQFHERPSDPEGPEEKEEDMDKRPAQR
AtHDA6      DPSPMENLNTPKDMERIRNTLLEQLSGLIHAPSVQFQHTPPVNRVLDTPEDDMETRPK--

TaHD1       SRLWSGGAY-DSDTEDPDNMKTEANDLSANSIMKDAS----------NDDL-----
AtHDA6      PRIWSGTATYESDSDDDDKPLHGYSCRGGATTDRDSTGEDEMDDDNPEPDVNPPSS
```

B

```
TaHDAC2       MEFWGLEVKPNQSVKVSPDDDHFLHLSQGALGEVK-KDDKATMFVKIGDQKLAIGTLSTD
ATHDT2        MEFWGVAVTPKNATKVTPEEDSLVHISQASLDCTVKSGESVVLSVTVGGAKLVIGTLSQD

TaHDAC2       KFPQIQFDLVFEKEFELSHNSKTSSVFFSGYKVFQPAEGDEMDFDSEDDSEEEEDKIIP-
ATHDT2        KFPQISFDLVFDKEFELSHSGTKANVHFIGYKSPNIEQD---DFTSSDDEDVPEAVPAPA

TaHDAC2       -ALTKENGKPEAKEQKKQVKIDTA---APSKSKAAAKDVGKSKKDDDSDDDDDSDEDNSE
ATHDT2        PTAVTANGNAGAA----VVKADTKPKAKPAEVKPA-EEKPESDEEDESDDEDESE----E

TaHDAC2       DDSGDDGALIPMEDDSDDSEDGDDSSDDNEDSSDEEEEETPKKQE-TGKKRAAGSVLKTP
ATHDT2        DDDSEKG----MDVDEDD-----SDDDEEEDSEDEEEEETPKKPEPINKKRPNESVSKTP

TaHDAC2       VTDKKAKIAT---PSGQKTGDKKGAVHVATPHPAKKAGKTPATSEKSPKSGGSVACKSCS
ATHDT2        VSGKKAKPAAAPASTPQKTEEKKKGGHTATPHPAKKGGKSPVNANQSPKSGGQSSGGNNN

TaHDAC2       -KTFNSEGALASHSK-AKHEAK
ATHDT2        KKPFNSGKQFGGSNNKGSNKGK
```

C

```
TaHDAC3      MDPSSAGAGGNSLPSVGPDGQKRRVCYFYDSEVGNYYYGQGHPMKPHRIRMTHSLLAQYG
AtHDA19      MDT-----GGNSL-ASGPDGVKRKVCYFYDPEVGNYYYGQGHPMKPHRIRMTHALLAHYG

TaHDAC3      LLDQMQVLRFNPARDRDLCRFHADDYISFLRSVTPETQQDQIRALKRFNVGEDCPVFDGL
AtHDA19      LLQHMQVLKFFPARDRDLCRFHADDYVSFLRSITPETQQDQIRQLKRFNVGEDCPVFDGL

TaHDAC3      YSLCQTYAGASVGGAVKLNHGL-DIAINWSGGLHHAKKCEASGFCYVNDIVLAILELLKH
AtHDA19      YSFCQTYAGGSVGGSVKLNHGLCDIAINWAGGLHHAKKCEASGFCYVNDIVLAILELLKQ

TaHDAC3      HQRVLYVDIDIHHGDGVEEAFYTTDRVMTVSFHKFGDYFPGTGDVRDIGHSKGKYYSLNV
AtHDA19      HERVLYVDIDIHHGDGVEEAFYATDRVMTVSFHKFGDYFPGTGHIQDIGYGSGKYYSLNV

TaHDAC3      PLDDGIDDESYQSLFKPIMAKVMEVFQPGAVVLQCGADSLSGDRLGCFNLSIRGHAECVK
AtHDA19      PLDDGIDDESYHLLFKPIMGKVMEIFRPGAVVLQCGADSLSGDRLGCFNLSIKGHAECVK

TaHDAC3      YMRSFSVPLLLLGGGGYTIRNVARCWCYETGVALGQELEDKMPVNEYYEYFGPDYTLHVA
AtHDA19      FMRSFNVPLLLLGGGGYTIRNVARCWCYETGVALGVEVEDKMPEHEYYEYFGPDYTLHVA

TaHDAC3      PSNMENKNTRYELDNIRTKLLDNLSKLRHAPSVQFQERPPDTEFPEPDEDEEDQDERHDD
AtHDA19      PSNMENKNSRQMLEEIRNDLLHNLSKLQHAPSVPFQERPPDTETPEVDEDQEDGDKRWDP

TaHDAC3      HDSDMELDY-HTPLEDSARRSTIQGTRVKRESAGAETKDQQDGSRVTGEHRGSEPMAEDI
AtHDA19      -DSDMDVDDDRKPIPS----------RVKREAVEPDTKDKDGLKGIMERGKGCEVEVDES

TaHDAC3      SPSKQ-----AHVDANAMAVDEPGNVKTESGSSTKLPDPPAIYQKP
AtHDA19      GSTKVTGVNPVGVEEASVKMEEEGTNK--GGAEQAFP--PKT----
```

D

```
TaHDAC4      MLLHSEMEIKPNPHPERPNRLRAIAASLAAAGIFPSKCALVPPRETTKEELVMVHTSDHV
AtHDA15      MLLHSEFEVKAQPHPERPDRLRAIAASLATAGVFPGRCLPINAREITKQELQMVHTSEHV

TaHDAC4      ESVEQTKNMLYSYFTSDTYANGHSACAAKLAAGLCADLASLMVSEHFQNGFALVRPPGHH
AtHDA15      DAVDTTSQLLYSYFTSDTYANEYSARAARLAAGLCADLATDIFTGRVKNGFALVRPPGHH

TaHDAC4      AGVKQAMGFCLHNNAAVAALAAQKAGAKKVLIVDWDVHHGNGTQEIFEGNKSVLYISLHR
AtHDA15      AGVRHAMGFCLHNNAAVAALVAQAAGAKKVLIVDWDVHHGNGTQEIFEQNKSVLYISLHR

TaHDAC4      HEDGSFYPGTGAADEVGVLDGKGFSVNIPWSCGGVGDNDYIFAFQHVVLPIATEFAPDIT
AtHDA15      HEGGNFYPGTGAADEVGSNGGEGYCVNVPWSCGGVGDKDYIFAFQHVVLPIASAFSPDFV

TaHDAC4      IISAGFDAARGDPLGCCDVTPAGYSQMTSMLTACSEGKLLVILEGGYNLRSISSSATEVV
AtHDA15      IISAGFDAARGDPLGCCDVTPAGYSRMTQMLGDLCGGKMLVILEGGYNLRSISASATAVI

TaHDAC4      KVLLGDGPSYGTN-AAAPSKEGMQTALQVLDIQQKYWPVLVPIFASLQAQQGPTSSKYVN
AtHDA15      KVLLGENPENELPIATTPSVAGLQTVLDVLNIQLEFWPSLAISYSKLLSELEAR--LIEN

TaHDAC4      AENKLKRRMLTGGPGPVWWKWGSKRLLYEVLFEGRRPRKSRAKGE
AtHDA15      KKNQMKRKV---VRVPTWWKWGRKKLLYNFLSARMISRSK-----
```

Figure 4.15. Histone Deacetylase Multiple Sequence Alignments. Multiple sequence alignments showing homology between A) the wheat HDAC TaHD1 and Arabidopsis HDAC AtHDA6, B) the wheat HDAC TaHDAC2 and Arabidopsis HDAC AtHDT2, C) the wheat HDAC TaHDAC4 and Arabidopsis HDAC AtHDA13 and D) the wheat HDAC TaHDAC4 and Arabidopsis HDAC AtHDA15. Created using Clustal Omega (1.2.1) with identical residues highlighted in red.

4.5. Identification of HATS and HDACs in Wheat

Histone acetylation is most commonly associated with more active transcription of the associated genes (Berger 2007), and HDACs have previously been shown to be involved in plant defence; HISTONE DEACTYLASE19 (HDA19) of Arabidopsis is induced by *Pseudomonas syringae* infection, and positively regulates defence by repression of two WRKY transcription factors (Kim *et al*., 2008), while SIRTUIN2 (SRT2) negatively regulates this response through suppression of biosynthesis of Salicylic Acid (Wang *et al*., 2010). While no HATs yet have a definitively proven role in plant defence, a number have been suggested to have a role in defence responses (Liu *et al*., 2012). As a result it was decided to identify HATs and HDACs in wheat and investigate any potential interaction with TaR1.

Using the NCBI Genbank database (Benson *et al*., 2013) a number of HATs and HDACs within the wheat genome were found to have been previously identified (Yao *et al*. 2005; Dai *et al.*, unpublished). These were *TaHAT1* (Genbank accession number DQ656605.1), *TaHAT2* (DQ656606.1), *TaHD1* (AY736125.1), *TaHDAC2* (DQ656602.1), *TaHDAC3* (DQ656603.1) and *TaHDAC4* (DQ656604.1). These sequences were aligned with HATs and HDACs previously seen in Arabidopsis. This is seen in Figures 4.14 and 4.15. which show that there is similarity between these sequences and those of known HATs and HDACs. Cloning was instigated for all of these genes, including fragments for VIGS. However, due to time constraints this could not be completed within the timeframe of the project.

4.6. Conclusions

4.6.1. TaR1 Function

From the results of alignments and phylogenetic trees within this chapter (Figure 4.1) as well as that in Chapter 3, it can be concluded that TaR1 shows a strong homology to a group of Alfin1-like PHD domain proteins, which are conserved across the plant kingdom (Lee *et al*. 2009), from Arabidopsis and rice, as well as Alfin1, a PHD domain originally discovered in alfalfa (Bastola *et al*. 1998). From this it can be concluded that TaR1 is likely a wheat Alfin1-like protein.

In the same study that identified AL1-7 (Lee *et al*. 2009) it was found that many proteins containing the canonical PHD domain sequence were also predicted to localise to the nucleus and regulate or interact with chromatin. We have shown (Figure 4.3. 4.4. and 4.5.) that TaR1 is also nuclear localised. This suggests that it could have a role associated with chromatin and, given that six of the seven homologous Arabidopsis AL proteins bind to the H3k4me3 modification, this was likely to be the mode of TaR1-chromatin interaction.

In Figure 4.6. and Figure 4.7. it was shown that TaR1 is capable of binding to TaH3 *in planta*, while Figure 4.9. shows that TaR1 binds specifically to H3k4me2/3. Equally, it shows that disruption of a residue important in forming the aromatic cage prevents binding. Together these suggest that TaR1 is a histone-binding protein, which specifically recognises the H3k4me3 modification, and that its binding is in the same manner as other AL proteins.

While little else is known of OsAL1, AtAL1-5 or AtAL7, other than their possession of a PHD domain and homology to other AL proteins, AtAL6 has been found to form part of a complex, which affects the transcription of seed development genes (Molitor *et al*. 2014). As the recruitment of chromatin-remodelling complexes is a common function of PHD domain proteins (Shi *et al*. 2006; Taverna *et al.* 2006; Wysocka *et al*. 2006) it is likely that, if TaR1 does interact with chromatin, it will be through this method.

If TaR1 is interacting with chromatin through association with a chromatin-remodelling complex, it is possible that this complex would also involve a HAT or HDAC, as the action of these has been linked with that of PHD domains often (Schindler *et al*, 1993; Shi *et al*., 2006; Taverna *et al*., 2006; Li *et al*., 2007.). Figures 4.14. and 4.15. show that a number of HATs and HDACs do exist within the genome. While there was not time to further analyse these genes within this project, an investigation into a possible interaction between these and TaR1 would be a good starting point for a future investigation into the mechanism for TaR1 function.

In particular, *TaHDAC3* shows specific similarity to *AtHDA19*, a positive regulator of plant defence (Kim *et al*., 2008) while *TaHDAC4* shows a close homology to *AtSRT2,* which acts negatively in the plant defence response (Wang *et al*., 2010). These two

wheat HDACs may, therefore, be the best candidates for an interactor of TaR1, which would alter chromatin structure in response to pathogen recognition.

4.6.2. Role of TaR1 in *Z. tritici* Infection

The results of Chapter 3 had already shown that *Z. tritici* infection is altered in *TaR1* silenced wheat, with fewer spores produced. In Figure 4.12. this result was reproduced with half as many spores developing on *TaR1*-silenced plants compared to the mock silenced control. It is also shown in Figure 4.13. that fewer picnidia are produced by *Z. tritici* on *TaR1* silenced plants. This suggests that the reduction in spores is as a result of fewer picnidia developing, rather than each producing fewer spores.

Figure 4.11. shows a graphical representation of the development of disease symptoms in *TaR1* silenced and mock silenced wheat lines infected with *Z. tritici*. For each line tested, eight leaves were selected to analyse development of symptoms. Leaves were photographed daily and the green area present on each leaf was calculated. The green area measurement was carried out using the image analysis software imageJ. However, due to the varying shades of greens present across the leaves, and the range of yellow and brown shades produced during infection, the programme was not able to adequately distinguish between healthy areas and some lesions. As a result, the green area had to be individually drawn and measured for each leaf. This method does show the same overall trend: that lesions develop faster in *TaR1* silenced plants.

Due to the requirement for human intervention to differentiate between infected and non-infected leaf tissue, the quantification of the green and brown leaf areas is no more useful than close observation of each leaf. This method was employed in Figure 4.10. In this figure, it can be clearly seen that the earliest symptoms of *Z. tritici* infection appear up to two days earlier in *TaR1* silenced plants, supporting what is seen in Figure 4.11. Silencing *TaR1*, therefore, brings forward disease symptoms, but reduces spore production.

Z. tritici relies on stealth pathogenesis to avoid host sensing during its biotrophic growth phase (Goodwin *et al.* 2011). During this time it increases biomass, until the switch to necrotrophism and the production of picnidia within necrotic lesions. It is possible, therefore, that the reduction in spore production in *TaR1* silenced plants is due to an earlier host recognition event, leading to a Hypersensitive Response (HR). The cell

death of HR would force *Z. tritici* to switch to necrotrophic growth and its reproductive phase earlier, and possibly before it reaches the desired levels of biomass. Reproducing before reaching this biomass then is the cause for the reduction in picnidia and spores.

This mechanism would suggest that, as part of its stealth pathogenesis approach, *Z. tritici* is hi-jacking an existing cell death-repressing role of TaR1 within the plant to prevent a response in case of recognition. Such hi-jacking of host signalling is seen by many pathogens (Robert-Seilaniantz *et al.* 2011) including *Z. tritici* (Hammond-Kosack and Rudd 2008).

In summary, it seems from the results in this chapter that *TaR1* plays a role in repressing cell death. It is assumed that this is achieved by recruiting a chromatin remodelling complex onto specific areas of chromatin and, in doing so, altering the transcription of certain target genes. This function is then hi-jacked by *Z. tritici* in order to prevent a host cell death response until it has reached the required biomass for completely efficient reproduction.

While the role of TaR1 has been examined though loss-of-function gene silencing experiments, Chapter 5 will attempt to compliment this with a stable transgenic line over expressing *TaR1*.

Chapter 5

Analysis of Transgenic *TaR1* Overexpressing Lines

5.1. Introduction

Having identified TaR1 as a target involved in the interaction between wheat and *Zymoseptoria tritici* in Chapter 3, Chapter 4 analysed the function of TaR1, and also confirmed the phenotype of a loss-of-function of TaR1. In order to examine this further, transgenic lines overexpressing *TaR1* was produced. These lines were tested, to see if they possessed opposite infection phenotype, an increased susceptibility to *Z. tritici*, and whether there were any differences to growth or development.

Transgenic plants were produced by the National Institute of Agricultural Botany (NIAB, Huntingdon Road, Cambridge) under their BBSRC funded Community Resource for Wheat Transformation. Agrobacterium-mediated transformation was used to transform Fielder variety wheat plants with an Agrobacterium strain containing the *TaR1* sequence within the vector pSC4Act-R1R2-SCV (Biogemma.com). This vector overexpresses genes via the rice actin promoter and contains the kanamycin resistant selection gene *NPTII (*Carrer *et al*., 1993).

After production of transgenic plants, these plants were tested by PCR at NIAB for presence of the *TaR1* sequence, using *TaR1*-specific primers, and for the full-length insert, using a forward primer from the rice actin promoter and a reverse primer from the Nos terminator sequence. The copy number of the transgene in these plants was also determined at NIAB by qPCR using Taqman probes (Applied Biosystems) targeted to the *NPTII* selection gene.

In order to determine the level of protein expressed in these lines it was decided to produce an anti-TaR1 antibody, using the Durham University antibody production

facility. This antibody was produced in rabbits, using purified His-TaR1 protein, as seen in Chapter 4.

Once it had been determined that these lines are indeed overexpressing *TaR1*, they could be infected, to test whether they show the opposite infection phenotype to *TaR1* silenced plants. However, since the silencing phenotype had only been established in Avalon variety plants, it would first need to be verified that *TaR1* could be silenced in fielder.

As well as the infection phenotype, the generation of a stable transgenic line, rather than the transient effects of BSMV VIGS, would allow a more in depth analysis of the growth of plants with altered *TaR1* expression under normal conditions. As such, a sample of the lines were grown to maturity and allowed to set seed, so that phenotypic measurements of the growth and development of these plants could be compared with the wild type.

5.2. Transgenic *TaR1* Overexpression Lines

30 T_0 transformants, along with four non-transformed controls, were provided by NIAB, as listed in Table 5.1. Each of these plants was grown to maturity, and the seed from each was collected as independent lines. It was then decided, from these, to only work on those that NIAB had identified as being one or two copy number. The lines chosen were TaR1 OX11, 12, 13, 17, 23, 25, 27, 32. This is shown in Table 5.1., along with the presence of the full-length construct, as demonstrated by PCR using a forward primer from the promoter region and reverse primer from the terminator is included.

Table 5.1. TaR1 Transgenic Lines

Plant Number	Line Name	Copy Number qPCR	Promoter – > Terminator PCR
CW5.1	TaR1 OX1	2	+
CW5.2	TaR1 OX2	4+	+
CW5.3	TaR1 OX3	4+	+
CW5.4	TaR1 OX4	2	+
CW5.5	TaR1 OX5	4	+
CW5.6	TaR1 OX6	4+	+
CW5.7	TaR1 OX7	2	+
CW5.8	TaR1 OX8	4+	+
CW5.10	TaR1 OX10	2	+
CW5.11	TaR1 OX11	1	+
CW5.12	TaR1 OX12	1	+
CW5.13	TaR1 OX13	1	+
CW5.14	TaR1 OX14	2	+
CW5.15	TaR1 OX15	4+	+
CW5.16	TaR1 OX16	4+	+
CW5.17	TaR1 OX17	2	+
CW5.18	TaR1 OX18	4+	+
CW5.19	TaR1 OX19	4+	+
CW5.21	TaR1 OX21	4+	+
CW5.22	TaR1 OX22	4	+
CW5.23	TaR1 OX23	1	+
CW5.24	TaR1 OX24	4+	+
CW5.25	TaR1 OX25	1	+
CW5.26	TaR1 OX26	3	+
CW5.27	TaR1 OX27	1 or 2	+
CW5.28	TaR1 OX28	3	+
CW5.29	TaR1 OX29	4	+
CW5.30	TaR1 OX30	4+	+
CW5.31	TaR1 OX31	4+	+
CW5.32	TaR1 OX32	1	+
CW5.con1	-	0	-
CW5.con2	-	0	-
CW5.con3	-	0	-
CW5.con4	-	0	-

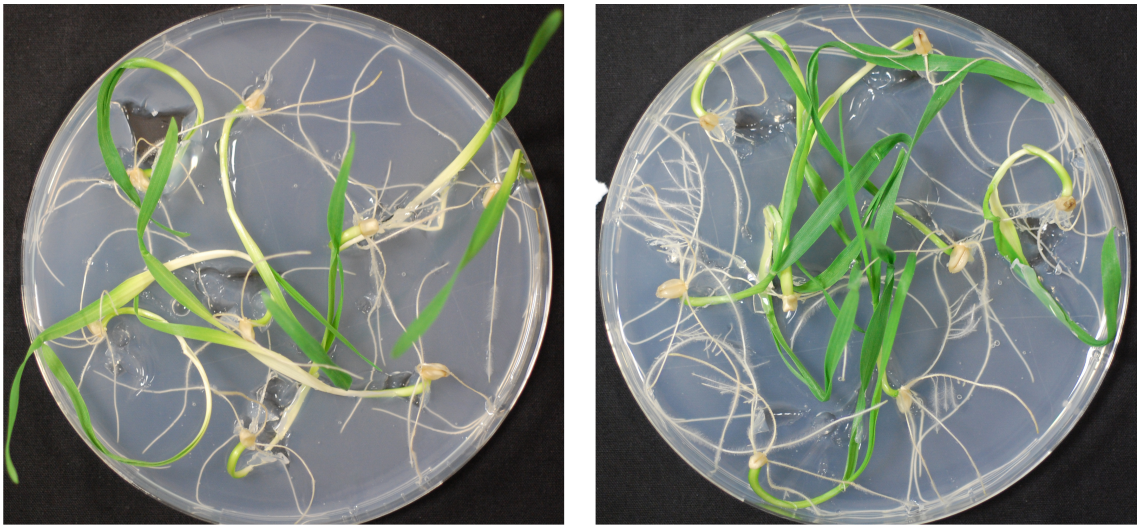

Figure 5.1. Kanamycin Selection Plates. Photographs showing germination of wild type seeds and the TaR1 OX11 *TaR1* overexpressing lines on 600µg/ml kanamycin plates.

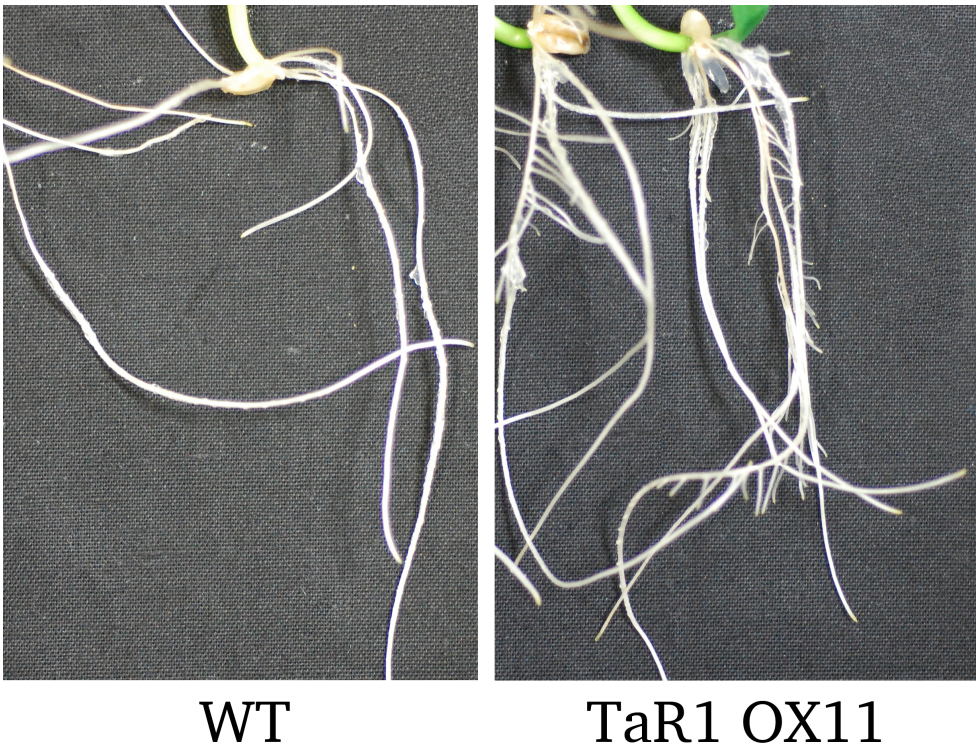

Figure 5.2. Kanamycin Selection Lateral Roots. Photographs showing no lateral roots develop on wild type (WT) seedlings grown on 600µg/ml kanamycin plates, while they develop fully on the TaR1 OX11 *TaR1* over expressing line under the same conditions.

5.3. Transgenic Plant Selection

The seeds used for these experiments were T_1, and thus is it was necessary to select for transformants. The vector used for transformation contains the kanamycin resistance gene *NPTII*, and so plants were grown on solid media with kanamycin. Unfortunately, as is seen in Figure 5.1. almost all seeds sown germinated on kanamycin selection plates, including the non-transformed fielder wild type plants, even at a concentration of 600µg/ml.

However, on closer inspection it was noted that, while most plants from the transformed lines did produce lateral roots, none of the wild type plants produced lateral roots on any kanamycin selection plate (figure 5.2.). It was speculated that, while these concentrations are sufficient to kill plants such as Arabidopsis, the much larger seed of wheat allows it to survive for much longer. It has also been noted that, among many defects of Arabidopsis grown on kanamycin is a complete lack of lateral root formation (Duan *et al*., 2009). Although this has not previously been reported in wheat, it was suggested that those with lateral roots on kanamycin selection contained the transgene.

In order to test this hypothesis, genomic DNA was extracted from seedlings with and without lateral roots and PCR was carried out using primers designed to amplify the *NPTII* gene. As can be seen in Figure 5.3. these primers did produce a band in the wild type fielder plants. However, a second band of the correct anticipated size was present in the positive control (a vector containing the *NPTII* gene) as well as all samples from plants with lateral roots, but not plants without. This suggests that plants that develop lateral roots on kanamycin selection all contain the transgene, and that germinating seeds on these plates and selecting those which develop lateral roots, is a suitable form of transgenic selection. While one plant without lateral roots does produce the band, this could be because those roots were slower in developing or were missed. However, false negatives such as this were considered to be acceptable as long as there were no false positives.

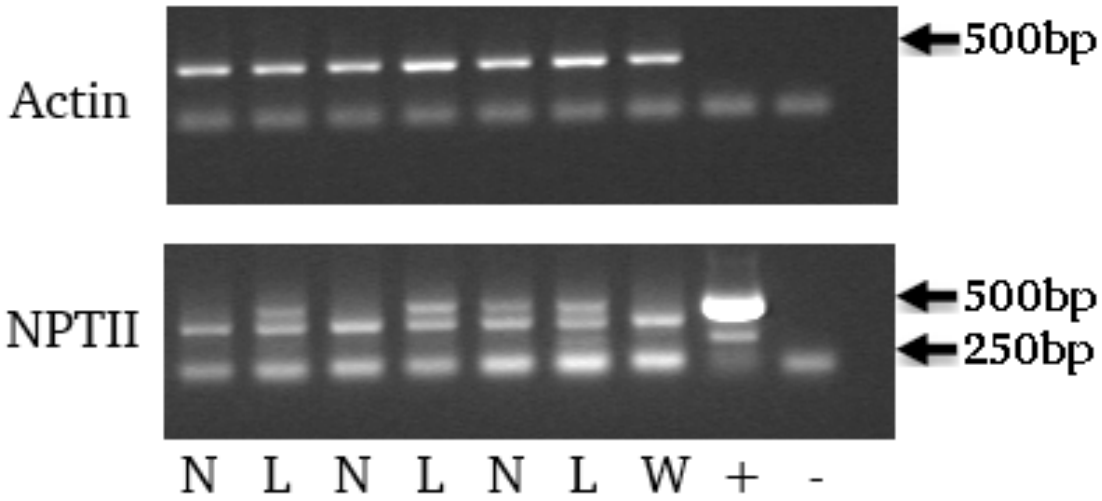

Figure 5.3. PCR Amplification of *NPTII*. Gel image showing the PCR product after amplification with primers designed to the *NPTII* gene (expected size: 493bp). Included are three independent pooled samples of *TaR1* over expressing lines without lateral roots (N) or with lateral roots (L) as well as a wild type sample (W), a positive control (+) containing the kanamycin resistant plasmid pEARLYGATE104 and a negative control (-) containing no cDNA. Actin is included as a positive control for each cDNA.

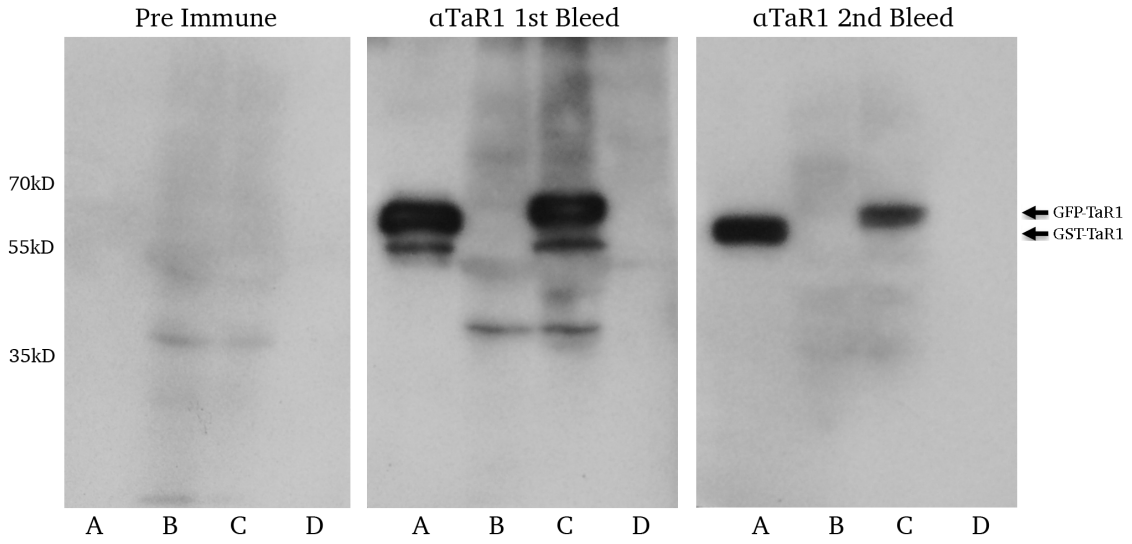

Figure 5.4. αTaR1 Test. Western blot probed with Pre-immune and two separate bleeds of αTaR1 at a 1:1000 concentration, incubated for two hours, using anti-rabbit secondary antibody at 1:20000 incubated for one hour. In each blot, each lane contains the following: A) purified GST-TaR1, B) pEARLYGATE104:00 infiltrated *N. benthamiana*, C) pEARLYGATE104:TaR1 infiltrated *N. benthamiana*, D) wheat total protein extract.

5.4. Analysing RNA and Protein Expression in Over Expression Lines

5.4.1 Testing Anti-TaR1 Antibody

As mentioned in the introduction, an anti-TaR1 antibody was produced in rabbit at the Durham University antibody production facility. Before it could be used to determine the levels of TaR1 in various lines, it first had to be tested to ensure that it could detect the TaR1 protein. Purified TaR1, protein extract from *Nicotiana benthamiana* leaves transiently expressing YFP-TaR1 and total protein extract from wheat leaves were run on an acrylamide gel and probed with the anti-TaR1 antibody, as well as the pre-immune serum as a control. As can be seen in Figure 5.4. anti-TaR1 is capable of detecting bands at the expected size for both the purified TaR1 and the *N. benthamiana* expressed TaR1, while it is not seen in the pre-immune. However, no band of the expected size is seen in the wheat extract. This could be due to very low expression of TaR1, and so a number of methods were attempted to visualise TaR1 in wheat protein extracts.

5.4.2. Improving TaR1 Detection by αTaR1

As anti-TaR1 was unable to detect TaR1 in wheat total protein extract, the method required altering in order to see the protein. It had been assumed that the problem resulted from the low expression of TaR1, and so the first modification was to concentrate the TaR1 protein, and run a much larger volume on the gel. However, as seen in Figure 5.5. this was not successful, and still no band was present for TaR1.

Attempts were then made to optimise the Western Blotting conditions, with the aim that the optimal antibody concentration, incubation time or blocking reagent might improve the overall quality of anti-TaR1 Western Blotting, and thereby allow the band for TaR1 to be seen in the wheat extract. A wide range of conditions were used, ranging the incubation time from one hour to three hours and the concentration of anti-TaR1 from 1:500 to 1:5000, using milk and BSA as blocking reagents from 1-5% and including the blocking reagent at 1% with the primary antibody. A sample of results from these attempts are shown in Figure 5.6. but, unfortunately, none were able to detect TaR1.

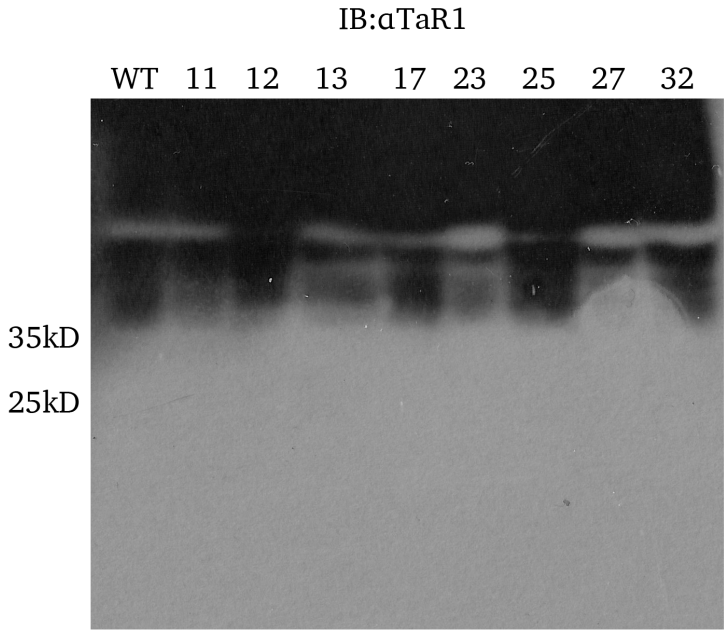

Figure 5.5 High Protein Concentration αTaR1 Western Blot. A western blot of total protein of wild type (WT) and *TaR1* over expressing lines (11,12,13,17,23,25,27,32) samples concentrated to 5mg/ml, probed with αTaR1.

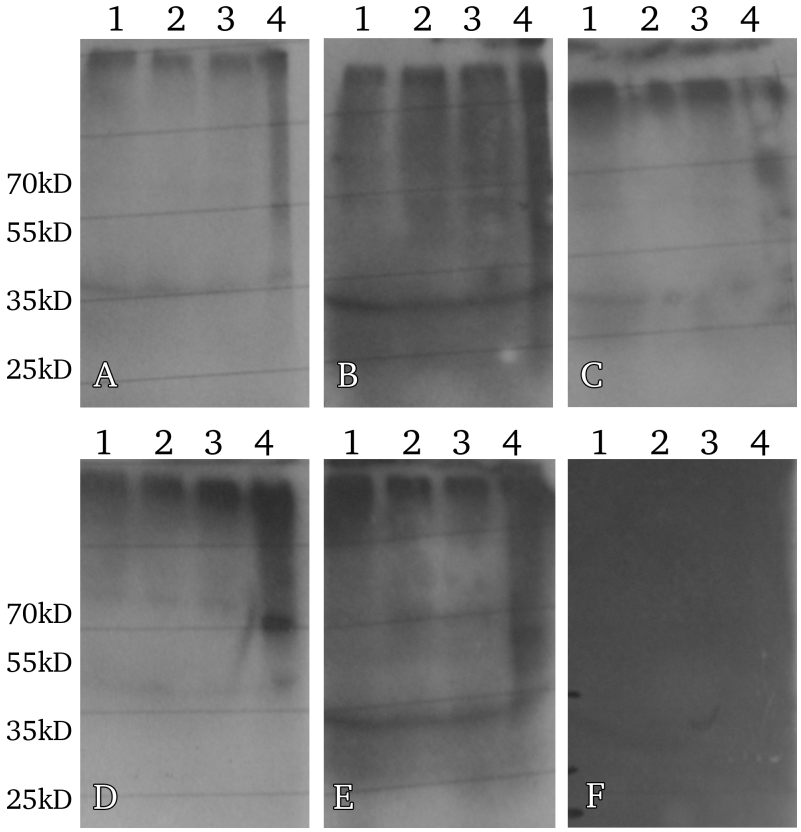

Figure 5.6. αTaR1 Western Blot Optimisation. Western blots of total protein from: 1) wild type, 2) BSMV:TaR1_A, 3) TaR1 OX11, 4) GST-TaR1, under various conditions. A) 1:5000 primary (5% milk), B) 1:5000 (0% milk), C) 1:5000 (5% BSA), D) 1:10000 (5% milk), E) 1:10000 (0% milk), F: 1:1000 (5%milk).

Since we had previously shown that TaR1 was present in the nucleus, it was hypothesised that a low level of *TaR1* expression might result in it not being present at a high enough concentration to visualise because of the large amount of cytosolic protein in the sample. It was, therefore, decided to isolate the nuclei of wheat leaves, using a method adapted from Sikorskaite *et al*. (2013). The method was verified, as shown in Figure 5.7. by probing with antibodies for UGPase, as a cytosolic control, and for Histone 3, as a nuclear control. Figure 5.7. shows that UGPase is present only in the total extract, and not in the nucleus, while Histone 3 is present in the total extract, but is enriched in the nuclear fraction. This is as expected, as some nuclear proteins will be present in a total protein extract, but cytosolic proteins should not be present in the nucleus. However, no band for TaR1 appears in either the total or the nuclear fraction.

After this, it was speculated that, rather than an issue of protein concentration, the antibody itself was pure enough to detect high levels of protein, such as those seen in the purified and transiently over expressed samples, but not in the total wheat extract. As a result, the antibody was purified, using the AminoLink® Plus Immobilization Kit (Thermo Scientific). This method produced six different fractions of purified antibody, which were used to probe purified TaR1 protein, in order to ascertain which fractions contained the purified antibody, and which of those were the most efficient at detecting TaR1. The results of this are shown in Figure 5.8. and suggest that the second fraction is the best for further use. However, when this fraction was used to probe a wheat total protein extract (Figure 5.9.) no band for TaR1 was seen. While a band of approximately 50kD was seen in wheat total protein extract in these blots, it was considerably larger than the predicted size of TaR1 (28kD) and at this point it was decided to determine the levels of TaR1 overexpression via qPCR to detect the levels of RNA transcribed.

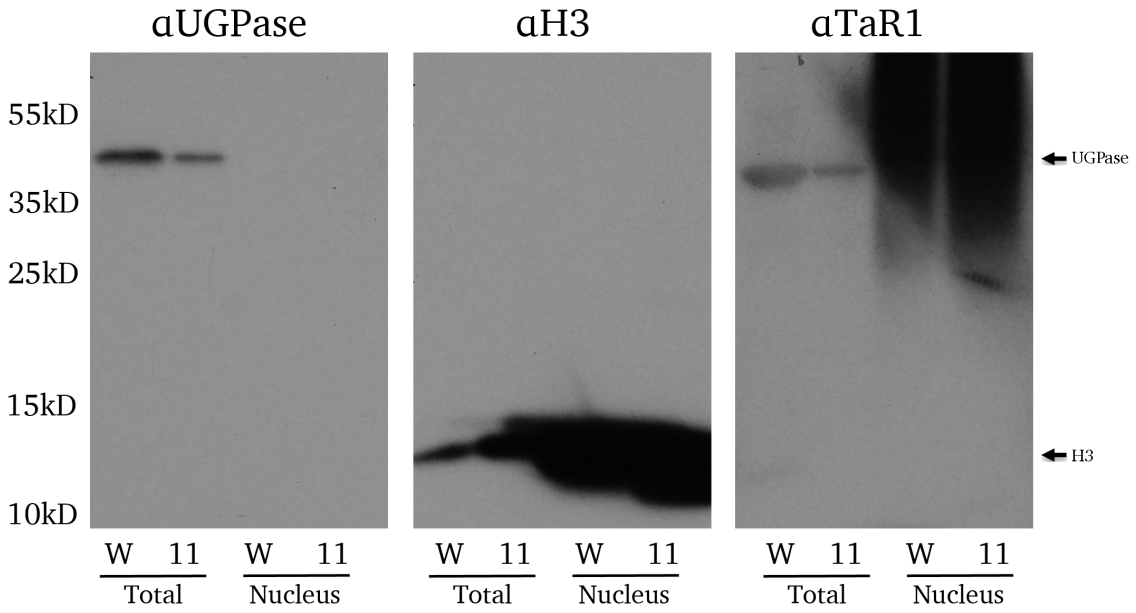

Figure 5.7. Nuclear Isolation Western Blot. Western blot of total protein extract (Total) and isolated nuclei protein extract (Nucleus) from wild type (W) and TaR1 OX11 (11) leaves, probed with αUGPase, αH3 and αTaR1.

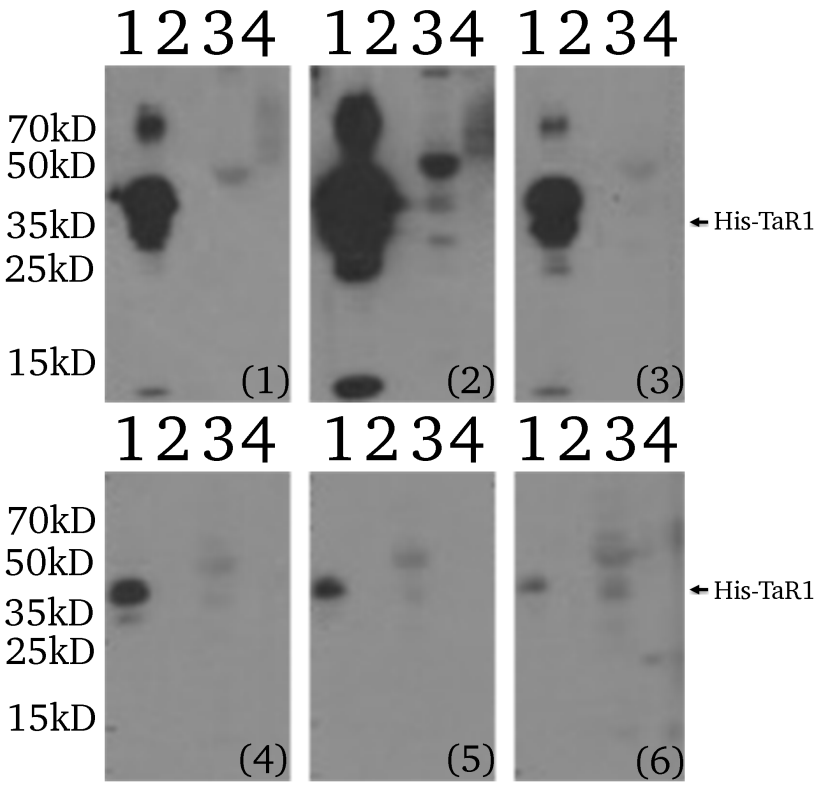

Figure 5.8. Antibody Purification Western Blot. Western blot probed with six αTaR1 elutions from AminoLink® Plus Immobilization Kit, labelled (1), (2), (3), (4), 5), (6). Each blot consists of the following four lanes: 1) Purified His-TaR1, 2) Non-transformed *E. coli* protein extract, 3) Wheat total protein extract, 4) Wheat nuclear protein extract.

5.4.3. Analysing *TaR1* Overexpression by qPCR

In order to test whether *TaR1* was being transcribed at higher levels in the *TaR1* overexpression lines, seeds were germinated on plates with 200 μg/ml kanamycin for all of the selected lines, and those which developed lateral roots were taken, and their RNA extracted. As a control, plants which did not develop lateral roots and therefore were considered to be null segregants, were also taken in one pooled sample, as were wild type fielder seedlings grown on plates without kanamycin. cDNA was the produced from each of these RNA samples, and all equalised to the same concentration.

qPCR was carried out on all of the cDNA samples, to compare the levels of *TaR1* expression. The results of this (Figure 5.10.) show that the majority of the lines are within the same levels of expression as the wild type and null segregants, which suggest that these lines are not over expressing *TaR1*. Meanwhile, lines OX25 and OX32 show a slight upregulation of TaR1 compared to the wild type and null segregants. However, even these lines are still well below the threshold of 2x expression.

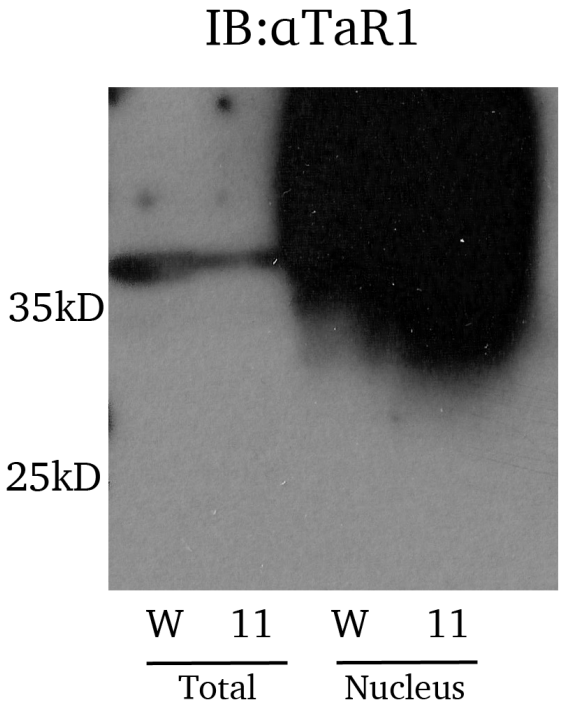

Figure 5.9. Western Blot with Purified αTaR1. A western blot of total protein extract (Total) and isolated nuclei protein extract (Nucleus) from wild type (W) and TaR1 OX11 (11) leaves, probed with purified αTaR1 (elution 2 from Figure 5.8).

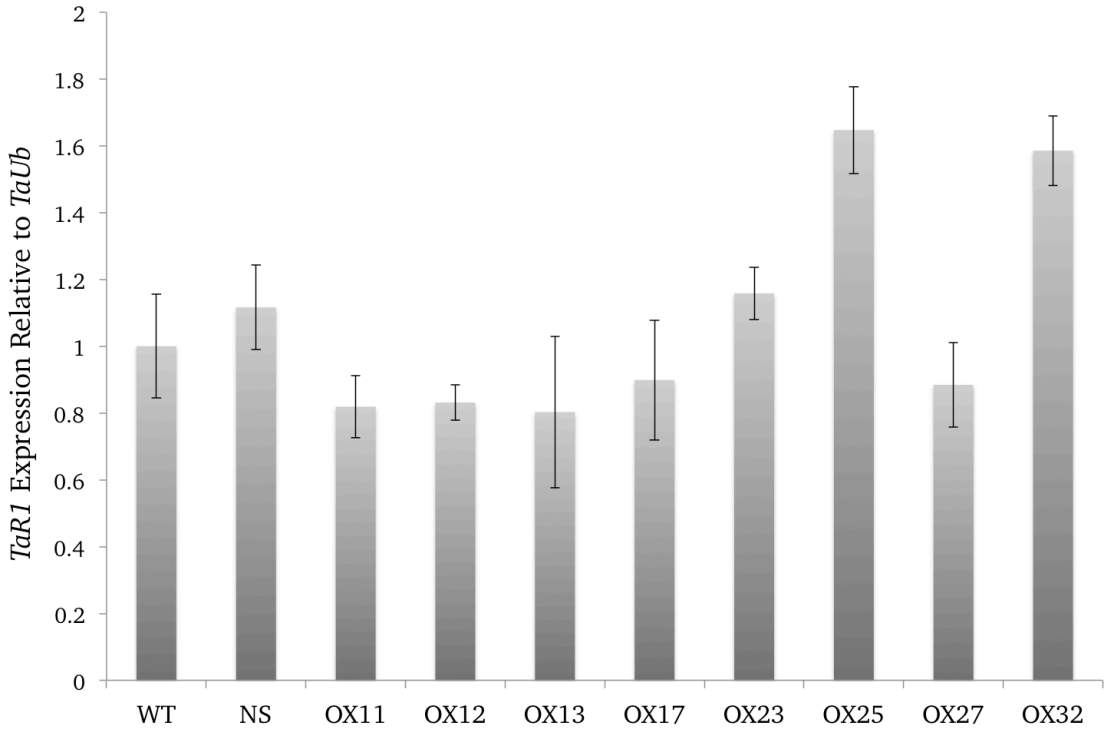

Figure 5.10. *TaR1* Expression qPCR. Real Time qPCR data showing the level of expression of *TaR1* in wild type (WT) leaves compared to null segregants (Null) and *TaR1* over expressing transgenic lines (TaR1 OX11,12,13,17,23,25,27,32).

5.5. *TaPDS* Silencing in Fielder Variety Wheat

While all previous work had been carried out in avalon variety wheat, the *TaR1* over expressing lines were transformed into fielder variety. In order to be able to directly compare *TaR1* silenced plants with *TaR1* over expressing plants, it was therefore necessary to determine whether BSMV VIGS was effective in the Fielder variety. As before, this was tested using the BSMVγ:*TaPDS* construct. Figure 5.11. shows that the wheat leaf phenotype expected from *TaPDS* silencing is clearly present in the leaves infiltrated with the BSMVγ:*TaPDS*, but not in those infiltrated with the BSMV:00 control.

5.6. Infection of Fielder Variety Wheat with *Z. tritici*

Anticipating that *TaR1* over expressing lines would be verified, and given that BSMV VIGS was effective in Fielder, an infection assay was set up, as before with a spore concentration of $7.5x10^5$ spores/ml of the *Z. tritici* strain IPO323, on fielder variety wheat, so that conditions could be optimised for a further experiment with all of the selected over expression lines and the BSMV:TaR1_A and BSMV:TaR1_B silencing lines. However, after 28 days, no obvious visible symptoms of infection could be seen, suggesting that no infection was possible using the Fielder variety and IPO323 under the previously used conditions.

In order to test this further, another assay was arranged, using only wild type Fielder plants, with a range of spore concentrations from $5x10^5$ to $5x10^6$ spores/ml. This infection was left for 42 days, well past the normal length of infection, but still no major symptoms of infection were visible, as seen in Figure 5.12. This result was repeated, after which it was decided not to continue with the infection phenotype analysis, due to a lack of time to further trouble-shoot the infection assay.

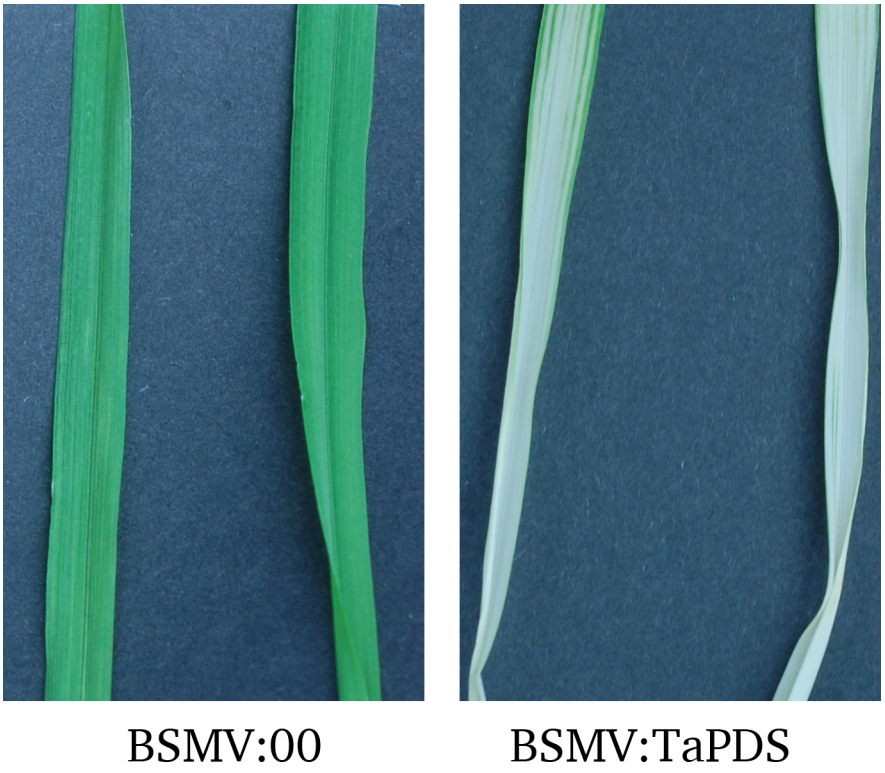

Figure 5.11. *TaPDS* Silencing in Fielder Wheat. Photographs showing green leaves of mock silenced (BSMV:00) fielder variety wheat and *TaPDS* silenced leaves (BSMV:TaPDS) with a distinct white pattern.

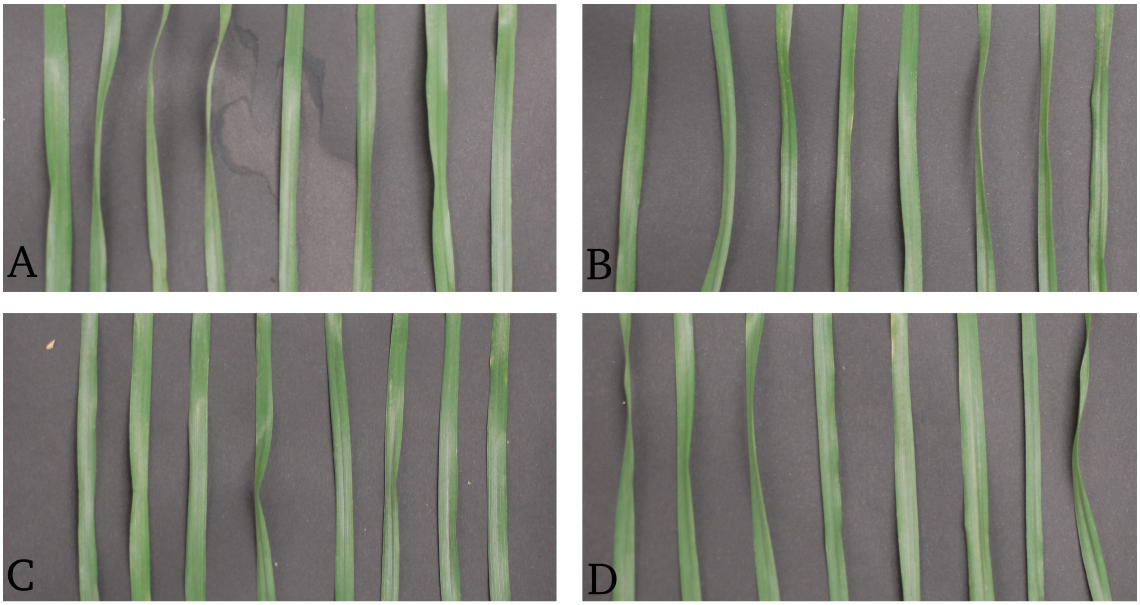

Figure 5.12. Fielder Infection with *Z. tritici* IPO323. Fielder variety wheat leaves 42 days after infection with *Z. tritici* strain IPO323 at A) $5x10^5$, B) $1x10^6$, C) $2x10^6$, D) $5x10^6$ spores/ml.

5.7. Analysis of Growth and Development of *TaR1* Overexpressing Lines

5.7.1. Growth of *TaR1* Overexpressing Lines

All of the selected *TaR1* overexpressing lines were allowed to grow to maturity, along with wild type Fielder plants. Growth data for each line was taken, measuring the overall height of each plant, as well as the number of leaves produced, the internode length and the number of tillers produced on each plant. While the data is only shown for the wild type and TaR1 OX25 and 32 lines, all lines were grown and, as a result, limited space allowed for only two plants of each line. These results were averaged out over lines and are shown in Table 5.2. along with a Student's *t*-test comparing each line to the wild type.

No statistically significant difference was seen in the height or node length of the lines, suggesting that their overall growth was similar. TaR1 OX25 did produce fewer tillers than the wild type, but TaR1 OX32 did not. Given the small sample size and low numbers involved, this effect could very easily be by chance, and would not be seen in a larger sample size. While the leaf number showed no statistical significance, there does appear to be a difference between the lines. However, any difference could be explained by tiller number, with each line producing a very similar number of leaves per tiller (WT: 5.3, TaR1 OX25: 5.5, TaR1 OX32: 5).

Table 5.2. *TaR1* Overexpression Adult Plant Growth Analysis

	Height (mm)	**Height *t*-test**	**Tillers**	**Tillers *t*-test**	**Leaves**	**Leaves *t*-test**	**Node Length (mm)**	**Node Length *t*-test**
Wild Type	580.5	X	3.5	x	18.5	x	106.8	x
TaR1 OX25	597.5	0.375	2	0.048*	11	0.054	103.9	0.161
TaR1 OX32	583.5	0.478	3	0.211	15	0.162	93.8	0.211

- Statistically significant (p value < 0.05).

5.7.2. Flowering Development of *TaR1* Overexpressing Lines

In order to assess whether there were differences in the development of flowering between the wild type and lines overexpressing *TaR1* the age of each plant at the point of head appearance was recorded, along with the height of the plant at this stage. The results of this are displayed in Table 5.3. along with a Student's *t*-test comparing each line to the wild type.

As seen above in tiller production, there is a significant difference between one OX line (TaR1 OX25) and the wild type, but not with the other (TaR1 OX32) in the age at flowering. This result could also be explained by the small sample size, but there was a large difference between the latest flowering TaR1 OX25 plant and the earliest of any other line, suggesting the result could be genuine. The height at flowering, however, showed no difference between any lines, suggesting that any difference in flowering time is not related to faster growth.

Table 5.3. *TaR1* Overexpression Flowering Development Analysis

	Flowering Age (days)	**Flowering Age *t*-test**	**Flowering Height (mm)**	**Flowering Height *t*-test**
Wild Type	71.5	x	412.5	x
TaR1 OX25	61.5	0.038*	411	0.485
TaR1 OX32	70.5	0.382	408	0.456

* Statistically significant (p value < 0.05).

5.7.3. Yield of *TaR1* Overexpressing Lines

To assess any differences in yield between the wild type and lines over expressing *TaR1*, all plants were allowed to set seed, which was dried and collected. The total weight of seed produced by each plant was recorded. In order to better determine whether any yield differences were the result of a higher number of seeds, or a higher seed quality or size, the weight per 100 grains was calculated for each line. The results of these measurements are displayed in Table 5.4. along with a Student's *t*-test comparing each line to the wild type.

The 100-grain weight is consistent between lines, with no significant differences, and so it can be assumed that all seeds produced were of a similar size and quality. There was a difference, however, in the total yield, with TaR1 OX32 producing a much larger yield than the other two lines. Once again, a significant difference has been shown for one OX line, but the other. Although this could again be due to the small sample size, there is also the possibility that this disparity is caused by the different tiller production.

While TaR1 OX25 produced a similar yield to the wild type, it did so from four total heads, while the TaR1 OX32 and the wild type yields were produced from six and seven heads respectively. Adjusted numbers show that TaR1 OX25 and 32 produced a similar yield per head (62.5g and 59.3g), this number for the wild type was considerably lower (37.9g).

Table 5.3. *TaR1* Overexpression Yield Analysis

	Total Yield (g)	**Total Yield *t*-test**	**100-Grain Weight (g)**	**100-Grain Weight *t*-test**
Wild Type	132.5	x	270.5	x
TaR1 OX25	125.5	0.123	267	0.392
TaR1 OX32	178	0.007*	276	0.353

* Statistically significant (p value < 0.05).

5.8. Conclusions

As direct transformants were received from NIAB, it was necessary to allow these plants to grow to maturity and to harvest the seeds produced. In order to keep multiple biological replicates for any phenotype testing, the seeds produced by each plant were kept separate and treated as independent lines. Before any experimentation could be carried out on these lines, it was first essential to devise and verify a method of selecting transformants from the T_1 seedlings.

The vector used for transformation contained the kanamycin selection marker gene *NPTII*. Therefore, it was decided to germinate the seeds first on solid media with

kanamycin before transferring to soil. However, it was found (Figure 5.1.) that wild type seeds were able to germinate on these plates, and so this would not be a viable method of removing null segregants from population before experimentation.

In spite of this, it was noted that, whereas wild type plants did germinate, they did not produce lateral roots, and that *TaR1* over expressing lines produced a mixture of plants, with and without lateral roots (Figure 5.2). It was hypothesised that those seedlings, which produced lateral roots, possessed the *NPTII* selection and, therefore, the transgene, while those with no lateral roots were the null segregants. In order to test this, PCR reactions with primers designed to the *NPTII* gene were carried out with gDNA extracted from seedlings with and without lateral roots. The result of this (Figure 5.3.) suggested that all plants with lateral roots did possess the *NPTII* selection marker and, consequently, that germination on kanamycin plates and transferring to soil only those seedlings, which produced lateral roots, was a viable method of selecting *TaR1* over expressing transgenic plants for further analysis.

Once it had been certified that transgenic plants were being selected, it was next imperative to determine that *TaR1* was being overexpressed as intended. Initially the intention was to do this by observing the level of protein present in the leaves by Western Blotting. This was to be achieved using a specific αTaR1 antibody, which was produced at Durham University. This antibody was tested, and was found to be capable of detecting TaR1 when purified from *E. coli* or transiently expressed in *N. benthamiana*, but unable to do so in wheat leaf extracts (Figure 5.4.).

Since *TaR1* is expressed at a relatively low level, it was assumed that the inability to detect it in wheat was due to only a very small amount of protein being present in samples. Therefore, a number of further tests to devised to attempt to visualise TaR1 in protein extracted from wheat (Figure 5.5. 5.6. 5.7. 5.9.), but none of these proved successful. As a result, it was determined that Western Blotting with the anti-TaR1 antibody would not be a practicable method for determining the extent of *TaR1* over expression. It was thus resolved to instead investigate the levels of RNA by qPCR.

qPCR analysis of *TaR1* expression (Figure 5.10.) suggests that many of the lines tested show expression similar or lower than in the wild type. Even those lines, which show a slightly higher expression, OX25 and OX32, are well below 2x the wild type expression

level, and so it cannot be concluded that these are upregulated. It has been previously shown that endogenous overexpression of genes can trigger gene silencing in plants (van der Krol *et al*., 1990), and so this could be the reason.

Although no lines were considered to be definitely overexpressing *TaR1*, phenotypic data under healthy conditions was collected and analysed for the two lines, which looked mostly to be over expressing *TaR1*, TaR1 OX25 and 32. The plants showed no obvious differences and, while a significant difference was seen for some features, none was consistent across both lines for growth or flowering.

The seed quality also appeared to consistent between the lines, with no difference seen in the 100-grain weight, with average seed weight considered an important test of seed quality, which can affect a number of traits in seedlings and the adult plants produced (Moshatati and Gharineh, 2012). In total yield, however, there is a potential difference between the lines. While, again, this is only seen with one line, the yield produced per head does appear to show a strong difference between the two OX lines and the wild type.

As no infection appeared to take place on fielder with IPO2323 under our conditions, no further analysis could be undertaken to examine their *Z. tritici* infection phenotype. Unfortunately, time did not permit further testing of the infection assay conditions or the use of different pathogen strains, but these would both be areas for continued work.

Chapter 6

Discussion

6.1. Introduction

Wheat is a very important food crop worldwide, with the latest 2014/15 yield estimate at 729.5 million tonnes, accounting for 28.6% of the global cereal market (FAO 2015). In particular, wheat accounts for 42.3% of all arable land area and 67.5%, by weight, of total cereal production, worth 9.5% of the total UK farming economic output (DEFRA 2015).

Farming yields are constantly at risk of loss due to abiotic factors such as drought or cold, as well as biotic stresses. Septoria leaf blotch, caused by the fungus *Zymoseptoria tritici*, is the most damaging foliar disease of wheat in the United Kingdom, capable of causing 30-50% yield losses (Eyal *et al.*, 1987). In 2014, a national annual survey of wheat disease found *Z. tritici* to be present on 99% of examined plants (CropMonitor 2015). This survey found 11.5% of mean leaf area to be affected. This was much higher than the long-term mean of 4.5%, but both are considerably higher than the second highest, powdery mildew (0.1%).

A notable aspect of the *Z. tritici* lifecycle is a long period of symptomless growth within the host tissue, followed by a sudden switch to necrotrophic growth accompanied by host cell death (Kema *et al.*, 1996). During this asymptomatic period, which can persist for up to two weeks, the pathogen relies on its ability to evade detection by the host (Goodwin *et al.* 2011). The switch to necrotrophy is a key stage in the disease development and is associated with large-scale transcriptional changes in both host and pathogen (Rudd *et al.*, 2015) and yet little is known about the underlying processes.

6.2. Virus-Induced Gene Silencing

In order to gain a better understanding of individual host genes involved in this plant pathogen interaction, Virus Induced Gene Silencing (VIGS) was employed to knock down expression of target genes in the host, which could then be infected with *Z. tritici*. VIGS was chosen as the method of gene alteration as during the initial stages of this investigation there was a large number of target genes, and, unlike stable transformants, VIGS provides results within a short timeframe.

VIGS is a technique used to reduce expression of host genes, based on the plant response to recognition of double stranded DNA (dsDNA), in which small interfering RNAs (siRNA) are produced to target degradation complexes onto mRNA (Baulcome *et al.*, 2004). Insertion of a plant gene into the viral genome will, therefore, result in the production of siRNA, which will target not the plant gene, as well as the plant derived sequence within the virus. VIGS experiments were originally carried out in *Nicotiana benthamiana* (Kumagai *et al.*, 1995), and have since been proven to be effective at reducing gene expression in a wide range of plants, including *Solanum* species (Liu *et al.* 2002; Brigneti *et al.* 2004), Arabidopsis (Burch-Smith *et al.*, 2006), barley (Holzburg *et al.* 2002) and wheat (Scofield *et al.* 2005).

The VIGS system used in this project was one specifically adapted for use in wheat, using the Barley Stripe Mosaic Virus (BSMV) as a vector (Yuan *et al.*, 2011). In order to verify the function of BSMV VIGS on the wheat varieties at our disposal under the conditions available, it was used to silence the carotenoid biosynthesis gene *PHYTOENE DESATURASE* (*TaPDS*). Silencing *TaPDS* produces a discernible white leaf phenotype and has regularly been used as a marker of VIGS function (Kumagai *et al.* 1995; Ruiz *et al.* 1998; Burch-Smith *et al.* 2006). We have shown that, under our conditions, BSMV VIGS is capable of successfully silencing avalon (Figure 3.2) and fielder (Figure 5.11) variety wheat.

Using this system, a number of target genes, selected by their homology to known Ubiquitin Proteasome System (UPS) components in Arabidopsis and a change in expression level in wheat following *Z. tritici* infection, were silenced in wheat, which was then infected with *Z. tritici*. Using this method, at least one candidate, *TaR1*, was identified as altering the process of infection when silenced (Figure 3.11; Figure 4.10-

4.13.). As such, the use of BSMV VIGS to test the function of a short list of candidate genes can be considered successful. Once a candidate has been verified, stable transgenic lines may be more useful that the transient VIGS system for the most thorough investigation of the effects of the gene, but until the phenotype of this gene has been certified, the higher-throughput nature and lower cost of the VIGS system makes it a very useful tool.

6.3. TaR1 Is Involved in the Interaction Between Wheat and *Z. tritici*

Z. tritici is a fungal pathogen wheat, notable for an unusually long period of growth within the leaf tissue, during which time no response is seen from the host, before a shift to necrotrophic growth, and the production of lesions on the host tissue, in which the pathogen reproduces (Kema *et al*., 1996). The action of the fungus during this infection is currently much better understood than that of the host.

Initial access to the host tissue is achieved through stomatal entry, and colonisation of the substomatal cavities, which allows for more extensive hyphal growth, and multiple infection sites from a single penetration. Efficient colonisation of the substomatal cavities requires the activity of an ATP-binding cassette (ABC) transporter, which may be used to reduce the effect of host-derived anti-fungal compounds (Kema *et al*., 1996; Duncan and Howard 2000; Stergiopoulos *et al*., 2003).

That *Z.* tritici then avoids host detection by variety of stealth pathogenesis tools has been well observed (Godwin *et al*., 2011; Marshall *et al*., 2013; Lee *et al*., 2014). However, little is known about the switch to cell death and necrotrophic growth, which takes place after this symptomless period, other than the existence of significant changes in transcription in both the host and the pathogen (Yang *et al*., 2013; Rudd *et al*., 2015). The only host components linked with this is the possible involvement of a Mitogen-Activated Protein Kinase (MAPK) signalling cascade, which may be hi-jacked by unknown fungal effectors (Rudd *et al*., 2008).

As mentioned above, TaR1 was shown to have a role in the virulence of wheat by *Z. tritici*, as knocking down *TaR1* expression by BSMV VIGS altered development of disease symptoms and the reproduction of the pathogen. More precisely, silencing of

TaR1 lead to an earlier onset of disease symptoms in host leaves and reduced sporulation at the end of the infection cycle. This shift in the appearance of symptoms suggests that TaR1 is involved in the previously discussed switch from biotrophic to necrotrophic growth.

The earlier development of symptoms, when *TaR1* is silenced, indicates that TaR1 may be acting to delay the onset of cell death. However, given that its silencing leads to a decrease in the viability of the pathogen, it appears that TaR1 is a negative regulator of pathogen defence. Considering this, it is possible that the regular function of TaR1 is to prevent unnecessary cell death under normal conditions, but is hi-jacked by *Z. tritici*, in order to prevent a cell death response upon recognition by the host. Such a hi-jacking of host cellular processes is already an established mechanism in this host-pathogen interaction (Hammond-Kossack and Rudd 2008).

Z tritici is said to depend upon 'stealth pathogenesis' and has previously been revealed to employ a system to prevent recognition by the plant, even at the earliest stages by preventing chitin recognition by host receptors (Marshall *et al*. 2011). However, this would not preclude further mechanisms, acting downstream in the plant signalling, to prevent a response in the event of recognition. Recognition is more likely further into the infection, as fungal biomass within the host is higher, and so it would follow that these systems would be more required later in infection. *TaR1* expression reaches its peak shortly before the onset of symptoms (Lee *et al*., 2015) and, if pathogen hi-jacking is causing this increase in expression, this would be consistent with this theory.

Plant responses to pathogen recognition often lead to cell death. While *Z. tritici* is capable of feeding in a necrotrophic manner, it goes to great lengths to avoid recognition and cell death. The fungus increases biomass through a long biotrophic phase, and then reproduces through picnidia in necrotic tissue (Ponomarenko *et al*., 2011), and so it can be assumed that it is important for the fungus to attain a certain biomass before beginning to reproduce. It is possible, therefore, that the function of hi-jacking TaR1 is to prevent a cell death response before this biomass is reached. Consequently, when *TaR1* is silenced and recognition, and hence cell death, occur sooner, the pathogen is forced into its reproductive phase before the ideal biomass is achieved. This may be the reason behind the reduced reproductive capacity of *Z. tritici* in *TaR1* silenced wheat.

Although the experiments undertaken to find these results were repeated and found consistent outcomes, further work could be undertaken to improve certainty. For example, qPCR on DNA extracted from *Z. tritici* infected wheat leaves has been used previously as a measure of the increase in fungal biomass throughout an infection cycle (Marshall *et al*., 2011). This would give a much more accurate view on the spread of the fungus within the leaf, and so would provide a more detailed impression of how this is affected by *TaR1* silencing.

It would also be of interest to examine the role of TaR1 in interactions with other pathogens. Given that it is implicated in the cell death response, it is possible that TaR1 may function more generally in pathogen defence, rather than as a specific involvement with *Z. tritici*. Conversely, if it is indeed hi-jacked by *Z. tritici* effectors, other pathogens may have no corresponding system in place, and thus TaR1 would play no role in the interaction.

6.4. TaR1 as a Link Between Defence and Chromatin Remodelling

Chromatin remodelling refers to the mechanism of altering the architecture of DNA and other associated structures, so as to affect the transcription of genes, often by changing the accessibility of promoter regions of DNA to transcription factors or other transcription machinery (Hirschorn *et al.,* 1992). Changes to the structure or positioning of nucleosomes in relation to promoter regions directly affects gene expression (Whitehouse *et al*., 2007; Henikoff 2008).

Positioning of these nucleosomes can be altered directly by ATP-dependent chromatin remodelling complexes (Teif and Rippe 2009). However, the main method of chromatin remodelling focussed on here is through alteration, by post-transcriptional modification, to the histone subunits, which make up the nucleosomes. Histones can be modified in a large number of ways, including methylation, acetylation, phosphorylation and ubiquitination (Tan *et al*., 2011). These modifications can change the binding affinity of the histones to DNA, and therefore the expression of associated genes, as a lower affinity leads to easier transcriptional access (Teif and Rippe 2009).

As considered above, TaR1 appears to play a role in wheat defence against *Z. tritici*, but the mode of action for its involvement was still unknown. Sequence analysis (Figure 3.12-13; Figure 4.1-2.) suggested that TaR1 contained a Plant Homeodomain (PHD) domain, and showed strong similarity to a group of previously defined Alfin1-like proteins from Arabidopsis and rice (Lee *et al*., 2009). These proteins were demonstrated to bind to Histone 3, di- or trimethylated at lysine 4 (H3k4me2/3). A protocol modified from this investigation was used to demonstrate that TaR1 also specifically binds to H3k4me2/3 *in vitro* (Figure 4.9.), while a co-immunoprecipitation (co-IP) assay was also devised to show that transiently expressed tagged TaR1 constructs were capable of binding TaH3 *in planta*.

Lee *et al*. (2009) also provided evidence of which amino acid residues within the PHD domain were crucial for its binding function, highlighted in Figure 4.1. Amongst these was an Aspartic Acid residue at position 215, which, when mutated to an asparagine, removed the binding capability of the protein. This Aspartic Acid aligned with an Aspartic Acid at position 221 in the TaR1 sequence (Figure 4.1.). When this was mutated to an Asparagine, the resulting protein, TaR1ΔD221N, was unable to bind any histone peptides, suggesting that the binding of TaR1 is through the same mechanism as these Alfin-like proteins.

Combined, these data give a strong indication that TaR1 is a histone binding protein, able to distinguish between specific methylation states. In order to strengthen these results, some of these assays could be repeated in wheat, rather than in *Nicotiana benthamiana*. TaR1 was shown to localise to the nucleus when expressed transiently in *N. benthamiana* with fluorescent tags, but a particle bombardment technique could be used to express similar constructs in wheat (Wang *et al*., 1988). Further to this, immunolocalisation would allow the protein to be seen in wheat without any possible effect of the tag. However, this would require a good antibody, which will be reviewed later. Similarly, the co-IP could also be carried out in wheat leaves through bombardment, or even without need for transient over expression with the aforementioned antibody.

In order to further investigate the functions of TaR1, it would be interesting to discover whether there is any involvement in other pathogen interactions, as mentioned before. Additionally, *TaR1* silencing or over expressing plants ought to be subjected to tests of

their abiotic tolerance as well as various developmental aspects. The closely related AtAL5, which was found to regulate seed development through a chromatin remodelling complex (Mollitor *et al*., 2014), had previously been indicated to have a role in phosphate deficiency (Chandrika *et al*., 2013), displaying an ability of these Alfin-like proteins to have an effect on a wide range of processes.

Although the function of TaR1 seems clear from the assays conducted, how this relates to a role in pathogen defence is still unknown. Many other PHD domain proteins have been shown to bind to H3k4me3 and, in doing so, alter downstream transcription through modification to chromatin structure. However, this action is usually associated with another protein or complex (De Lucia *et al*. 2008; Molitor *et al.* 2014), most often containing histone acetyltransferases (HATs) or histone deactylases (HDACs) (Shi *et al*., 2006; Taverna *et al*., 2006; Li *et al*., 2007.). Considering their ability to read specific methylation markers on histones, the most likely role for a PHD domain protein within such a complex would be to recruit the chromatin remodelling proteins onto a specific area of chromatin. A model based on this concept can be seen in Figure 6.1.

The H3k4me3 modification is most often associated with being a signal for active transcription of connected genes (Bernstein *et al*., 2002; Santos-Rosa *et al*., 2002). Meanwhile, acetylation of histones decreases their affinity for DNA (Hong *et al*. 1993), allowing easier access to the DNA for transcription factors and other transcriptional machinery (Lee *et al.*, 1993; Vettese-Dadey *et al*., 1996), meaning acetylation generally results in increased transcription, while deacetylation results in reduced transcription (Kadosh and Struhl 1998). As a result, complexes targeting H3k4me3, which alter the acetylation of histones, are able to regulate the expression of transcriptionally active genes. Accordingly, TaR1, through HAT/HDAC interactions could play a role in the switch between biotrophic and nectrotrophic growth through contribution to the large scale transcriptional reprogramming seen in the host during this time (Rudd *et al*., 2015).

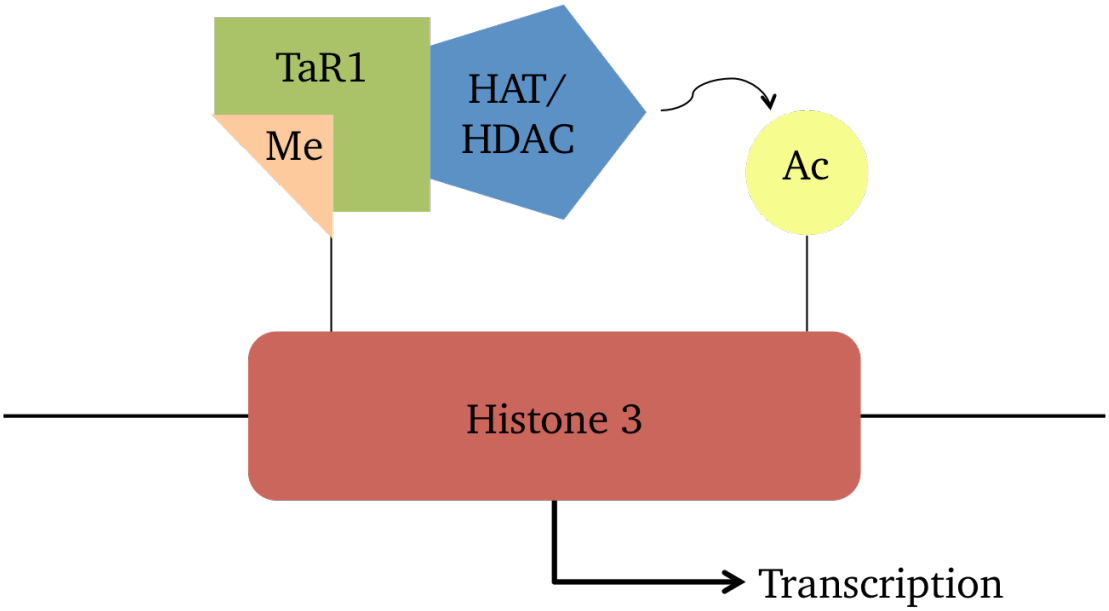

Figure 6.1. Possible Mechanism for TaR1 Function. TaR1 (green) is able to read the methylation code of Histone 3 (red) and bind only to a specific methylation (orange). Any chromatin remodelling proteins, such as HATs or HDACs (blue), bound to TaR1, would then be recruited onto this area of chromatin. From there, it could alter the pattern of histone acetylations (yellow) and, hence, the overall chromatin structure. This would result in changes to transcription of genes associated with this area.

Nevertheless, any connection between TaR1 and other chromatin remodelling proteins remains entirely theoretical and much further work would be required to sufficiently link the two. Towards that end, a number of HATs and HDACs of wheat were identified (Figure 4.14-15.). The first stage in an investigation into whether TaR1 was involved in such a complex would be to verify whether it associates with any of these HATs or HDACs. This could be achieved through a number of methods; further co-IP assays, such as those already performed with TaH3, would be the most consistent with the work already completed, though other techniques such as yeast two hybrid or bimolecular fluorescence complementation could also be utilised. Should no interaction of any kind be found, a chromatin remodelling complex would still not be ruled out as histones can be modified in a variety of other ways, including phosphorylation, ubiquitination and sumoylation (van Attikum and Gasser 2005; Wurtele and Verreault 2006).

In response to possible chromatin remodelling involving TaR1, almost any genes could be transcriptionally altered, and it would be difficult to predict which without a chromatin immunoprecipitation (ChIP) assay using either TaR1 or any protein shown to associate with it. Through this method, genes associated with the chromatin, to which these proteins bind, could be ascertained. qPCR analysis of these genes in *TaR1* silenced and *TaR1* over expressing lines would then give a clearer indication of whether there was a relationship present. One gene family that would seem the most likely to be involved, without further evidence, are the WRKY transcription factors.

WRKYs are a large family of transcription factors conserved throughout the plant kingdom (Wen *et al*., 2014). As a family they are involved in a wide array of cellular processes, most markedly in response to environmental stresses. In particular they are implicated in the response to pathogen attack (Pandey and Somssich 2009), and a number of wheat WRKY genes have been shown to change expression on *Z. tritici* infection (Lee *et al*., 2015). Regulation of a transcription factor such as these would allow TaR1 to produce a larger downstream response, and therefore, more of a contribution to the large-scale changes seen at the onset of *Z. tritici* symptoms. As a result, of all possible genes, WRKY transcription factors seem the most likely to be related to this system, but a large amount more evidence would need to be acquired before any link could be suggested.

Despite the strong indications of the previous evidence, it should be noted that, while Lee *et al.* (2009) confirmed the H3k4me3 binding function of three of the six AL proteins predicted to bind, a further three were left untested. Meanwhile, more recently, six of the seven AL proteins were indicated to be involved in a direct protein-DNA interaction by a gel shift assay (Wei *et* al., 2015). Among these six, AL5, which was not proven to bind H3k4me3, has been shown to have a role in plant abiotic stress, through this direct interaction with promoter sequences.

This binding, however, was also shown to be dependent on a conserved Valine residue at position 34, which TaR1 does not possess. AL6, the only Arabidopsis AL protein without a Valine at position 34 does not show binding in the gel shift assay, even though it does possess a Valine at position 35.

Nonetheless, the supposedly important residues for DNA binding do fall within the highly conserved Alfin-like domain shown in figure 4.2. In this alignment, it can be seen that while there is no Valine 34 in TaR1, when aligned by the Alfin-domain, the Valine in position 43 aligns with the conserved Valine 34 from other alfin and alfin-like proteins. This study also highlighted the importance of a Glutamine, Glutamic Acid or Aspartic Acid residue following the Valine 34. The Valine 43 in TaR1 is followed by a Glutamic Acid at position 44.

It, therefore, would be vital to repeat the gel shift assay seen in the Wei *et al.* experiment, to test whether TaR1 is capable of maintaining this DNA binding capacity. If this were the case, it would provide a function for the strong conservation shown in this Alfin-like region across the AL proteins. It would also provide an alternative mechanism for TaR1 function, not requiring the formation of a complex.

AL5 was shown to act as a transcriptional repressor, and bound to the promoter regions of a number of genes, including the transcription factor *AtWRKY11*, which has also previously been linked to pathogen defence (Journot-Catalino *et al*., 2006). TaR1, therefore, could also, while still 'reading' the methylation code as a target, bind to promoters of genes and effect their transcription. As a negative regulator of transcription, this would also seem to fit the concept of TaR1 as a repressor of cell death.

Further to this, cell death on infection was reduced in *wrky11* mutants. Therefore, if TaR1 was to work in a similar manner to AtAL5, it might negatively regulate the function of a wheat homolog of AtWRKY11. Since it would function as a negative regulator, this would reduce transcription of the wheat *WRKY* gene and, assuming it maintained its function in wheat, a reduction in cell death on infection would be seen. This would explain the phenotype, which is seen in *TaR1* silenced plants, where reduction of *TaR1* leads to an increase in cell death, possibly by an increase in the levels of the hypothetical WRKY.

To test this hypothesis, it would first be necessary to find wheat WRKY sequences, which are most similar to *AtWRKY11*. Primers designed to these sequences would then be used to determine, by qPCR, which WRKYs changed in transcription on TaR1 silencing, with a particular note of which increased in expression. If any of these gene

were shown to have altered expression on *TaR1* silencing, the ChIP assays carried out by on AL5 Wei *et al*. (2015) could be repeated for TaR1, looking for the promoter sequence of the wheat WRKY gene in question.

If the results were to find that this hypothesis was held up, and that the mode of action was through direct DNA binding, rather than recruitment of histone modifiers, it would suggest that TaR1 had no action, direct or indirect in bringing about chromatin remodelling. However, as it would still rely on TaR1 correctly reading the signals of histone methylation, it would nonetheless provide evidence for TaR1 as a link between chromatin remodelling and wheat defence against *Z. tritici*.

6.5. Stable Transgenics Overexpressing *TaR1*

A *TaR1* over expressing construct, driven by the rice actin promoter sequence, was transformed, by NIAB, into fielder variety wheat with the vector pSC4Act-R1R2-SCV (Biogemma.com), to create stable transgenic plants. These plants were allowed to reach maturity and set seed, which was maintained as 30 independent *TaR1* over expressing (TaR1 OX) lines (Table 5.1.). Of these lines, those which were identified as single copy number transformations were taken forward for further analysis. These lines were TaR1 OX 11,12,13,17,23,25,27,32.

Unfortunately, due to issues discussed in the following section, the difference in protein levels between these and wild type fielder plants could not be measured. Instead, it was decided to determine the level of over-expression by qPCR (Figure 5.10.). However, these results suggested that there was no significant upregulation in *TaR1* in any of the lines tested.

The qPCR analysis was only carried out for one biological replicate for each of these lines, and testing of further replicates would be important, particularly for lines OX25 and OX32, which did appear to have very slightly raised *TaR1* expression. In addition to this, the remaining lines, which were not tested, ought to be analysed, as these may yet over express *TaR1*.

Nonetheless, a phenotypic analysis was carried for the TaR1 OX25 and TaR1 OX32 lines, compared to the wild type. No differences were clear for the growth of either line,

but it is possible that there is a yield difference, as both of these lines produced a higher yield per head than the wild type (seen in 5.7.3.). However, due to the large differences in tiller and head production, it is hard to be confident in these results. Further testing of this, with a larger sample size, would be necessary before any strong conclusions could be made for any of these factors.

The TaR1 OX25 line also produced significantly earlier flowers (5.7.2. Flowering Development of *TaR1* Overexpressing Lines) than the wild type, although TaR1 OX32 showed a similar flowering to the wild type. This discrepancy between the two overexpressing lines, along with the small sample sizes involved, show that this requires much further testing. However, chromatin remodelling has previously shown a large involvement in flowering time, with disruption often leading to early flowering (Piniero *et al.*, 2013; Sacharowski *et al.*, 2015). No such involvement has previously been demonstrated in wheat, but this is an interesting observation, and ought to be examined through further experimentation with larger sample sizes.

Although the initial tests of the *Z. tritici* infection phenotype, using strain IPO323 on the fielder variety wheat, showed no sign of disease progression (5.12), other strains could be acquired and tested.

6.6. TaR1-Specific Antibody

An antibody for TaR1 was developed in rabbit from a recombinant His-TaR1 protein, purified from *E. coli* using the Gateway expression vector pDEST17. When tested on other recombinant TaR1 protein, or transiently expressed YFP-TaR1 in *N. benthamiana* protein extract, this antibody appeared to detect TaR1, while remaining specific, as no auxiliary bands were seen (Figure 5.4.).

However, the initial purpose of the development of this antibody was to verify protein levels in *TaR1* silenced and over expressing lines, and yet the antibody was unable to detect TaR1 in wheat total protein extract (Figure 5.4.). Numerous attempts were made through a variety of methods in an effort to detect the protein in wheat, but all were ultimately unsuccessful (Figure 5.5-5.9.). The reason behind this inability to detect native TaR1 is still unknown.

As the antibody was created from a tagged construct, produced from a Gateway vector, it is possible that the antibody is not binding to the TaR1 protein, but to some other area of Gateway-specific sequence. Figure 5.4. shows that the antibody is capable of binding to proteins other the His tag used in the original protein, which suggests this is not the area recognised. However, there could be areas of link sequence between the tag and TaR1 protein, which is consistent across all three constructs. Binding to this would explain why the antibody is able to detect GST-TaR1 and GFP-TaR1, but not TaR1.

In order to rectify this situation, a new antibody would need to be produced, either by attempting the same method again, or by synthesis of a peptide antibody (Trier *et al*., 2012). By either method, production of a functional antibody, capable of specific recognition of TaR1 would be instrumental to further studies on this topic; not only would it then be possible to quantify the changes in protein level between wild type and *TaR1* silenced and over expressing lines, but several other interesting techniques, as mentioned above would then become accessible.

Firstly, it was seen that, while nuclear localisation of TaR1 was consistent, the use of different fluorescent tags did somewhat change the protein's cellular distribution (Figure 4.3-4.5.). Immunolocalisation, using an antibody specific to TaR1 would eliminate this issue entirely. Concerns of the co-IP assays being undertaken in a heterologous system, with TaR1 under the influence of a 35S promoter could also be removed, as pulldown assays could be undertaken by directly pulling down native TaR1 from wheat leaves, and probing with the Histone 3 antibody used previously in this study.

Further experimentation, rather than improvements to existing results, would also be possible through this antibody. Chief amongst those would be a ChIP assay, in order to detect which genes are most likely to associate to the areas of chromatin, to which TaR1 is binding.

6.7. Summary

Septoria leaf blotch, caused by the fungal pathogen *Z. tritici* is a devastating disease of wheat, a key food crop both worldwide and in the United Kingdom. We have shown that the previously unidentified wheat gene *TaR1* has an involvement in this plant pathogen interaction, and that silencing of *TaR1* leads to earlier development of visible symptoms and reduced sporulation by the pathogen.

The mechanism, by which TaR1 affects this interaction, is still currently unknown. However, it is likely to involve either or both the histone binding capacity of the PHD domain and the possible DNA binding function of the Alfin-like domain. Either of these functions would allow an involvement in the regulation of gene transcription, and therefore potentially in the key switch in the pathogen from necrotrophic to biotrophic.

Appendix

Primer List

Primer Code	Function	Sequence
PDS F	*TaPDS* Expression	TCAGTCTTTGGGTGGTGAGGT
PDS R	*TaPDS* Expression	AGGTTCGCAGTTCGGGAC
RT_PDS F	*TaPDS* qPCR	GTCCCGAACTGCGAACCT
RT_PDS R	*TaPDS* qPCR	GCCAGGTATTTCTGCTTTGTGT
JL2 F	*TaU1_A* Cloning	AAGGAAGTTTAAGCGAAGAAAAGGAGCTTATCATGGC
JL2 R	*TaU1_A* Cloning	AACCACCACCACCGTGTAGTCCGGGGGGGAAATGGATATTC
JL3 F	*TaU1_B* Cloning	AAGGAAGTTTAAGCATATGCCTTGACATTCTGAAGG
JL3 R	*TaU1_B* Cloning	AACCACCACCACCGTTCATCCCATGGCATACTTCTGCG
RT_JL2 F	*TaU1* qPCR	GCTGCTTACCGACCCTAACC
RT_JL2 R	*TaU1* qPCR	CGGGCTGTCGTCTCATACTT
JL5 F	*TaU2_A* Cloning	AAGGAAGTTTAAATGGCATCAAAGCGCATCCTC
JL5 R	*TaU2_A* Cloning	AACCACCACCACCGTACCTTTGGTGGCTTGAAGGGG
JL 6 F	*TaU2_B* Cloning	AAGGAAGTTTAAGCATATGCCTTGATATTCTTAAGG
JL6 R	*TaU2_B* Cloning	AACCACCACCACCGT TCAACCCATGGCGTACTTCTGCG
JL8 F	*TaU3_A* Cloning	AAGGAAGTTTAAAGCGGAAGCAGGAGGCAGAGAG
JL8 R	*TaU3_A* Cloning	AACCACCACCACCGTCCACCGGAATATGGGCTGTCAG
JL9 F	*TaU3_B* Cloning	AAGGAAGTTTAAGGAGCATTTGTCTGGACATCC
JL9 R	*TaU3_B* Cloning	AACCACCACCACCGTTTACATGGCATACCTTTGCGTC
JL14 F	*TaU5_A* Cloning	AAGGAAGTTTAAAGGAGGAAGGGAAGATTTCATC
JL14 F	*TaU5_A* Cloning	AACCACCACCACCGTGTTCTACTCTAACCTTCCAGAC

JL15 F	*TaU5_B* Cloning	AAGGAAGTTTAAGTACCCAAATCCGTCTGATCC
JL15 R	*TaU5_B* Cloning	AACCACCACCACCGTCCACTATATCCTCATCGCCGG
JL16 F	*TaR1* Cloning	CACCATGGACGCCTCCTACCGCCGC
JL16 R	*TaR1* Cloning	CTACTGCCTAGGTCTCTTGGAGC
JL17 F	*TaR1_A* Cloning	AAGGAAGTTTAAATCACGAGAGGCGGCGCCCCC
JL17 R	*TaR1_A* Cloning	AACCACCACCACCGTCCGCGGGCAGCGCCACCTCCC
JL18 F	*TaR1_B* Cloning	AAGGAAGTTTAACAATCGAAGGAGAGGGACAGATC
JL18 R	*TaR1_B* Cloning	AACCACCACCACCGTCGCACTTGCCATGGTACCAC
RT_JL18 F	*TaR1* qPCR	CAAAGCATACAGTCGAGGCG
RT_JL18 R	*TaR1* qPCR	GCATAAGGTCTCGCTGTGGT
D221N F	Site-directed mutagenesis	ATTGGTTGCAATGTGTGCGA
D221N R	Site-directed mutagenesis	TCGCACACATTGCAACCAAT
JL23 F	*TaR3_A* Cloning	AAGGAAGTTTAACGGGGGAGGCACGCATCGCACG
JL23 R	*TaR3_A* Cloning	AACCACCACCACCGTCTCATCCATCCCATCCCGAGC
JL24 F	*TaR3_B* Cloning	AAGGAAGTTTAACTAAGCCATCTCGCCAGCCAG
JL24 R	*TaR3_B* Cloning	AACCACCACCACCGTCATTTGTAGTGCTTGATGTGC
JLACT F	*TaActin* Expression	GCCACACTGTTCCAATCTATGA
JLACT R	*TaActin* Expression	TGATGGAATTGTATGTCGCTTC
RT_UB F	qPCR Reference	TTGACAACGTGAAGGCGAAG
RT_UB R	qPCR Reference	TGGATGTTGTAGTCCGCCAAG
TaH3 F	*TaH3* Cloning	CACCATGGCCCGCACCAAGCAGA
TaH3 R	*TaH3* Cloning	CTAGGCCCTCTCGCCACGGA
NPTII F	*NPTII* Expression	TGCTCGACGTTGTCACTGAA
NPTII R	*NPTII* Expression	TAAAGCACGAGGAAGCGGTC

Bibliography

Aasland R, Gibson TJ, Stuart AF. **1995**. The PHD finger: implications for chromatin-mediated transcriptional regulation. Trends in Biochemical Sciences 20: 56–9.

Abramovich RB, Anderson JC, Martin GB. **2006**. Bacterial elicitation and evasion of plant innate immunity. Nature Review Molecular Cell Biology 7: 601-11.

Agriculture and Horticulture Development Board. **2012**. Septoria tritici in winter wheat. http://cereals.ahdb.org.uk/media/178045/ts113_septoria_tritici_in_winter_wheat.pdf

Ahuja I, Kissen R, Bones AM. **2012**. Phytoalexins in defence against pathogens. Trends in Plant Science 17: 73-90.

Alfano JR, Collmer A. **1996**. Bacterial Pathogens in Plants: Life up against the Wall. Plant Cell 88: 1683–98.

Allfrey VG, Faulkner R, Mirsky AE. **1964**. Acetylation and methylation of histones and their possible role in the regulation of RNA synthesis. Proceedings of the National Academy of Science USA 51: 786–94.

Álvarez-Venegas R, Abdallat AA, Guo M, Alfano JR, Avramova Z. **2007**. Epigenetic control of a transcription factor at the cross section of two antagonistic pathways. Epigenetics 2: 106–13.

Asai T, Tena G, Plotnivkova J, Willmann MR, Chiu W-L, Gomez-Gomez L, Boller T, Ausubel FM, Sheen J. **2002**. MAP kinase signalling cascade in Arabidopsis innate immunity. Nature 415: 977-83.

van Attikum H, Gasser SM. **2005**. The histone code at DNA breaks: a guide to repair? Nature Reviews Molecular Cell Biology 6: 757–65.

Austin MJ, Muskett P, Kahn K, Feys BJ, Jones JDG, Parker JE. **2002**. Regulatory Role of *SGT1* in Early *R* Gene-Mediated Plant Defenses. Science 295: 2077-80.
Azevedo S, Sadanandom A, Kitagawa A, Freialdenhoven A, Shirasu K, Schulze-Lefert T. **2002**. The RAR1 Interactor SGT1, an Essential Component of R Gene–Triggered Disease Resistance. Science 295: 2073-6.

Bannister AJ, Zegerman P, Partridge JF, Miska EA, Thomas JO, Allshire RC, Kouzarides T. **2001**. Selective recognition of methylated lysine 9 on histone H3 by the HP1 chromodomain. Nature 410: 120–4.

Bannister AJ, Kouzarides T. **2011**. Regulation of chromatin by histone modifications. Cell Research 21: 381-95.

Bastola DR, Pethe VV, Winicov I. **1998**. Alfin1, a novel zinc-finger protein in alfalfa roots that binds to promoter elements in the salt-inducible MsPRP2 gene. Plant Molecular Biology 38: 1123–35.

Baulcombe D. **2004**. RNA Silencing in plants. Nature 431: 356-63.
Benson DA, Cavanaugh M, Clark K Karsh-Mizrachi I, Lipman DJ, Ostell J, Sayers EW. **2013**. Genbank. Nucleic Acids Research 41: 36-42.

Berg JM, Tymoczko JL, Stryer L. **2002**. Covalent Modification Is a Means of Regulating Enzyme Activity. In Biochemistry. 5th edition. New York: W H Freeman.

Berger SL. **2007**. The complex language of chromatin regulation during transcription. Nature 447: 407-12.

Bernstein BE, Humphrey EL, Erlich RL, Schneider R, Bouman P, Liu JS, Kouzarides T, Schreiber SL. **2002**. Methylation of histone H3 Lys 4 in coding regions of active genes. Proceedings of the National Academy of Science USA 99: 8695–700.

Bienz M. **2006**. The PHD finger, a nuclear protein-interaction domain. Trends in Biochemical Sciences 31: 35–40.

van der Biezen EA, Jones JDG. **1998**. Plant disease resistance proteins and the gene-for-gene concept. Trends in Biochemical Sciences 23: 454-6.

Boch J, Bonas U, Lahaye T. **2014**. TAL effectors – pathogen strategies and plant resistance engineering. New Phytologist 204: 823–32.

Bochar DA, Savard J, Wang W, Lefleur DW, Moore P, Cote J, Shiekhattar J. **2000**. A family of chromatin remodeling factors related to Williams syndrome transcription factor. Proceedings of the National Academy of Science of USA 97: 1038-43.

Boter M, Amigues B, Peart J, Breuer C, Kadota Y, Casais C, Moore G, Kleanthous C, Ochsenbein F, Shirasu K, Gurois R. **2003**. Structural and Functional Analysis of SGT1 Reveals That Its Interaction with HSP90 Is Required for the Accumulation of Rx, an R Protein Involved in Plant Immunity. The Plant Cell 19: 3791-3804.

Bragg JN, Jackson AO. **2004.** The C-terminal region of the barley stripe mosaic virus γb protein participates in homologous interactions and is required for suppression of RNA silencing. Molecular Plant Pathology 5: 465-81.

Boller T, Felix G. **2009**. A renaissance of elicitors: perception of microbe associated molecular patterns and danger signals by pattern recognition receptors. Annual Review of Plant Biology 60: 379-406.

Brigneti G, Martin-Hernandez AM, Jin H, Chen J, Baulcombe DC, Baker B, Jones JD. **2004**. Virus-induced gene silencing in *Solanum* species. Plant Journal 39: 264-72.

Brown JKM, Chartrain L, Lasserre-Zuber P, Saintenac C. **2015**. Genetics of resistance to *Zymoseptoria tritici* and applications to wheat breeding. Fungal Genetics and Biology 79: 33-41.

Burch-Smith TM, Schiff M, Liu Y, Dinesh-Kumar SP. **2006**. Efficient virus-induced gene silencing in Arabidopsis. Plant Physiology 142(1): 21-7.

van den Burg HA, Tsitsigiannis DI, Rowland O, Lo J, Rallapalli G, Maclean D, Takken FLW, Jones JDG. **2008**. The F-box protein ACRE189/ACIF1 regulates cell death and defense responses activated during pathogen recognition in tobacco and tomato. Plant Cell 20: 697–719.

Camacho C, Coulouris G, Avagyan V, Ma N, Papadopoulos J, Bealer K, Madden TL. **2008**. BLAST+: architecture and applications. BMC Bioinformatics 10: 421.

Cantu D, Segovia V, MacLean D, Bayles R, Chen X, Kamoun S, Dubcovsky J, Saunders DGO, Uauy C. **2013**. Genome analyses of the wheat yellow (stripe) rust pathogen *Puccinia striiformis* f. sp. *tritici* reveal polymorphic and haustorial expressed secreted proteins as candidate effectors. BMC Genomics 14:270.

Carrer H, Hockenberry TN, Svab Z, Maliga P. **1993**. Kanamycin resistance as a selectable marker for plastid transformation in tobacco. Molecular and General Genetics 241: 49-56.

Chandrika NNP, Sundaravelpandian K, Schmidt W. **2013**. A PHD in histone language. Plant Signalling Behaviour 8: e24381.

Chang JH, Rathjen JP, Bernal AJ, Staskawicz BJ, Michelmore RW. **2000**. avrPto enhances growth and necrosis caused by Pseudomonas syringae pv. tomato in tomato lines lacking either Pto or Prf. Molecular Plant Microbe Interactions 13: 568–571.

Chen RS, McDonald BA. **1996**. Sexual reproduction plays a major role in the genetic structure of populations of the fungus *Mycosphaerella graminicola*. Genetics 142: 1119–27.

Chen D, Ma H, Hong H, Koh SS, Huang SM, Schurter BT, Aswad DW, Stallcup MR. **1999**. Regulation of transcription by a protein methyltransferase. Science 284: 2174–7.

Chinchilla D, Zipfel C, Robatzek, Kemmerling B, Nurnberger T, Jones JDG, Felix G, *Boller T*. **2007**. A flagellin-induced complex of the receptor FLS2 and BAK1 initiates plant defence. Nature 448: 497-500.

Chivasa S, Murphy AM, Hamilton JM, Lindsey K, Carr JP, Slabas AR. **2009**. Extracellular ATP is a regulator of pathogen defence in plants. Plant Journal 60: 436–48.

Choi J, Tanaka K, Cao Y, Qi Y, Qiu J, Liang Y, Lee SY, Stacey G. **2014**. Identification of a plant receptor for extracellular ATP. Science: 343 290–4.

Ciechanover A. **1998.** The ubiquitin–proteasome pathway: on protein death and cell life. The EMBO Journal 17: 7151-60.

CropMonitor. **2015**. Winter wheat commercial crops survey 2014. http://www.cropmonitor.co.uk/cmsReport.cfm?id=34 (accessed 21.07.2015)

Cools HJ, Fraaije BA. **2013**. Update on mechanisms of azole resistance in *Mycosphaerella graminicola* and implications for future control. Pesticide Management Science 69: 150–155.

Cools HJ, Mullins JGL, Fraaije BA, Parker JE, Kelly DE, Lucas JA, Kelly SL. **2011**. Impact of recently emerged sterol 14 alpha-demethylase (CYP51) variants of *Mycosphaerella graminicola* on azole fungicide sensitivity. Applications of Environmental Microbiology 77: 3830–37.

Dai Y, Ni ZF, Zhao T, Yao YY, Nie XL, Sun QX. Isolation and expression analysis of genes encoding putative histone acetyltransferase and deacetylase un wheat (Triticum aestivum L.). Unpublished.

Daayf F, El Hadrami A, El-Bebany AF, Henriquez MA, Yao Z, Derksen H, El-Hadrami I, Adam LR. **2012**. Phenolic Compounds in Plant Defense and Pathogen Counter-Defense Mechanisms, in Recent Advances in Polyphenol Research, Volume 3 (eds V. Cheynier, P.

Sarni-Manchado and S. Quideau), Wiley-Blackwell, Oxford, UK. doi: 10.1002/9781118299753.ch8

Dean R, Van Kan JAL, Pretorius ZA, Hammond-Kosack KE, Di Pietro A, Spanu PD, Rudd JJ, Dickman M, Kahmann R, Ellis J, Foster GD. **2012**. The Top 10 fungal pathogens in molecular plant pathology. Molecular Plant Pathology 13: 414–30.

Deller S, Hammond-Kosack KE, Rudd JJ. **2011**. The complex interactions between host immunity and non-biotrophic fungal pathogens of wheat leaves. Plant Physiology 168: 63–71.

De Lucia F, Crevillen P, Jones AM, Greb T, Dean C. **2008**. A PHD-polycomb repressive complex 2 triggers the epigenetic silencing of FLC during vernalization. Proceedings of the National Academy of Science USA 105: 16831-6.

Department for Food and Rural Affairs. **2015**. Agriculture in the United Kingdom 2014. https://www.gov.uk/government/uploads/system/uploads/attachment_data/file/430411/auk-2014-28may15a.pdf

Deslandes L, Olivier J, Peeters N, Feng DX, Khounlotham M, Boucher C, Somssich IE, Genin S, Marco Y. **2003**. Physical interaction between RRS1-R, a protein conferring resistance to bacterial wilt, and PopP2, a type III effector targeted to the plant nucleus. Proceedings of the National Academy of Science USA 100: 8024–9.

Ding L, Xu H, Yi H, Yang L, Kong Z, Zhang L, Xue S, Jia H, Ma Z. **2011**. Resistance to Hemi-Biotrophic F. graminearum Infection Is Associated with Coordinated and Ordered Expression of Diverse Defense Signaling Pathways. PLoS ONE 6(4): e19008.

Djamei A, Schipper K, Rabe F, Ghosh A, Vincon V, Kahnt J, Osorio S, Tohge T, Fernie AR, Feussner I, Feussner K, Meinicke P, Stierhof YD, Schwartz H, Macek B, Mann M, Kahmann R. **2011**. Metabolic priming by a secreted fungal effector. Nature 478: 395–398.

Dombrecht B, Xue GP, Sprague SJ, Kirkegaard JA, Ross JJ, Reid JB, Fitt GP, Sewelam N, Schenk PM, Manners JM, Kazan K. **2007**. MYC2 differentially modulates diverse jasmonate-dependent functions in *Arabidopsis*. Plant Cell 19: 2225–45.

Donald R, Jackson AO. **1994**. The barley stripe mosaic virus γb protein encodes a multifunctional cysteine-rich protein that affects pathogenesis. Plant Cell 6 1593-1606.

Duan H, Ding X, Song J, Duan Z, Zhou Y, Zhou C. **2009**. Effects of kanamycin on growth and development of *Arabidopsis thaliana* seedling, cotyledon and leaf. Pakistani Journal of Botany 41: 1611-8.

Duncan KE, Howard RJ. **2000**. Cytological analysis of wheat in- fection by the leaf blotch pathogen *Mycosphaerella graminicola*. Mycological Research 104: 1074-82.

Duplan V, Rivas S. **2014**. E3 ubiquitin-ligases and their target proteins during regulation of plant immunity. Frontiers in Plant Science 5:42. doi: 10.3389/fpls.2014.00042

Earley KW, Haag JR, Pontes O, Opper K, Juehne T, Song K, Pikaard CS. **2006**. Gateway-compatible vectors for plant functional genomics and proteomics. The Plant Journal 45:616–629.

Ekengren SK, Liu YL, Schiff M, Dinesh-Kumar SP, Martin GB. **2003**. Two MAPK cascades, NPR1, and TGA transcription factors play a role in Pto-mediated disease resistance in tomato. Plant Journal 36: 905–17.

Eyal Z, Schare AL, Prescott JM, van Ginkel M. **1987**. The Septoria Diseases of Wheat: Concepts and Methods of Disease Management. Mexico, DF: CIMMYT.

Felix G, Duran JD, Volko S, Boller T. **1999**. Plants have a sensitive perception system for the most conserved domain of bacterial flagellin. The Plant Journal 18: 265–76.

Flor HH. **1971**. Current status of the gene-for-gene concept. Annual Review of Phytopathology 9: 275-96.

Food and Agriculture Organisation of the United States. **2012**. Second Global Conference on Agricultural Research for Development. http://www.fao.org/docs/eims/upload/306175/Briefing%20Paper%20(3)-Wheat%20Initative%20-%20Hélène%20Lucas.pdf

Food and Agriculture Organisation of the United States. **2015**. Food Outlook. Biannual report on global food market. http://www.fao.org/3/a-I4581E.pdf

Frederick RD, Thlimony RL, Sessa G, Martin GB. **1998**. Recognition Specificity for the Bacterial Avirulence Protein AvrPto Is Determined by Thr-204 in the Activation Loop of the Tomato Pto Kinase. Molecular Cell 2: 241-5.

Freeman BC, Beattie GA. **2008**. An overview of plant defences against pathogens and herbivores. The Plant Health Instructor DOI: 10.1094/PHI-I-2008-0226-01.

Fraaije BA, Cools HJ, Fountaine J, Lovell DJ, Motteram J, West JS, Lucas JA. **2005**. Role of ascospores in further spread of QoI-resistant cytochrome b alleles (G143A) in field populations of *Mycosphaerella graminicola*. Phytopathology 95: 933–41.

Gabriëls SHEJ, Vossen JH, Ekengren SK, van Ooijen G, Abd-El-Haliem AM, van den Berg GCM, Rainey DY, Martin GB, Takken FLW, de Wit PJGM, Joosten MHAJ. **2007**. An NB-LRR protein required for HR signalling mediated by both extra- and intracellular resistance proteins. The Plant Journal 50: 14–28.

Gaetani M, Matafora V, Saare M, Spiliotopoulos D, Mollica L, Ouilici G, Chignola, F, Manella V, Zucchelli C, Peterson P, Bachi A Musco G. **2012**. AIRE-PHD fingers are structural hubs to maintain the integrity of chromatin-associated interactome. Nucleic Acids Research 40: 11756-68.

Gao Y, Liu X, Stebbing JA, He D, Laroche A, Gaudet DS, Xing T. **2011**. *TaFLRS*, a novel mitogen-activated protein kinase in wheat defence responses. European Journal of Plant Pathology 131: 643-51.

Gilchrist DG. **1998**. Programmed cell death in plant disease: the purpose and promise of cellular suicide. Annual Review of Phytopathology 36: 393–414.

Gimenez-Ibanez S, Hann DR, Ntoukakls V, Petutschnig E, Lipka V, Rathjen JP. **2009**. AvrPtoB targets the LysM receptor kinase CERK1 to promote bacterial virulence on plants. Current Biology 19: 423–9.

Glazebrook J. **2005**. Contrasting Mechanisms of Defense Against Biotrophic and Necrotrophic Pathogens. Annual Review of Phytopathology 43: 205-27.

Gohari AM, Ware SB, Wittenberg AHJ, Mehrabi R, Ben M'Barek S, Verstappen ECP, van der Lee TAJ, Robert O, Schouten, HJ, de Wit PPJGM, Kema GHJ. **2015**. Effector discovery in the fungal wheat pathogen Zymoseptoria tritici. Molecular Plant Pathology 16: 931–45.

Gohre, V, Spallek T, Haweker H, Mersmann S, Mentzel T, Boller T, de Torres M, Mansfield JW, Robatzek S. **2008**. Plant pattern-recognition receptor FLS2 is directed for degradation by the bacterial ubiquitin ligase AvrPtoB. Current Biology 18: 1824-32.

Gogoi, R, Singh, DV, Srivastava, KD. **2001**. Phenols as a biochemical basis of resistance in wheat against Karnal bunt. Plant Pathology 50: 470–476.

Gomez-Gomez L, Boller T. **2000**. An LRR receptor like kinase involved in the perception of the bacterial elicitor flagellin in Arabidopsis. Molecular Cell 5: 1003-11.

González-Lamothe R, Tsitsigiannis DI, Ludwig AA, Panicot M, Shirasu K, Jones JDG. **2006**. The U-box protein CMPG1 is required for efficient activation of defense mechanisms triggered by multiple resistance genes in tobacco and tomato. Plant Cell 18: 1067–83.

Goodwin SB, M'Barek SB, Dhilon B, Wittenberg AHJ, Crane CF, Hane JK, Foster AJ, Van der Lee TAJ, Grimwood J, Aerts A, Antoniw J, Bailey A, Bluhm B, Bowler J, Bristow J, Van der Burgt Canto-Canche B, Churchill ACL, Conde-Ferraez L, Cools HJ, Coutinho PM, Csukai M, Dehai M, De Wit P, Donzelli B, van de Geest HC, van Ham RCHJ, Hammond-Kosack KE, Henrissat B, Kilian A, Kobayashi AK, Koopmann E, Kourmpetis Y, Kuzniar A, Lindquist E,

Lombard V, Maliepaard C, Martins N, Mehrabi R, Nap PHJ, Ponomarenko A, Rudd JJ, Salamov, Schmutz J, Schouten HJ, Shapiro H, Stergiopolous I, Torriani SFF, Tu H, de Vries RP, Waalwijk C, Ware SB, Wiebenga A, Zwiers L-H, Oliver SP, Grigoriev IV, Kema GHJ. **2011**. Finished Genome of the Fungal Wheat Pathogen Mycosphaerella graminicola Reveals Dispensome Structure, Chromosome Plasticity, and Stealth Pathogenesis. PLoS Genetics 7: e1002070. doi: 10.1371/journal.pgen.1002070

Gouache D, Bensadoun A, Brun F, Page C, Makowski D, Wallach D. **2013**. Modelling climate change impact on Septoria tritici blotch (STB) in France: Accounting for climate model and disease model uncertainty. Agricultural Forest Meteorology 170: 242-252.

Govrin EM, Levine A. **1999**. The hypersensitive response facilitates plant infection by the necrotrophic pathogen *Botrytis cinerea*. Current Biology 10: 751-7.

Gozani O, Karuman P, Jones DR, Ivanov D, Cha J, Lugovskoy AA, Baird CL, Zhu H, Field SJ, Lessnock SJ, Villasnor J, Mehrota B, Chen J, Rao VR, Brugge JS, Ferguson CG, Payrastre B, Myszka DG, Cantley LC, Wagner G, Divecha N, Prestwich GD, Yuan J. **2003**. The PHD finger of the chromatin-associated protein ING2 functions as a nuclear phosphoinositide receptor. Cell 114: 99–111.

Gudesblat GE, Torres PS, Vojnov AA. **2009**. Stomata and pathogens. Welfare at the gates. Plant Signalling and Behaviour 4: 1114-6.

Halterman D, Zhou F, Wei F, Wise RP, Schulze-Lefert P. **2001**. The MLA6 coiled-coil, NBS-LRR protein confers AvrMla6-dependent resistance specificity to Blumeria graminis f. sp. hordei in barley and wheat. The Plant Journal 25: 335-48.

Hammond-Kosack KE and Rudd JJ. **2008**. Plant resistance signalling hijacked by a necrotrophic fungal pathogen. Plant Signalling and Behaviour 3: 993-5.

Hargreaves DC and Crabtree GR. **2011**. ATP-dependent chromatin remodelling: genetics, genomics and mechanisms. Cell Research 21: 396-420.

Hatfield PM, Gosink MM, Carpenter TB, Vierstra RD. **1997**. The ubiquitin-activating enzyme (E1) gene family in *Arabidopsis thaliana*. Plant Journal 11: 213–26.

Hayafune, M, Berisio R, Marchetti R, Silipo A, Kayama M, Desaki Y, Arima S, Squeglia F, Ruggiero A, Tokuyasu K, Molinaro A, Kaku H, Shibuya N. **2014**. Chitin-induced activation of immune signalling by the rice receptor CEBiP relies on a unique sandwich-type dimerization. Proceedings of the National Academy of Science USA 111: 404-13.

Hemetsberger C, Herrberger C, Zechmann B, Hillmer M, Doehlemann G. **2012.** The *Ustilago maydis* effector Pep1 suppresses plant immunity by inhibition of host peroxidase activity. PLoS Pathogens 8: e1002684.

Henikoff S. **2008**. Nucleosome destabilization in the epigenetic regulation of gene expression. Nature Reviews Genetics 9: 15–26.

Hershko A, Ciechanover A. **1998**. The ubiquitin system. Annual Review of Biochemistry 67: 425–79.

Hirschorn JN, Brown SA, Clark CD, Winston F. **1992**. Evidence that SNF2/SWI2 and SNF5 activate transcription in yeast by altering chromatin structure. Genes and Development 6: 2288-98.

Holzburg S, Brosio P, Gross C, Pogue GP. **2002**. Barley stripe mosaic virus-induced gene silencing in a monocot plant. Plant Journal 30: 315-27.

van der Hoorn RAL, Kamoun S. **2008**. From guard to decoy: a new model for perception of plant pathogen effectors. The Plant Cell 20: 2009-17.

Hong L, Schroth GP, Matthews HR, Yau P, Bradbury EM. **1993**. Studies of the DNA binding properties of histone H4 amino terminus. Thermal denaturation studies reveal that acetylation markedly reduces the binding constant of the H4 “tail” to DNA. Journal of Biological Chemistry 268 :305–14.

Howard RJ, Ferrari MA, Roach DH, Money NP. **1991**. Penetration of hard substrates by a fungus employing enormous turgor pressures. Proceedings of the National Academy of Science of USA 88: 11281-4.

Hubbard A, Lewis CM, Yoshida K, Ramirez-Gonzalez RH, de Vallavieille-Pope C, Thomas J, Kamoun S, Bayles R, Uauy C, Saunders DGO. **2015**. Field pathogenomics reveals the emergence of a diverse wheat yellow rust population. Genome Biology 16:23.

Hubert HA, Tomero P, Belkhadir Y, Krishna P, Takahashi A, Shirasu K, Dangl JL. **2003**. Cytosolic HSP90 associates with and modulates the Arabidopsis RPM1 disease resistance protein. EMBO Journal 22: 5679-89.

Jackson AO, Lim H-S, Bragg J, Ganesan U, Lee MY. **2009**. Hordevirus replication, movement and pathogenesis. Annual Review of Phytopathology 47: 385-422.

Jacobs AK, Lipka V, Burton RA, Panstruga R, Strizhov N, Schulze-Lefert P, Fincher GB. **2003**. An Arabidopsis callse synthase, GSL5, is required for wound and papillary callose formation. Plant Cell 15: 2503-13.

James TC, Elgin SC. **1986**. Identification of a nonhistone chromosomal protein associated with heterochromatin in *Drosophila melanogaster* and its gene. Molecular Cell Biology 6: 3862–72.

Ji Z-Y, Xiong L, Zou L-F, Li Y-R, Ma W-X, Liu L, Zakria M, Ji G-H, Chen G-Y. **2014**. AvrXa7-Xa7 mediated defense in rice can be suppressed by transcriptional activator-like effectors TAL6 and TAL11a from *Xanthomonas oryzae* pv. *oryzicola*. Molecular Plant–Microbe Interactions 27: 983–95.

Jia Y, McAdams SA, Bryan GT, Hershey HP, Valent B. **2000**. Direct interaction of resistance gene and avirulence gene products confers rice blast resistance. EMBO Journal 19: 4004–14.

Jin H, Axtell MJ, Dahlback D, Ekwenna O Zhang S, Staskawicz B, Baker B. **2002**. Developmental Cell 3: 291-7.

de Jonge R, van Esse HP, Kombrink A, Shinya T, Desaki Y, Bours R, van der Krol S, Shibuya N, Joosten MH, Thomma BP. **2010**. Conserved fungal LysM effector Ecp6 prevents chitin-triggered immunity in plants. Science 329: 953–5.

Jones JD, Dangl JL. The plant immune system. **2006**. Nature 444: 323–9.

Journot- Catalino, N, Somssich IE, Roby D, Kroj T. **2006**. The transcription factors WRKY11 and WRKY17 act as negative regulators of basal resistance in Arabidopsis thaliana. Plant Cell 18: 3289-302.

Kadosh D, Struhl K. **1998**. Targeted recruitment of the Sin3- Rpd3 histone deacetylase complex generates a highly localized domain of repressed chromatin in vivo. Molecular Cell Biology 18: 5121–7.

Kadota Y, Shirasu K, Guerois R. **2010**. NLR sensors meet at the SGT1-HSP90 crossroad. Trends in Biochemical Science 35: 199-207.

Kaku H, Nishizawa Y, Ishii-Minami N, Akimoto-Tomiyama C, Dohmae N, Takio K, Minami E, Shibuya N. **2006**. Plant cells recognise chitin fragments for defence signalling through a plasma membrane receptor. Proceedings of the National Academy of Science USA 103: 11086-91.

van Kan J.A. **2006**. Licensed to kill: the lifestyle of a necrotrophic plant pathogen. Trends in Plant Science 118: 247–53.

Karimi M, de Meyer B, Hilson P. **2005**. Modular cloning in plant cells. Trends in Plant Science

Karve TM, Cheema AK. **2011**. Small change huge impact: the role of protein posttranslational modification in cellular homeostasis and disease. Journal of Amino Acids 2011: 207691.

Keon J, Antoniw J, Carzaniga R, Deller S, Ward JL, Baker JM, Beale MH, Hammond-Kosack K, Rudd JJ. **2007**. Transcriptional adaptation of *Mycosphaerella graminicola* to programmed cell death of its susceptible wheat host. Molecular Plant–Microbe Interactions 20: 178–93.

Kim J, Guermah M, McGinty RK, Lee J-S, Tang Z, Milne TA, Shilatifard A, Muir TW, Roeder RG. **2009**. RAD6-mediated transcription-coupled H2B ubiquitylation directly stimulates H3K4 methylation in human cells. Cell 137: 459–71.

Kim KC, Lai Z, Fan B, Chen Z. **2008**. Arabidopsis WRKY38 and WRKY62 transcription factors interact with histone deacetylase 19 in basal defence. Plant Cell 20: 2357-2371.

Kim YJ, Lin NC, Martin GB. **2002**. Two distinct Pseudomonas effector proteins interact with the Pto kinase and activate plant immunity. Cell 109: 589-98.

King SRF, McLellan H, Boevink PC, Armstrong MR, Bukharova T, Sukarta O, Win J, Kamoun S, Birch PRJ, Banfield MJ. **2014**. Phytophthora infestans RXLR Effector PexRD2 Interacts with Host MAPKKKe to Suppress Plant Immune Signaling. Plant Cell 26: 1345-59.

Kislev ME. **1984**. Emergence of wheat agriculture. Paléorient 10: 61-70.

Kema GHJ, Yu D, Rijkenberg FHJ, Shaw MW, Baayen RP. **1996**. Histology of the pathogenesis of *Mycosphaerella graminicola* in wheat. Phytopathology 86: 777–86.

Kraft E, Stone SL, Ma L, Su N, Gao Y, Lau O-S, Deng X-W, Callis J. **2005**. Genome analysis and functional characterisation of the E2 and RING-type E3 ligase ubiquitination enzymes of Arabidopsis. Plant Physiology 139: 1597-1611.

van der Krol AR, Mur LA, Beld M, Mol JN, Stuitje AR. **1990**. Flavonoid genes in petunia: addition of a limited number of gene copies may lead to suppression of gene expression. Plant Cell 2: 291-9.

Kobe B, Diesenhofer J. **1994B**. The leucine-rich repeat: a versatile binding motif. Trends in Biochemical Science 19: 415-21.

Koncz C, Schell J. **1986**. The promoter of the TL-DNA gene 5 controls the tissue-specific expression of chimaeric genes carried by a novel type of Agrobacterium binary vector. Molecular and General Genetics 204: 383-96.

Kouzarides T. **2000**. Acetylation: a regulatory modification to rival phosphorylation? EMBO Journal 19: 1176-9.

Kumagai MH, Donson J, della-Cioppa G, Harvey D, Hanley K, Grill LK. **1995**. Cytoplasmic inhibition of carotenoid biosynthesis with virus-derived RNA. Proceedings of the National Academy of Science USA 92(5): 1679-83.

Lachner M, O'Carroll D, Rea S, Mechtler K, Jenuwein T. **2001**. Methylation of histone H3 lysine 9 creates a binding site for HP1 proteins. Nature 410: 116–20.

Lambert K, Bekal S. **2002**. Introduction to plant-parasitic nematodes. The Plant Health Instructor DOI: 10.1094/PHI-I-2002-1218-01.

Lee DY, Hayes JJ, Pruss D, Wolffe AP. **1993**. A positive role for histone acetylation in transcription factor access to nucleosomal DNA. Cell 72 :73–84.

Lee J, Orosa B, Milyard L, Edwards M, Kanyuka K, Gatehouse A, Rudd J, Hammond-Kosack K, Pain N, Sadanandom A. **2015**. Functional analysis of a wheat homeodomain protein, TaR1, reveals that host chromatin remodelling influences the dynamics of the switch to necrotrophic growth in the phytopathogenic fungus Zymoseptoria tritici. New Phytologist 206: 598-605.

Lee W-S, Rudd JJ, Hammond-Kosack KE, Kanyuka K. 2014. Mycosphaerella graminicola LysM effector-mediated stealth pathogenesis subverts recognition through both CERK1 and CEBiP homologues in wheat. Molecular Plant Microbe Interactions 27: 236-243. 10.1094/MPMI-07-13-0201-R.

Lee W-S, Devonshire BJ, Hammond-Kosack KE, Rudd JJ, Kanyuka K. **2015**. Deregulation of Plant Cell Death Through Disruption of Chloroplast Functionality Affects Asexual Sporulation of *Zymoseptoria tritici* on Wheat. Molecular Plant-Microbe Interactions 28: 590-604.

Lee WY, Lee D, Chung W-I, Kwon CS. **2009**. Arabidopsis ING and Alfin1-like protein families localise to the nucleus and bind to H3K4me2/3 via Plant HomeoDomain fingers. The Plant Journal 58: 511-24.

Li B, Gogol M, Carey M, Lee D, Seidel C, Workman JL. **2007**. Combined action of PHD and chromo domains directs Rpd3S HDAC to transcribed chromatin. Science 316: 1050-4.

Li L, Li M, Yu L, Zhou Z, Liang X, Liu Z, Cai G, Gao L, Zhang X, Wang Y, Chen S, Zhou M. **2014**. The FLS2-mediated kinase BIK1 directly phosphorylates the NADPH oxidase RbohD to control plant immunity. Cell Host and Microbe 15: 329-38.

Libault M, Wan J, Czechowski T, Udvardi M, Stacey G. **2007**. Identification of 188 Arabidopsis transcription factor and 30 ubiquitin-ligase genes responding to chitin, a plant defense elicitor. Molecular Plant Microbe Interactions 20: 900-11.

Liu J, Park CH, He F, Nagano M, Wang M, Bellizzi M, Zhang K, Zeng X, Liu W, Ning Y, Kawano Y, Wang G-L. **2015**. The RhoGAP SPIN6 Associates with SPL11 and OsRac1 and Negatively Regulates Programmed Cell Death and Innate Immunity in Rice. PLoS Pathogens 11: e1004807.

Liu Q, Feng Y, Zhu Z. **2009**. Dicer-like proteins in plants. Functional and Integrative Genomics 9(3): 277-86.

Liu T, Liu Z, Song C, Hu Y, Han Z, She J, Fan G, Wang J, Jin C, Chang J, Zhou J-M, Chai J. **2012**. Chitin-induced dimerization activates a plant immune receptor. Science 336: 1160-4.

Liu T, Song T, Zhang X, Yuan H, Su L, Li W, Xu J, Liu S, Chen L, Chen T, Zhang M, Gu L, Zhang B, Dou D. **2014**. Unconventionally secreted effectors of two filamentous pathogens target plant salicylate biosynthesis. Nature Communications 5: 4686 doi:10.1038/ncomms5686

Liu X, Luo M, Zhang W, Zhao J, Zhang J, Wu K, Tian L, Duan J. **2012**. Histone acetyltransferase in rice (Oryza sativa L.): phylogenetic analysis, subcellular localisation and expression. BMC Plant Biology 12:145.

Liu Y, Schiff M, Dinesh-Kumar SP. **2002**. Virus-induced gene silencing in tomato. Plant Journal 31: 777-86.

Liu Z, Faris JD, Oliver RP, Tan KC, Solomon PS, McDonald MC, McDonald BA, Nunez A, Lu S, Rasmussen JB, Friesen TL. **2009**. Sn TOZ3 acts in effector triggered susceptibility to induce disease on wheat carrying the Snn3 gene. PLoS Pathogens 5: e1000581.

Lorenzo O, Chico JM, Sanchez-Serrano JJ, Solano R. **2004**. JASMONATE-INSENSITIVE1 encodes a MYC transcription factor essential to discriminate between different jasmonate-regulated defense responses in *Arabidopsis*. Plant Cell 16: 1938–50.

Lu, D Wu S, Gao X, Zhang Y, Shan L, He P. **2010**. A receptor-like cytoplasmic kinase, BIK1, associates with a flagellin receptor complex to initiate plant innate immunity. Proceedings of the National Academy of Science USA 107: 496–501.

Lu D, Lin W, Gao X, Wu S, Cheng C, Avila J, Heese A, Devarenne TP, He P, Shan L. **2011**. Direct ubiquitination of pattern recognition receptor FLS2 attenuates plant innate immunity. Science 332: 1439–42.

Mansfield RE, Musselman CA, Kwan AH, Oliver SS, Garske AL, Davrazou F, Denu JM, Kutateladze TG, Mackay JP. **2011**. Plant homeodomain (PHD) fingers of CHD4 are histone H3-binding modules with preference for unmodified H3K4 and methylated H3K9. Journal of Biological Chemistry 284: 11779-91.

Mao G, Meng X, Liu Y, Zheng Z, Chen Z, Zhang S. **2011**. Phosphorylation of a WRKY transcription factor by two pathogen-responsive MAPKs drives phytoalexin biosynthesis in *Arabidopsis*. Plant Cell 23: 1639–53

Marchler-Bauer A, Derbyshire MK, Gonzales NR, Lu S, Chitsaz F, Geer LY, Geer RC, He J, Gwadz M, Hurwitz DI, Lanczycki, Lu F, Marchler GH, Song JS, Thanki N. Yamashita YA, Zhang D, Zheng C, Bryant SH. **2015**. CDD: NCBI's Conserved Domain Database. Nucleic Acids Research 43: 222-6.

Marino D, Peeters N, Rivas S. **2012**. Ubiquitination during plant immune signaling. Plant Physiology 160(1): 15-27.

Marshall R, Kombrink A, Motteram J, Loza-Reyes E, Lucas J, Hammond-Kosack KE, Thomma BPHJ, Rudd JJ. **2011**. Analysis of two in planta expressed LysM homologs from the fungus *Mycosphearella graminicola* reveals novel functional properties and varying contributions to virulence on wheat. Plant Physiology 156: 756-69.

McConn M, Creelman RA, Bell E, Mullet JE, Browse J. **1997**. Jasmonate is essential for insect defense in. Arabidopsis. Proceedings of the National Academy of Sciences USA 94: 5473-7.

Melech-Bonfil S, Sessa G. **2010**. Tomato MAPKKKe is a positive regulator of cell-death signaling networks associated with plant immunity. Plant Journal 64: 379-91.

Mellor J. **2006**. It takes a PHD to read the histone code. Cell 126: 22–24.

Melotto M, Underwood W, Koczan J, Nomura K He SY. **2006**. Plant stomata function in innate immunity against bacterial invasion. Cell 126: 969-80.

Mengiste T. **2012.** Plant Immunity to necrotrophs. Annual Review of Phytopathology 50: 267-94.

Mentlak TA, Kombrink A, Shinya T, Ryder LS, Otomo I, Saitoh H, Terauchi R, Nishizawa Y, Shibuya N, Thomma BP, Talbot NJ. **2012**. Effector-mediated suppression of chitin-triggered immunity by *Magnaporthe oryzae* is necessary for rice blast disease. Plant Cell 24**:** 322–35.

Miya A, Albert K, Shinya T, Desaki Y, Ichimura K, Shirasu K, Narusaka Y, Kawakami N, Kaku H, Shibuya N. **2007**. CERK1, a LysM receptor kinase, is essential for chitin elicitor signaling in Arabidopsis. Proceedings of the National Academy of Science of USA 104: 19613-8.

Molitor AM, Bu Z, Yu Y, Shen W-H. **2014**. Arabidopsis AL PHD-PRC1 Complexes Promote Seed Germination through H3K4me3-to-H3K27me3 Chromatin State Switch in Repression of Seed Developmental Genes. PLOS Genetics 10(1): e1004091.

Morais do Amaral A, Antoniw J, Rudd JJ, Hammond-Kosack KE. **2012**. Defining the Predicted Protein Secretome of the Fungal Wheat Leaf Pathogen *Mycosphaerella graminicola*. PLoS ONE 7: e49904.

Moreira FG, dos Reis S, Ferreira Costa MA, de Souza CGM, Peralta RM. **2005**. Production of hydrolytic enzymes by the plant pathogenic fungus Myrothecium verrucaria in submerged cultures. Brazilian Journal of Microbiology 36: 7-11.

Moshatati A, Gharineh MH. **2012**. Effect of grain wheat on germination and seed vigor of wheat. International Journal of Agriculture and Crop Sciences 4: 458-60.

Mwale VM, Chilembwe EHC, Uluko HC. **2014**. Wheat powdery mildew (*Blumeria graminis* f. sp. *tritici)*: Damage effects and genetic resistance developed in wheat (*Triticum aestivum*). International Research Journal of Plant Science 5: 1-16.

Najar A, Makkouk KM, Kumari SG. **2000**. First record of barley yellow striate mosaic virus, barley stripe mosaic virus and wheat dwarf virus infecting cereal crops in Tunisia. Plant Disease 84: 1045.

Nakayama J, Rice JC, Strahl BD, Allis CD, Grewal SI. **2001**. Role of histone H3 lysine 9 methylation in epigenetic control of heterochromatin assembly. Science 292: 110–3.

Nathan D, Ingvarsdottir K, Sterner DE, Bylebyl GR, Dokmanovich M, Dorsey JA, Whelan KA, Krsmanovich M, Lane WS, Meluh PB, Jonson ES, Berger SL. **2006**. Histone sumoylation is a negative regulator in *Saccharomyces cerevisiae* and shows dynamic interplay with positive-acting histone modifications. Genes and Development 20: 966–76.

Navarro L, Zipfel C, Rowland O, Keller I, Robatzek S, Boller T, Jones JD. **2004**. The transcriptional innate immune response to flg22. Interplay and overlap with Avr gene-dependent defense responses and bacterial pathogenesis. Plant Phyiology 135: 1113-28.

Ni X, Tian Z, Liu J, Song B, Xie C. **2010**. Cloning and molecular characterization of the potato RING finger protein gene StRFP1 and its function in potato broad-spectrum resistance against Phytophthora infestans. Journal of Plant Physiology 167: 488-96.

Ogasawara Y, Kaya H, Hiraoka G, Yumoto F, Kimura S, Kadota Y, Hishinuma H, Senzaki E, Yamagoe S, Nagata K, Nara M, Suzuki K, Tanokura M, Kuchitsu K. **2008**. Synergistic activation of the Arabidopsis NADPH oxidase AtrbohD by Ca2+ and phosphorylation. Journal of Biological Chemistry 283: 8885-92.

Oki M, Aihara H, Ito T. **2007**. Role of histone phosphorylation in chromatin dynamics and its implication in diseases. Subcellular Biochemistry 41: 319-36.

Oliver RP, Solomon PS. **2010**. New developments in pathogenicity and virulence of necrotrophs. Current Opinion in Plant Biology 13: 415–9.

Omrane S, Sghyer H, Audéon C, Lanen C, Duplaix C, Walker A-S, Fillinger S. **2015**. Fungicide efflux and the MgMFS1 transporter contribute to the multidrug resistance phenotype in *Zymoseptoria tritici* field isolates. Environmental Microbiology 17: 2805–23.

Orton ES, Deller S, Brown JK. **2011**. Mycosphearella graminicola: from genomics to disease control. Molecular Plant Pathology 12: 413-424.

Pacheco-Arjona JR, Ramirez-Prado JH. **2014**. Large-Scale Phylogenetic Classification of Fungal Chitin Synthases and Identification of a Putative Cell-Wall Metabolism Gene Cluster in Aspergillus Genomes. PLoS ONE 9: e104920.

Palomar MK, Brakke MK, Jackson AO. **1977**. Base sequence homology in the RNAs of barley stripe mosaic virus. Virology 77(2); 471-80.

Pandey SP, Somssich IE. **2009**. The role of WRKY transcription factors in plant immunity. Plant Physiology 150: 1648-55.

Pandey SP, Roccaro M, Schon M, Logemann E, Somssich, IE. **2010**. Transcriptional reprogramming regulated by WRKY18 and WRKY40 facilitates powdery mildew infection of *Arabidopsis*. Plant Journal 64: 912–23.

Park CH, Chen S, Shirsekar G, Zhou B, Khang CH, Songkumarn P, Afzal AJ, Ning Y, Wang R, Bellizzi M, Valent B, Wang G-L. **2012**. The *Magnaporthe oryzae* effector AvrPiz-t targets the RING E3 ubiquitin ligase APIP6 to suppress pathogen-associated molecular pattern- triggered immunity in rice. Plant Cell 24**:** 4748–62.

Peña RJ, Braun HJ, Mollins J. **2014**. "Anti-Wheat Fad Diets Undermine Global Food Security Efforts: Wheat consumption healthy despite claims in self-help publications". CIMMYT Wheat Discussion Paper. Mexico, D.F.

Pickart CM, Fushman D. **2004**. Polyubiquitin chains: polymeric protein signals. Current Opinion in Chemical Biology 8: 610–6.

Piniero M, Gomez-Mena C, Schaffer R, Martinez-Zapater JM, Coupland G. **2003**. EARLY BLOTING IN SHORT DAYS is related to chromatin remodeling factors and regulates flowering in Arabidopsis by repressing FT. Plant Cell 15: 1552-67

.

Piquerez SJ, Balmuth AL, Sklenar J, Jones AM, Rathjen JP, Ntoukakis V. **2014**. Indentification of post-translational modifcations of plant protein complexes. Journal of Visualised Experiments 22: e51095.

Ponomarenko A, Goodwin SB, Kema GHJ. **2011**. Septoria tritici blotch (STB) of wheat. Plant Health Instructor DOI:10.1094/PHI-I-2011-0407-01

del Pozo O, Pedley KF, Martin GB. **2004**. MAPKKKα is a positive regulator of cell death associated with both plant immunity and disease. EMBO Journal 23: 3072-82.

Privalksy ML. **1998**. Depudecin makes a debut. Proceedings of the National Academy of Science USA 95: 3335-7.

Punja ZK, Zhang Y-Y. **1993**. Plant chitinases and their roles in resistance to fungal diseases. Journal of Nematology 25: 526-40.

Qiu JL, Fiil BK, Petersen K, Nielsen HB, Botanga CJ, Thorgrimson S, Palma K, Suarez-Rodriguez MC, Sandbech-Clausen S, Lichota J, Brodersen P, Grasser KD, Mattsson O, Glazebrook J, Mundy J, Petersen M. **2008**. *Arabidopsis* MAP kinase 4 regulates gene expression through transcription factor release in the nucleus. EMBO Journal 27: 2214–21.

Ratcliff F, Harrison BD, Baulcombe DC. **2001**. Tobacco rattle virus as a vector for analysis of gene function by silencing. Plant Journal 25: 237-45.

Rea S, Eisenhaber F, O'Carroll D, Strahl BD, Sun ZW, Schmid M, Opravil S, Mechtler K, Ponting CP, Allis CD, Jenuwein T. **2000**. Regulation of chromatin structure by site-specific histone H3 methyltransferases. Nature 406: 593–9.

Reymond P, Grünberger S, Paul K, Müller M, Farmer EE. **1995**. Oligogalacturonide defense signals in plants: large fragments interact with the plasma membrane in vitro. Proceedings of the National Academy Of Science USA 92 4145–9

Robatzek S. **2006**. Ligand-induced endocytosis of the pattern recognition receptor FLS2 in Arabidopsis. Genes & Development 20: 537–42.

Robert-Seilaniantz A, Grant M, Jones JDG. **2011**. Hormone Crosstalk in Plant Disease and Defense: More Than Just JASMONATE-SALICYLATE Antagonism**.** Phytopathology 49: 317-43.

Ron M, Avni A. **2004**. The receptor for the fungal elicitor ethylene-inducing xylanase is a member of a resistance-like gene family in tomato. Plant Cell 16: 1604–15.

Rovenich H, Boshoven JC, Thomma BPHJ. **2014**. Filamentous pathogen effector functions: of pathogens, hosts and microbiomes. Current Opinion in Plant Biology 20: 96-103.

Rudd JJ, Keon J, Hammond-Kosack KE. **2008**. The wheat mitogen-activated protein kinases TaMPK3 and TaMPK6 are differentially regulated at multiple levels during compatible disease interactions with *Mycosphaerella graminicola*. Plant Physiology 147: 802–15.

Rudd J, Kanyuka K, Hassani-Pak K, Derbyshire M, Andongabo A, Devonshire J, Lysenko A, Saqi M, Desai N, Powers S, Hooper J, Ambroso L, Bharti A, Farmer A, Hammond-Kosack K, Dietrich R, Courbot M. **2015**. Transcriptome and metabolite profiling the infection cycle of Zymoseptoria tritici on wheat (Triticum aestivum) reveals a biphasic interaction with plant immunity involving differential pathogen chromosomal contributions, and a variation on the hemibiotrophic lifestyle definition. Plant Physiology 167: 1158-85.

Ruiz MT, Voinnet O, Baulcombe DC. **1998**. Initiation and maintenance of virus-induced gene silencing. The Plant Cell 10: 937-46.

Sacharowski SP, Gratkowska DM, Sarnowska EA, Kondrak P, Jancewicz I, Porri A, Bucior E, Rolicka AT, Franzen R, Kowalczyk J, Pawlikowska K, Huettel B, Torti S, Schmelzer E, Coupland G, Jerzmanowski A, Koncz C, Sarnowski TJ. **2015**. SWP73 Subunits of Arabidopsis SWI/SNF Chromatin Remodeling Complexes Play Distinct Roles in Leaf and Flower Development. Plant Cell 27: 1889-1906.

Sadanandom A, Bailey M, Ewan R, Lee J, Nelis S. **2012**. The ubiquitin-proteasome system: central modifier of plant siganlling. New Phytologist 196(1): 13-28.

Sadler JBA, Bryant NJ, Gould GW, Welburn CR. **2013**. Posttranslational modification of GLUT4 affect its subcellular localization and translocation. International Journal of Molecular Sciences 14: 9963-78.

Santos-Rosa H, Schneider R, Bannister AJ, Sherriff J, Bernstein BE, Emre NC, Schreiber SL, Mellor J, Kouzarides T. **2002**. Active genes are tri-methylated at K4 of histone H3. Nature 419: 407–11.

Scheel H, Hofmann K. **2003**. No evidence for PHD fingers as ubiquitin ligases. Trends in Cell Biology 13: 285–7.

Schindler U, Beckmann H, Cashmore AR. **1993**. HAT3.1, a novel Arabidopsis homeodomain protein containing a conserved cysteine-rich region. The Plant Journal 4: 137–50.

Scofield SR, Huang L, Brandt AS, Gill BS. **2005**. Development of a virus-induced gene silencing system for hexaploid wheat and its use in functional analysis of the *Lr21*-mediated leaf rust resistance pathway. Plant Physiology 138: 2165-73.

Serrano M, Coluccia F, Torres M, L'Haridon F, Metraux JP. **2014**. The cuticle and plant defence to pathogens. Frontiers in Plant Science 5: 274.

Shan LB, He P, Li JM, Heese A, Peck SC, Nürnberger T, Martin GB, Sheen J. **2008**. Bacterial effectors target the common signaling partner BAK1 to disrupt multiple

MAMP receptor-signaling complexes and impede plant immunity. Cell Host and Microbe 4: 17–27.

Shen Q-H, Saijo Y, Mauch S, Biskup C, Bieri S, Keller B, Seki H, Ulker B, Somssich IE, Schulze-Lefert P. **2007**. Nuclear activity of MLA immune receptors links isolate-specific and basal disease-resistance responses. Science 315: 1098–103.

Shetty NP, Jensen JD, Knudsen A, Finnies C, Geshi N, Blennow A, Collinge DB, Jorgensen HJL. **2009**. Effects of beta-1,3-glucan from *Septoria tritici* on structural defence responses in wheat. Journal of Experimental Botany 60, 4287–300.

Shi X, Hong T, Walter KL, Ewalt M, Michisita E, Hung T, Carney D, Pena P, Lan F, Kaadige MR, Lacoste N, Cayrou C, Davrazou F, Saha A, Cairns BR, Ayer DE, Kutateladze TG, Shi Y, Cote J, Chua K, Gozani O. **2006**. ING2 PHD domain links histone H3 lysine 4 methylation to active gene repression. Nature 442: 96–9.

Shiio Y, Eisenman RN. **2003**. Histone sumoylation is associated with transcriptional repression. Proceedings of the National Academy of Science USA 100: 13225–30.

Shimizu T, Nakano T, Takamizawa D, Desaki Y, Ishii-Minami N, Nishizawa Y, Minami E, Okada K, Yamane H, Kaku H, Shibuya N. **2010**. Two LysM receptor molecules, CEBiP and OsCERK1, cooperatively regulate chitin elicitor signalling in rice. Plant Journal 64: 204-14.

Shirasu K, Lahaye T, Tan M-W, Zhou F, Azevedo C, Schulze-Lefert P. **1999**. A Novel Class of Eukaryotic Zinc-Binding Proteins Is Required for Disease Resistance Signaling in Barley and Development in *C. elegans*. Cell 99: 355-66.

Sievers F, Wilm A, Dineen D, Gibson TJ, Karplus K, Li W, Lopez R, McWilliam H, Remmert M, Soding J, Thompson JD, Higgins DG. **2011**. Fast, scalable generation of high-quality protein multiple sequence alignments using Clustal Omega. Molecular Systems Biology 7: 539.

Sikorskaite S, Rajamaki M-L, Banilus D, Stanys V, Valkonen JPT. **2013**. Protocol: Optimised methodology for isolation of nuclei from leaves of species in the solanacaea and rosacaea families. Plant Methods 9: 31.

Spoel SH, Dong X. **2012**. How do plants achieve immunity? Defence without specialized immune cells. Nature Reviews Immunology 12: 89-100.

Soliman MA, Riabowol K. **2007**. After a decade of study-ING, a PHD for a versatile family of proteins. Trends in Biochemical Science 32: 509–19.

Staal J, Kaliff M, Dewaele E, Persson M, Dixelius C. **2008**. RLM3, a TIR domain encoding gene involved in broad-range immunity of *Arabidopsis* to necrotrophic fungal pathogens. Plant Journal 55: 188–200.

Stergiopoulos I, Zwiers LH, de Waard MA. **2003**. The ABC transporter MgAtr4 is a virulence factor of Mycosphaerella graminicola that affects colonization of substomatal cavities in wheat leaves. Molecular Plant Microbe Interactions 16: 689-98.

Strahl BD, Ohba R, Cook RG, Allis CD. **1999**. Methylation of histone H3 at lysine 4 is highly conserved and correlates with transcriptionally active nuclei in Tetrahymena. Proceedings of the National Academy of Science USA 96: 14967–72.

Strahl BD, Allis CD. **2000**. The language of covalent histone modifications. Nature 403: 41-5.

Strange RN, Scott PR. **2005**. Plant Disease: a threat to global food security. Annual Review of Phytopathology 43: 83-116.

Sun W, Dunning F, Pfund C, Weingarten R, Bent A. **2006**. Within-species flagellin polymorphism in *Xanthomonas campestris* pv *campestris* and its impact on elicitation of *Arabidopsis FLAGELLIN SENSING2*-dependent defenses. Plant Cell 18: 764–79.

Tan M, Luo H, Lee S, Jin F, Y JS, Montellier E, Buchou T, Cheng Z, Rousseaux, Rajagopal N, Lu Z, Ye Z, Zhu Q, Wysocka J, Ye Y, Khochbin S, Ren B, Zhao Y. **2011**. Identification of 67 histone marks and histone lysine crotonylation as a new type of histone modification. Cell 146: 1016-28.

Tang X, Frederick RD, Zhou J, Halterman DA, Jia Y, Martin GB. **1996**. Initiation of Plant Disease Resistance by Physical Interaction of AvrPto and Pto Kinase. Science 274: 2060-3.

Taverna SD, Ilin S, Rogers RS, Tanny JC, Lavender H, Li H, Baker L, Boyle J, Blair LP, Chait BT, Patel DJ, Aitchison JD, Tacket AJ, Allis CD. **2006**. Yng1 PHD finger binding to H3 trimethylated at K4 promotes NuA3 HAT activity at K14 of H3 and transcription at a subset of targeted ORFs. Molecular Cell 24: 785-96.

Teif VB, Rippe K. **2009**. Predicting nucleosome positions on the DNA: combining intrinsic sequence preferences and remodeler activites. Nucleic Acids Research 37: 5641-55.

Torres MA, Jones JDG, Dangl JL. **2006**. Reactive oxygen species in signaling response to pathogens. Plant Physiology 141: 373-8.

Traut TW. **1994**. The functions and consensus motifs of nine types of peptide segments that form different types of nucleotide-binding sites. European Journal of Biochemistry 222: 9-19.

Trier NH, Hansen PR, Houen G. **2012**. Production and characterization of peptide antibodies. Methods 56: 136-44.

Trujillo M, Ichimura K, Casais C, Shirasu K. **2008**. Negative regulation of PAMP-triggered immunity by an E3 ubiquitin ligase triplet in *Arabidopsis*. Current Biology 18: 1396–1401.

Trujillo M, Shirasu, K. **2010**. Ubiquitination in plant immunity. Current Opinion in Plant Biology 13:402-8.

Tsuda K, Sato M, Glazebrook J, Cohen JD, Katagiri F. **2008**. Interplay between MAMP-triggered and SA-mediated defense responses. Plant Journal 53: 763–75.

Underwood W. **2012**. The plant cell wall: a dymanic barrier against pathogen invasion. Frontiers in Plant Science 3: 85.

United States Department of Agriculture. **2015**. World agricultural production. http://apps.fas.usda.gov/psdonline/circulars/production.pdf

Vettese-Dadey M, Grant PA, Hebbes TR, Crane-Robinson C, Allis CD, Workman JL. **1996**. Acetylation of histone H4 plays a primary role in enhancing transcription factor binding to nucleosomal DNA in vitro. EMBO Journal 15 :2508–18.

Vierstra RD. **1996**. Proteolysis in plants: mechanisms and functions. Plant Molecular Biology 32: 275–302.

Vierstra RD. **2009**. The ubiquitin–26S proteasome system at the nexus of plant biology. Nature Reviews Molecular Cell Biology 10: 385–97.

Vleeshouwers VG, van Dooijeweert W, Govers F, Kamoun S, Colon LT. **2000**. The hypersensitive response is associated with host and nonhost resistance to *Phytophthora infestans*. Planta 210: 853–64.

Voitsik A-M, Muench S, Deising HB, Voll LM. **2013**. Two recently duplicated maize NAC transcription factor paralogs are induced in response to *Colletotrichum graminicola* infection. BMC Plant Biology 13: 85.

Walley JW, Rowe HC, Xiao Y, Chehab EW, Kliebenstein DJ, Wagner D, Dehesh K. **2008**. The chromatin remodeler SPLAYED regulates specific stress signaling pathways. PLoS Pathogens 4: e1000237.

Walton JD. **1996**. Host-selective toxins: agents of compatibility. The Plant Cell 88: 1723–33.

Walton JD. **2006**. HC-toxin. Phytochemistry 67: 1406-13.

Wang C, Gao F, Wu J, Dai J, Wei C, Li Y. **2010**. Arabidopsis putative deacetylase AtSRT2 regulates basal defence by supressing PAD4, EDS5 and SID2 expression. Plant Cell Physiology 51: 1291-1299.

Wang H, Wang L, Erdjument-Bromage H, Vidal M, Tempst P, Jones RS, Zhang Y. **2004**. Role of histone H2A ubiquitination in Polycomb silencing. Nature 431: 873–8.

Wang YC, Klein TM, Fromm M, Cao J, Sanford JC, Wu R. **1988**. Transient expression of foreign genes in rice, wheat and soybean cells following particle bombardment. Plant Molecular Biology 11: 433-9.

Wang YS, Pi LY, Chen X, Chakrabarty PK, Jiang J, De Leon AL, Liu G-Z, Li L, Benny U, Oard J, Ronald PC, Song W-Y. **2006**. Rice XA21 binding protein 3 is a ubiquitin ligase required for full Xa21-mediated disease resistance. Plant Cell 18: 3635–46.

Wei W, Zhang Y-Q, Tao J-J, Chen H-W, Li Q-T, Zhang W-K, Ma B, Lin Q, Zhang J-S, Chen S-Y. **2015**. The Alfin-like homeodomain finger protein AL5 supresses multiple negative factors to confer abiotic stress tolerance in Arabidopsis. The Plant Journal 81: 871-83.

Wen F, Zhu H, Li P, Jiang M, Mao W, Ong C, Chu Z. **2014**. Genome-Wide Evolutionary Characterization and Expression Analyses of WRKY Family Genes in *Brachypodium distachyon*. DNA Research 21: 327-39.

Whigham E, Qi S, Mistry D, Surana P, Xu R, Fuesrt GS, Pliego C, Bindschedler LV, Spanu P, Dickerson JA, Inner R, Nettleton D, Bogdanove AJ, Wise RP. **2015**. Broadly conserved fungal effector BEC1019 suppresses host cell death and enhances pathogen virulence in powdery mildew of barley (Hordeum vulgare L.). Molecular Plant Microbe Interactions http://dx.doi.org/10.1094/MPMI-02-15-0027-FI.

Whitehouse I, Rando OJ, Delrow J, Tsukiyama T. **2007**. Chromatin remodelling at promoters suppresses antisense transcription. Nature 450:1031–5.

Winicov I. **2000**. Alfin1 transcription factor overexpression enhances plant root growth under normal and saline condi- tions and improves salt tolerance in alfalfa. Planta, 210: 416– 22.

Winicov II, Bastola DR. **1999**. Transgenic overexpression of the transcription factor Alfin1 enhances expression of the endogenous MsPRP2 gene in alfalfa and improves salinity tolerance of the plants. Plant Physiology 120: 473–80.

Wilson ZA, Morrol SM, Dawson J, Swarup R, Tighe PJ. **2001**. The Arabidopsis MALE STERILITY1 (MS1) gene is a transcriptional regulator of male gametogenesis, with homology to the PHD-finger family of transcription factors. Plant Journal 28: 27-39.

Wolpert TJ, Dunkle LD, Ciuffetti LM. **2002**. Host-selective toxins and avirulence determinants: What's in a name? Annual Review of Phytopathology 40: 251–85.

Wong HL, Pinontoan R, Hayashi K, Tabata R, Yaeno T, Haegawa K, Kojima C, Yoshioka H, Iba K, Kawasaki T, Shimamoto K. **2007**. Regulation of rice NADPH oxidase by binding of Rac GTPase to its N-terminal extension. Plant Cell 19: 4022-34.

Wurtele H, Verreault A. **2006**. Histone post-translational modifications and the response to DNA double-strand breaks. Current Opinion in Cell Biology 18: 137–44.

Wysocka J, Swigut T, Xiao H, Milne TA, Kwon SY, Landry J, Kauer M, Tackett AJ, Chait BT, Badenhorst P, Wu C, Allis CD. **2006**. A PHD finger of NURF couples histone H3 lysine 4 trimethylation with chromatin remodelling. Nature 442: 86–90.

Xiang T, Zong N, Zou Y, Wu Y, Zhang J, Xing W, Li Y, Chang X, Zhu L, Chai J, Zhou JM. **2008**. *Pseudomonas syringae* effector AvrPto blocks innate immunity by targeting receptor kinases. Current Biology 18: 74–80.

Xiang T, Zhong N, Zou Y, Wu Y, Zhang J, Xing W, Li Y, Tang X, Zhu L, Chai J, Zhou J-M. **2008**. Pseudomonas syringae effector AvrPto blocks innate immunity by targeting receptor kinases. Current Biology 18: 74–80.

Yamaguchi K, Yamada K, Ishikawa K, Yoshimura S, Hayashi N, Uchihashi K, Ishihama N, Kishi-Kaboshi M, Takahashi A, Tsuge S, Ochiai H, Tada Y, Shimamoto K, Yoshioka H, Kawasaki T. **2013**. A receptor-like cytoplasmic kinase targeted by a plant pathogen effector is directly phosphorylated by the chitin receptor and mediates rice immunity. Cell Host and Microbe 13: 347-57.

Yang C-W, González-Lamothe R, Ewan RA, Rowland O, Yoshioka H, Shenton M, Ye H, O'Donnell E, Jones JDG, Sadanandom A. **2006**. The E3 ubiquitin ligase activity of arabidopsis PLANT U-BOX17 and its functional tobacco homolog ACRE276 are required for cell death and defense. Plant Cell 18: 1084–98.

Yang F, Li WS, Jorgensen HJL. **2013**. Transcriptional reprogramming of wheat and the hemibiotrophic pathogen *Septoria tritici* during two phases of the compatible interaction. PLoS ONE 8: e81606.

Yang XJ, Seto E. **2007**. HATs and HDACs: from structure, function and regulation to novel strategies for therapy and prevention. Oncogene 26: 5310–8.

Yao Y, Ni Z, Zhang Y, Chen Y, Ding Y, Han Z, Liu Z, Sun Q. **2005**. Identification of differentially expressed genes in leaf and root between wheat hybrid and its parental inbreds using PCR-based cDNA subtraction. Plant Molecular Biology 58: 367-84.

Yu Y, Xu W, Wang J, Wang L, Yao W, Yang Y, Xu Y, Ma F, Du Y, Wang Y. **2013**. The Chinese wild grapevine (*Vitis pseudoreticulata*) E3 ubiquitin ligase Erysiphe necator-induced RING finger protein 1 (EIRP1) activates plant defense responses by inducing proteolysis of the VpWRKY11 transcription factor. New Phytologist 200: 834–846.

Yuan C, Li C, Yan L, Jackson AO, Liu Z, Han C, Yu J, Li D. **2011**. A high throughput barley stripe mosaic virus vector for virus induced gene silencing in monocots and dicots. PLoS ONE 6: e26468. doi:10.1371/journal.pone.0026468

Zhan J, Pettway RE, McDonald BA. **2003**. The global genetic structure of the wheat pathogen *Mycosphaerella graminicola* is characterized by high nuclear diversity, low mitochondrial diversity, regular recombination, and gene flow. Fungal Genetics Biology 38: 286–97.

Zhang J, Li W, Xiang T, Liu Z, Laluk K, Ding Z, Zou Y, Gao M, Zhang X, Chen S, Mengiste T, Zhang y, Zhou J-M. **2010**. Receptor-like cytoplasmic kinases integrate signalling from multiple plant immune receptors and are targeted by a Pseudomonas synringae effector. Cell Host and Microbe 7: 290-301.

Zhang L, Kars I, Essenstam B, Liebrand TWH, Wagemakers L, Elberse J, Tagalaki P, Tjoitang D, van der Ackerveken G, van Kan JAL. **2014**. Fungal endopolygalacturonases are recognized as microbe-associated molecular patterns by the *Arabidopsis* receptor-like protein RESPONSIVENESS TO BOTRYTIS POLYGALACTURONASES1. Plant Physiology 164: 352–64.

Zhang Y, Feng D, Bao Y, Ma Y, Yin N, Xu J, Wang H. **2013**. A novel wheat related-to-ubiquitin gene *TaRUB1* is responsive to pathogen attack as well as to both osmotic and salt stress. Plant Molecular Biology Reporter 31: 151-9.

Zhou C, Zhang L, Duan J, Miki B, Wu K. **2005**. HISTONE DEACETYLASE19 is involved in jasmonic acid and ethylene signaling of pathogen response in *Arabidopsis*. Plant Cell 17: 1196–204.

Zhou XL, Han DJ, Gou HL, Wang QL, Zeng QD, Yuan FP, Zhan GM, Huang LL, Kang ZS. **2014**. Molecular mapping of a stripe rust resistance gene in wheat cultivar wuhan 2. Euphytica 196: 251-9.

Zipfel C, Robatzek S, Navarro L, Oakley EJ, Jones JDG, Boller T, Felix G. **2004**. Bacterial disease resistance in Arabidopsis through flagellin reception. Nature 428: 764-7.
Zipfel C. **2014**. Plant pattern-recognition receptors. Trends in Immunology 35: 345-51.